



Skolkovo Institute of Science and Technology

CARBON NANOTUBE FIBERS AS EMBEDDED ELECTRODES FOR THE DUAL-  
STAGE MONITORING OF MULTI-FUNCTIONAL CARBON NANOTUBE  
NANOCOMPOSITES  
*Doctoral Thesis*

by

HASSAAN AHMAD BUTT

DOCTORAL PROGRAM IN MATERIALS SCIENCE AND ENGINEERING

Supervisor  
Professor Albert G. Nasibulin  
Co-Supervisor  
Assistant Professor Dmitry V. Krasnikov

Moscow - 2023

© Hassaan Ahmad Butt 2023

I hereby declare that the work presented in this thesis was carried out by myself at Skolkovo Institute of Science and Technology, Moscow, except where due acknowledgement is made, and has not been submitted for any other degree.

Candidate (Hassaan Ahmad Butt)

Supervisor (Professor Albert G. Nasibulin)

Co-Supervisor (Assistant Professor Dmitry V. Krasnikov)

## **Abstract**

This thesis is devoted to the scientific foundations of carbon nanotube fiber (CNTF) and carbon nanotube (CNT) interactions in polymer nanocomposites. The work focuses on the application of CNTFs as embedded electrodes for the one-step manufacturing and lifecycle monitoring of CNT nanocomposites. The CNTFs are shown to be able to detect various parameters; manufacturing defects, lifecycle damage and functional properties of CNT nanocomposites.

The nanocomposites were manufactured using two types of CNTs, single- and multiwalled, at two weight percentages of 0.25 and 0.75, to which the CNTFs were integrated. The CNTFs were produced using the wet-pulling technique from SWCNT thin films of two widths to alter their diameter and conductivity. This allowed understanding of how the diameter and conductivity of the fibers affected dual-stage monitoring. Manufacturing monitoring consisted of electrical testing, with both the 2- and 4-point techniques, to determine CNTF sensitivity to CNT type, concentration and contact resistance. The performance was compared to embedded metallic electrodes, and the CNTFs were found to display no noise or contact resistance, diameter-free consistency and sensitivity to CNT type and concentration.

Post-manufacturing monitoring tested the electrical, mechanical and piezoresistive properties of the nanocomposites with the embedded CNTFs. Electrical measurements made by the CNTFs matched those of the standard silver-based electrodes and were 1-2 orders of magnitude smaller than metallic electrodes. Uniaxial tensile and cyclic testing

showed consistently measured piezoresistive response which matched the standard without causing any mechanical property loss, unlike metallic embedded electrodes.

Microstructural analysis showed that the porous nature of the CNTFs allowed higher wetting and adhesion from the nanocomposite matrices on the surface as well volume through infiltration. This caused their superior mechanical and electrical performance through CNT (matrix) to CNT (CNTF adhesion).

Thus, the CNTFs showed higher detection performance for both manufacturing and post-manufacturing monitoring. They were able to detect changes in the concentration of CNTs, were sensitive to both types, show no contact resistance and perform better than metallic electrodes. They perform as good as standard silver electrodes in all testing, with the added benefit of being useable as one-step dual stage solution. They did not cause any mechanical property loss after integration, unlike the embedded metallic electrodes.

This thesis is the first to show that CNTF based electrodes can be integrated into large-scale nanocomposite manufacturing and provide dual-stage in-situ monitoring. This concept, which is cheaper and as accurate as alternative techniques for both stages, has a strong potential to positively impact industrial production techniques for smart, self-diagnostic and multifunctional nanocomposites.

**Publications included in thesis:**

1. H.A. Butt, I.V. Novikov, D.V. Krasnikov, A.V. Sulimov, A.K. Pal, S.A. Evlashin, A.M. Vorobei, Y.I. Zuev, D. Ostrizhiniy, D. Dzhurinskiy, Y.A. Popov, O.O. Parenago, A.G. Nasibulin, Binder-free, pre-consolidated single-walled carbon nanotubes for manufacturing thermoset nanocomposites, *Carbon* 202 (2022) 450-463, 10.1016/j.carbon.2022.10.088

*Author's contribution:* Fabrication of samples (50%, with I.V. Novikov), DC conductivity testing and analysis (50%, with I.V. Novikov), data processing (50%, with I.V. Novikov), thermal property study, microstructural analysis (50%, with I.V. Novikov), and writing, reviewing and editing the original draft.

2. H.A. Butt, G.V. Rogozhkin, A. Starkov, D.V. Krasnikov, A.G. Nasibulin, Multifunctional Carbon Nanotube Reinforced Polymer/Fiber Composites: Fiber-Based Integration and Properties, in: L. Li (Ed.), Next Generation Fiber-Reinforced Composites - New Insights, IntechOpen, Online (London), 2022, pp. 1-25, 10.5772/intechopen.108810

*Author's contribution:* Data collection, visualization conception, writing, reviewing and editing the original draft.

3. **Submitted (Advanced composites and Hybrid Materials, Springer):** H. A. Butt, D. V. Krasnikov, V. A. Kondrashov, B. V. Voloskov, S. D. Konev, A. I. Vershinina, S. D. Shandakov, Z. Wang, A. M. Korsunsky, I. V. Sergeichev, A. G. Nasibulin, Multifunctional nanocomposite assessment using carbon nanotube fiber sensors

*Author's contribution:* Fabrication of samples, electrical testing, mechanical testing

*(with assistance from B. V. Voloskov, S. D. Konev, and I. V. Sergeichev), microstructural analysis and writing, reviewing and editing the original draft.*

4. **Partially included, submitted (Advanced Engineering Materials, Wiley):** M.R.

Chetyrkina, H. A. Butt, M. O. Bulavskiy, M. A. Zhilyaeva, D V. Krasnikov, F. S. Fedorov, B. Mikladal, S. D. Shandakov, and A. G. Nasibulin, Approaching Technological Limit for Wet Pulling Technique

*Author's contribution: Fabrication of samples (25%, with M.R. Chetyrkina), conductivity testing and analysis (25%, with M.R. Chetyrkina), data processing (25%, with M.R. Chetyrkina), and writing, reviewing and editing the original draft (25%, with M.R. Chetyrkina).*

**Publications during PhD related to, but not included in the thesis:**

1. H.A. Butt, S.V. Lomov, I.S. Akhatov, S.G. Abaimov, Self-diagnostic carbon nanocomposites manufactured from industrial epoxy masterbatches, Composite Structures 259 (2021), 10.1016/j.compstruct.2020.113244.
2. H.A. Butt, M. Owais, A. Sulimov, D. Ostrizhiniy, S.V. Lomov, I.S. Akhatov, S.G. Abaimov, Y.A. Popov, CNT/Epoxy-Masterbatch Based Nanocomposites: Thermal and Electrical Properties, 2021 IEEE 21st International Conference on Nanotechnology (NANO, IEEE explore), 2021, pp. 417-420.

## **Acknowledgements**

This thesis is a culmination of the work of not myself, but people who throughout my life, and especially during my PhD, have supported me to the point where completion was possible.

To my Mother and Late Father, who gave me a running start in life. I hope this makes you proud. To my Brother, without whom I would not have been able to be here worry-free, your shoulders can carry more than mine ever could. To my Wife, who's patience with my demeanor has kept both of us sane. Thank you.

To Professors Albert Nasibulin and Dmitry Krasnikov: Thank you for taking the chance on me and giving me your trust. Without your support, ideas, input and most importantly, personality and attitude, none of this would have been minutely possible. I am indebted to you for the kindness you have shown and the opportunities and trust that you have provided.

Dr. Anastasia Goldt, Dr. Vladislav Kondrashov, Dr. Ignat Rakov and Mr. Andrei Starkov, without your presence, neither would I have been able to conduct this research nor enjoy it. Your expertise during difficult experimentation and moral support have kept me afloat more than once. Ilya, Mikhail, Veronica, Javier, Nikita, Aleksei, Konstantin and Aram, you are the spirits which keep this lab alive and the joy and smiles that you have provided me have made this journey worth it.

To the Late Professor Alexei Buchachenko. My words for you are as sincere as they can be, because without you, this PhD would have ended prematurely. I thank you for your support at the most crucial of times. Words cannot express my gratitude for your actions

and assistance and how professional your demeanor was. Too much can be said about your academic achievements and contributions to Skoltech, of which you were undoubtedly one of the strongest cornerstones. Not once have I ever heard someone speak ill of you, which is in itself a testimony to how you carried yourself, both professionally and academically. This milestone, and whatever comes after it because of it, I shall credit most greatly and happily to you. Your presence is felt still, and missed even more.

To my collaborators from the Center of Materials Technologies, Dr. Ivan Sergeichev, Stepan Konev and Boris Voloskov, I would like to express my gratitude for never failing to provide expertise and equipment, and always giving a priority to me and this work. To Nikita Gudkov, hard times feel light because of good company. Thank you.

For all those mentioned and unmentioned, your presence, interaction and help have culminated in this thesis and my own personal growth. The memories and friendships that have come of this journey are to me, the most valuable of outcomes which cannot be replaced for anything the world has to offer.

This work was partially supported thanks to the Council on grants of the President of the Russian Federation grant number HIII-1330.2022.1.3.

## Table of Contents

Abstract.....	3
Publications.....	5
Acknowledgements.....	7
Table of Contents.....	9
<b>Chapter 1. Introduction .....</b>	<b>12</b>
<b>Chapter 2. Literature Review .....</b>	<b>15</b>
2.1 Carbon nanotubes.....	15
2.2 Carbon nanotube polymer nanocomposites .....	17
2.3 Carbon nanotube fibers .....	22
<b>Chapter 3. Materials and Methods.....</b>	<b>26</b>
3.1 Methodology and characterization.....	26
3.2 Precursor materials.....	27
3.3 Carbon nanotube fiber fabrication .....	28
3.4 Carbon nanotube nanocomposite manufacturing.....	29
3.5 Material selection and optimization.....	31
3.5.1 Carbon nanotube fiber density alteration.....	32
3.5.2 Bulk density alteration of carbon nanotubes.....	33
3.6 Nanocomposite fabrication with embedded electrodes .....	36
<b>Chapter 4. Nanocomposites with embedded electrodes .....</b>	<b>40</b>
4.1 Material selection and optimization.....	40
4.2 Embedded electrodes and multifunctional property monitoring .....	52

4.3 Carbon nanotube fibers .....	54
4.4 Manufacturing parameter monitoring .....	57
4.5 Post-manufacturing parameter monitoring .....	64
4.5.1 Electrical resistivity measurements.....	64
4.5.2 Tensile piezoresistive response and properties .....	67
4.5.3 Cyclic piezoresistive response and properties .....	75
4.5.4 Microstructural analysis and mechanism of working .....	80
<b>Chapter 5. Conclusions and Future Outlook .....</b>	<b>90</b>
<b>Bibliography .....</b>	<b>95</b>
<b>Appendix.....</b>	<b>105</b>

## **List of Symbols, Abbreviations**

CNT – Carbon nanotube

CNTF – Carbon nanotube fiber

CVD – Chemical vapor deposition

dc – Direct current

DIC – Digital image correlation

GF – Gauge factor

IG/ID – Ratio of Raman G and D mode intensities

MB – Masterbatch

MWCNT – Multi-wall carbon nanotubes

NP – Nanoparticle

RESS – Rapid expansion of supercritical suspensions

SEM – Scanning electron microscopy

SWCNT – Single-wall carbon nanotubes

TEM – Transmission electron microscopy

UTS – Ultimate tensile strength

## **Chapter 1. Introduction**

Polymer nanocomposites, a material class where nano-scale additions are added into a polymer matrix, incorporating carbon nanotubes (CNTs) have been used for a plethora of applications [1–3]. Most commonly seen is their combination with other materials to form nanocomposites [4], of which CNT polymer nanocomposites are the most popular due to their ease of manufacturing, multifunctional properties and spectrum of possible applications [5]. CNTs have been shown to be successfully applicable to both thermoset and thermoplastic nanocomposite manufacturing [1,6]. However, like any contemporary composite, they are susceptible to damage and defect generation either during their manufacturing or during their practical application. Current techniques, which were developed previously for contemporary composites, can be used for defect characterization and structural health determination, but have numerous drawbacks. They do not provide real-time monitoring, techniques used for monitoring manufacturing parameters cannot be used for structural health monitoring and vice versa, they often rely on capital and technology intensive techniques. Embedded sensors have attempted to solve this task, but their incorporation usually leads to defects generation, stress concentration and subsequent mechanical property loss.

This thesis addresses these technological problems by utilizing carbon nanotube fibers (CNTFs) as embedded electrodes for the dual-stage monitoring of CNT nanocomposites. Here, CNTFs produced through the wet pulling technique, the foundations for which were laid down by the Laboratory of Nanomaterials at Skoltech [7], are applied as a material-based solution for monitoring multifunctional properties directly

linked to defects associated with manufacturing and loss in structural integrity. To verify applicability and feasibility of the novel embedded electrodes, various testing and characterization techniques are utilized. For the manufacturing stage, DC electrical resistance readings are taken of the nanocomposite to determine whether the CNTFs display contact resistance, are sensitive to different types of CNTs, if they are sensitive to the concentration of CNTs within the chosen polymer and if their own diameters and electrical conductivity effect the measurement behavior in a significant way. The CNTFs were not removed after the manufacturing stage and used as electrical connections for monitoring the material during application. Nanocomposites were subjected to uniaxial tensile and cyclic testing, with their electrical properties monitored simultaneously. The testing aimed to substantiate if the CNTFs registered piezoresistive change, if their integration caused any mechanical property loss and if they showed consistent behavior. In both stages, performance was compared to commonly used metallic electrodes, such as surface applied silver paste and embedded metallic electrodes. Finally, a microstructural comparison of samples with various electrodes was conducted to elucidate on the mechanisms of interaction.

Hence, this thesis methodologically explores a new, novel application of CNTFs as multifunctional property-based electrodes which allow material property detection during the entire life of a nanocomposite, beginning from its manufacturing to practical application. The proposed solution for future advanced nanocomposites has benefits over traditional measurement techniques, such as low noise, no mechanical property loss, cost effectiveness and dual stage applicability and performs on par or better than traditionally

used materials. Its applicability, not just for the materials investigated within, but nanomaterials which rely on the same mechanisms of working, make the proposed solution robust and wide-spectrum.

## Chapter 2. Literature Review

### 2.1 Carbon nanotubes

Carbon nanotubes (CNTs) have been reported and investigated since the early 1950s [8,9], with various accounts showcasing what may be carbon nanotubes dating back even further [10,11]. However, large scale studies on carbon nanotubes, their properties and their eventual applications picked up following the famous publication by Iijima [12]. Due to their remarkable inherent thermal, optical and electrical properties [13], CNTs are uniquely suitable for manufacturing advanced composite materials systems [1,3,6], hierarchical material systems made by "top-down" or "down-up" fabrication [14,15] and CNT-based macrostructures such as fibers (CNTFs) [7,16,17]. In both self-conversion and in combination with other materials, CNTs have shown unique properties which have highlighted areas of potential applications, ranging from various types of sensors to complex electronics [18–22].

CNTs owe their inherently unique properties to their electronic structure, where the carbon bonding leads to  $sp^2$  hybridization. This hybrid carbon bond allows properties such as an extremely high Young's modulus and tensile strength, thermal conductivity which is theoretically higher than that of a diamond and extremely high electrical conductivity [23]. These properties have led to their investigation in a variety of applications and fields, some of which have been previously mentioned. In order to better group what range of properties are shown by CNTs, they are generally classified according to two main methods, the first being according to their physical properties and dimensions and the second according to their electronic properties [23,24]. According to physical characteristics, CNTs may be

classified as single-wall (SWCNT), double-wall (DWCNT) or multi-wall (MWCNT) [25]. Length is not chosen as a good display of properties since each type of CNT may be produced in a variety of lengths. An illustration of this type of classification is shown in Figure 1.

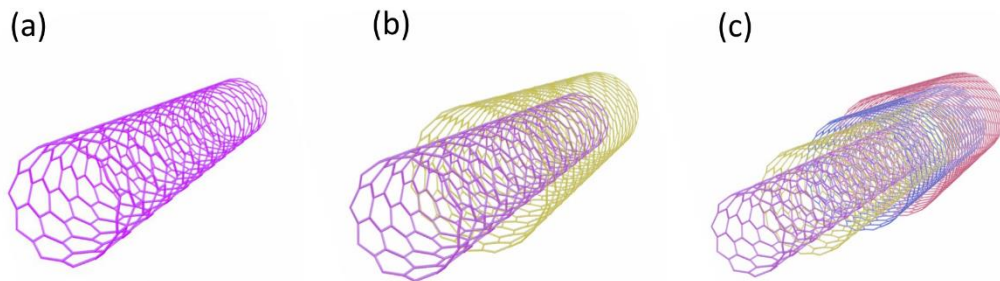


**Figure 1: Schematic representation of (a) single-wall, (b) double-wall and (c) multi-wall CNTs [2].**

The second type of classification which is useful for CNTs is their chirality. Chirality refers to the  $n$  and  $m$  vectors that showcase the degree or type of rolling that a CNT may have, since CNTs may be considered to be rolled up graphene sheets. This chirality is a good measure of whether CNTs may be considered to be metallic or semi-conducting in nature [26]. Metallic CNTs have an electronic structure similar to that of metals, meaning that they do not have a band gap which needs to be surpassed for electrical conduction, whereas semi-conducting CNTs do have such a gap present [26,27]. The chirality is also directly related to CNT diameter, with certain diameters corresponding to certain chiralities and thus certain electrical characteristics.

The characterization of CNTs is important in terms of final properties displayed by the nanocomposites these CNTs are used to manufacture. Through the addition of CNTs

to polymer matrices, the properties of CNTs may be transferred to the nanocomposites, as is further described in the next section. In this thesis, the first type of classification is relied upon, with the study contained within relating final nanocomposite properties with the CNT aspect ratios from SWCNT and MWCNT masterbatches.

## **2.2 Carbon nanotube polymer nanocomposites**

The addition of CNTs to polymers, both thermoset and thermoplastic [1,28], allow the transference of CNT properties to the matrix polymer, resulting in multifunctional CNT-polymer nanocomposites. When coupled with polymers, changes in mechanical behavior [3,4], electrical and thermal conductivity [5,6], piezoresistive response [29,30], corrosion resistance [31] and flame retardancy [32] have been noted, amongst other. When coupled with fiber reinforced polymer matrix composites, the same tendencies are shown [2,33], leading to CNT nanocomposites becoming a prime candidate for next generation multifunctional composite systems [34,35].

For thermoset matrices such as epoxy, the most popular way of inclusion of CNTs in the matrix is through homogeneous dispersion into one of the components, usually being the polymer component and not the hardening component [3,36,37]. This process, commonly known as in-situ polymerization, relies on dispersing the CNTs in the matrix in such a way that the critical percolation threshold is crossed [31], before the addition of the hardening agent which begins the polymerization process. The critical percolation threshold is defined as the least amount of particles required to obtain a functioning percolation network [38]. A percolation network is a series of connections of these particles which allows electric current to flow through either the tunneling mechanism or through

ohmic contacts [39,40]. In the case of CNT/polymer nanocomposites, the percolation is believed to be dependent solely upon the aspect ratio of the reinforcing particles and the matrix is not considered to be contributing in any way to the electrical conductivity [40,41]. A schematic representation of this technique and the resultant percolation network is shown in Figure 2.

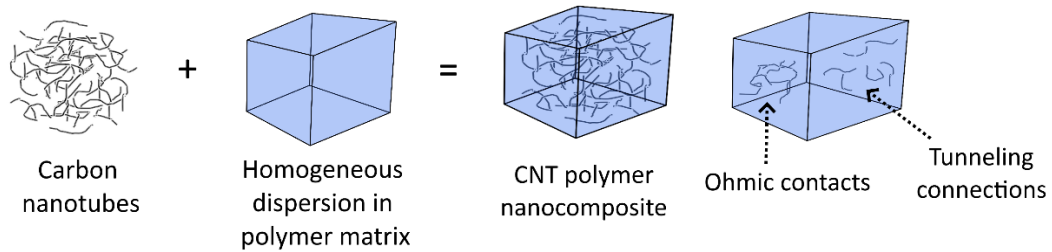


**Figure 2: Schematic representation of homogeneously dispersed CNT polymer nanocomposites**

Carbon nanotubes show poor dispersibility and conflict with conventional production routes for polymer composites [42–44]. Usually produced and shipped as powders, CNTs cause a dramatic viscosity increase when added to polymer matrices, resulting in agglomeration and thus a variety of advanced dispersion techniques being thoroughly investigated throughout literature [38,44,45]. For some functional properties, a degree of agglomeration is shown to be needed [46–48]. When it comes to integration into conventional production techniques for polymer composites, aerosolization of CNT powder limits the effective incorporation of nanotubes into polymer matrices and also poses a significant health risk. This causes the need for specialized safety protocol and handling and monitoring systems, increasing production costs [49–51]. CNT masterbatches (MBs) have become the prevalent strategy for industries working with CNT nanocomposites [3,47,52,53]. Masterbatches can be particularly useful for the large

volume production of such nanocomposites. Masterbatches are concentrates of carbon nanoparticles embedded or pre-mixed in a selected matrix. From an industrial point of view, such masterbatches allow economical integration of advanced materials into existing thermoset/thermoplastic production lines with minimum changes to the manufacturing route. Apart from the manufacturing advantages, the embedded particles have a much lower chance of becoming airborne, presenting no health hazards which have to be counteracted [54].

An area which has attracted particular attention is the field of nanocomposite self-diagnostic sensor materials [3,55]. Through the addition of the carbon nanoparticles to thermoplastic and thermoset matrices, multifunctional nanocomposites can be produced, granted that the electrical percolation limit is reached or surpassed [41,56]. Such nanocomposites are usually piezoresistive, showing a resistance change under certain stimuli such as mechanical force. This property is caused by three main factors: (1) the destruction of the percolation network through reduction of the number of connections between individual particles, (2) deformation of the particles present within the network causing an increase in their intrinsic resistivity due to dimensional change, and (3) change of current flow due to the tunneling mechanism [57,58]. Piezoresistivity based self-diagnostic materials allow measurement of stresses where traditional sensors cannot be used and may help in streamlining designs for a variety of applications.

Since piezoresistive response is often dependent upon factors such as the number of CNTs and their aspect ratios, the relationship between the weight percentage of nanoparticles and the resistivity of nanocomposites (which influences the piezoresistive

response) has well been studied [38,59]. The general trend seen is that the higher the additive percentage of CNTs, the lower the resistivity and piezoresistive response [3,29,60,61]. Lower concentrations of CNT's, nearing the percolation threshold, result in a higher piezoresistive response due to a weaker percolation network.

CNT nanocomposites are susceptible to defect generation either during their manufacturing [62,63] or usage lifecycle [64,65]. With the inclusion of CNTs, manufacturing defects for such materials increase to include mechanisms such as nanoparticle filtration, dead spaces due to increases in viscosity as well as a lowered degree of polymer curing [28,66]. Identifying such defects with commonly used technological solutions such as visual, acoustic, infrared, ultrasonic and x-ray inspection as well as online FTIR, NMR, DSC and TGA are often time and resource consuming, infeasible for a complete picture in their singularity, and are not representative of the entire part being manufactured [67,68]. Furthermore, most techniques for manufacturing defect detection and post-manufacturing defect development cannot be integrated to provide information for both stages. To address such issues, recent studies have focused on the usage of embeddable sensor systems which have the benefit of providing real time information during the manufacturing of composites regarding matrix properties and changes [69–71]. An added benefit of such sensors is that they offer a one-step sensor solution as they may double as sensors for the lifecycle structural health monitoring of the composite parts, without the need for removal or alteration. Although such technology has promising potential, the application of such sensors within composites and composite structures may alter their mechanical behavior [72–74]. In addition to this, the issue of nanoparticle

filtration, present within major forms of composite manufacturing used for nanocomposite production, is still an avenue which has not been researched in detail when combined with embeddable sensors [75].

Embeddable sensor technology for composite monitoring has employed, but is not limited to, the use of fiber optics [76], piezoelectric/piezoresistive materials [77], dielectric [78], acoustic [74] as well as electromagnetic materials and sensors [79]. For fiber optic-based sensors, successful application has allowed both manufacturing variable [80] and post-manufacturing structural health monitoring [81]. However, such sensor systems rely on the need for an additional optics systems, associated equipment, and face hinderance with CNT nanocomposites where the transmittance properties of the base material deteriorate with nanoparticle addition [82]. Piezoelectric and piezoresistive sensors and patches have also shown to be usable for monitoring both stages, but their dimensions, coupled with the electric wiring needed for their operation, causes regions of inhomogeneity within the composite [83]. Dielectric, acoustic and electromagnetic patches and sensors also have the same drawback, with their inclusion and wiring resulting in areas where composite failure might originate [78,84].

Hence, this thesis aims to address the issues, identified above, for CNT nanocomposites manufactured from masterbatches with embedded CNTFs electrodes capable of monitoring multifunctional properties and identifying defects, all while causing no loss in mechanical performance of the host material.

### **2.3 Carbon nanotube fibers**

CNTFs are fiber-shaped macro structures developed from the assembly of CNTs and have in themselves proven to show exceptional flexibility combined with electrical, thermal, mechanical and piezoresistive properties [7,85]. CNTFs may be produced through both wet and dry techniques [86,87], allowing specific tailoring of properties and performance through changes in density, porosity and surface morphology. Dry methods are characterized by the lack of liquid solvent or dispersant required during manufacturing, and they are usually created directly from a CNT aerosol or from other nanotube assemblies (film or forest) to obtain CNTFs [7]. Wet techniques entail the usage of liquid phases, usually a crystalline phase of CNTs in a superacid or production from a nanotube dispersion [86]. Both methods require specialized equipment and specific chemicals. Compared to these, the wet pulling method provides a novel yet simple methodology for manufacturing CNTFs from CNT thin films. It combines the surface tension of a wetting agent with directional pulling to ensure consolidation of a CNT film into a CNTF [7,85,88]. The electrical behavior of the CNTFs produced through the wet pulling method from SWCNT thin films is comparable with the values achieved by wet or dry spinning [85,89–94] and Figure 3 provides a visual example for CNTFs.

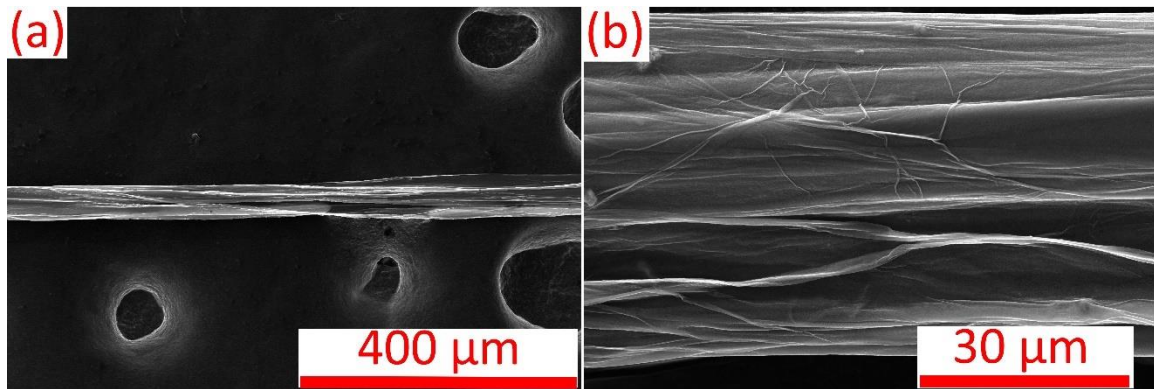


Figure 3: SEM images of a CNTF at (a) 500X and (b) 5000x

Carbon nanotube fibers (CNTFs) may offer a mechanically non-invasive solution for the embedded monitoring of advanced thermoset nanocomposites. In previous studies where CNTFs were applied for the manufacturing stage monitoring of resins and composites, they have shown to be sensitive to thermoset resin changes and chemical reagent concentrations [95]. The porosity and flexibility of the CNTFs allows infiltration of the resin into the fiber, resulting in distinct piezoresistive changes during each of the various stages of polymer reaction and solidification. The same piezoresistive principle is used for their application in structural health monitoring during composite usage, with the application of stress and strain causing changes in the number of connections between the CNTs which make up the CNTF, resulting in accurate sensors which can detect material health status and damage [96].

Some works have investigated using CNTFs as embedded sensors for fiber reinforced or unaltered polymer composites. They have studied both the manufacturing and lifecycle stages of such materials, but separately. No scientific work, to the best of the author's knowledge, has addressed their feasibility for monitoring multifunctional nanocomposites and their properties such as electrical conductivity and piezoresistive

response, especially those incorporating CNTs in the polymer matrix. To add, CNTFs have not been investigated for the possibility of offering a material-based sensing solution for detecting different concentrations of conductive nanoparticles, which may allow the filtration effect to be identified during manufacturing. CNTFs based on single-walled carbon nanotubes (SWCNTs) are extremely rare in literature, with the majority of fibers being produced using multi-walled carbon nanotubes (MWCNTs), leading to no literature showing their applications for multifunctional property detection. Finally, combining these diverse properties into a single embedded electrode system which performs these functions both during the manufacturing of CNT thermoset nanocomposites as well as during their usage without causing any mechanical property loss has not been investigated or reported.

Hence, to experimentally verify the feasibility of CNTFs as mechanically non-invasive functional property detecting electrodes, this thesis creates a hierarchical nanocomposite which utilizes CNTs as the matrix filling material for providing multifunctional properties and CNTFs as the mechanically non-invasive electrodes. The CNTFs, produced through the wet pulling technique utilizing SWCNT thin films, are studied for their feasibility of functional property monitoring, their sensitivity to MWCNTs and SWCNTs concentrations in the matrix, the effect that CNTF dimensions may have on detection performance and these properties are then compared to the standard methods employed in scientific works for a comparative analysis. The work not only shows that the one-step embeddable CNTFs perform as good as the currently utilized standard techniques, and in some cases higher, but identifies the mechanism of interaction between CNTFs and dispersed CNTs within the thermoset matrix, an area of research which currently has not

been reported on. The work is also the first to show the feasibility of the wet pulling technique and SWCNT-based CNTFs for manufacturing defect and post-manufacturing structural health monitoring and aims to pave the way for the use of CNTFs as novel electrodes for CNT-based multifunctional nanocomposite property detection.

## **Chapter 3. Materials and Methods**

### **3.1 Methodology and characterization**

As described above, this thesis required the production of two separate materials, which were then integrated together. The first is the thermoset nanocomposite which is intended to be measured for multifunctional properties, both during the manufacturing process and after. The second are the novel CNTF electrodes which are embedded into the nanocomposite during the manufacturing stage to measure the properties without affecting the final mechanical performance. Once the multifunctional nanocomposites were produced with the various electrode systems, they were tested for their electrical, mechanical and piezoresistive properties and a comparison between their performance was conducted.

Prior to CNTF fabrication, the SWCNT thin films were checked for their thickness, G/D ratio and sheet resistance using a Perkin Elmer Lambda 1050 UV-vis-NIR spectrometer, a ThermoScientific DXRxi Raman Imaging microscope, and a Jandal 4-point probe RM3000, respectively. CNTFs were characterized for their diameters and electrical resistance values using a Keithley multimeter and Leica DM4500 optical microscope. Masterbatches used for manufacturing nanocomposites were characterized at the manufacturer, and data sheets were provided. After nanocomposite production with embedded electrodes, electrical and piezoresistive properties were measured using a Keithley multimeter combined with an Instron 5969 and Instron Electropuls 3000. After mechanical testing, samples were visually inspected at sites of breakage, followed by SEM

visualization using a Helios G4 PFIB. Exact details for these techniques are included in the following sections describing the materials.

### 3.2 Precursor materials

In this thesis, two types of CNTs were used to manufacture the epoxy matrix nanocomposites. For health and safety reasons, and to make the thesis more geared towards materials which may be used in industrial settings, commercial masterbatches were used for nanocomposite manufacturing. The details of the CNTs used to manufacture the commercial masterbatches have been compiled in Table 1.

**Table 1: Commercial masterbatches used to manufacturing epoxy matrix nanocomposites**

Designation	Additive type	Aspect Ratio	Manufacturing
MW*	MWCNT	~6-1000	Twin screw extrusion
SW*	SWCNT	~ 2500-3000	Three-roll milling.

\*Note: Masterbatch producers are OCSiAl (SWCNT) and Graphistrength (MWCNT)

The masterbatches used were commercially purchased (SWCNTs-Tuball 301, OCSiAl, Russia, MWCNTs - Graphistrength C S1-25, Arkema, France) and used as received. The manufacturer data sheets of the SWCNT masterbatch showed the diameter to be  $1.6 \pm 0.4$  nm with a mean length of  $> 5$   $\mu$ m and the estimated aspect ratio of the SWCNTs is about 3000. For the MWCNT masterbatch, the manufacturer data sheets showed the diameter to be between 10-15 nm, while the length was stated to be 0.1-10  $\mu$ m, putting the aspect ratio between 6-1000. A bis-a-phenol/DGEBA epoxy resin (EPOLAM 2031, Axon, France), which is chemically the same as the matrix used for masterbatch production, was utilized as the matrix in this study. Nanocomposites were manufactured by adding CNTs to the epoxy matrix through an optimized, standardized processing route

based on both ultrasonication and high-speed homogenization, described further on in this thesis.

SWCNT thin films were used to fabricate CNTFs through the wet pulling technique. The CNTs had an average length of 20-40  $\mu\text{m}$  and an average diameter of 2.1 nm [97]. The films were synthesized by an aerosol (floating catalyst) chemical vapor deposition (CVD) technique described previously [98]. As shown in previous work, the thickness of the films used to fabricate the CNTFs have an effect on their final structure and conductivity [7,85]. Thus, the highest available thickness of 60% transmittance were used for CNTF production. Film G/D ratio was measured using a ThermoScientific DXRxi Raman Imaging microscope, thickness was calculated using a Perkin Elmer Lambda 1050 UV-vis-NIR spectrometer [99] and sheet resistance was measured using a Jandal 4-point probe RM3000. The measured G/D ratio was  $\sim 37$ , the thickness corresponded to  $\sim 53$  nm and the sheet resistance measured was  $48 \Omega/\text{sq}$ .

### **3.3 Carbon nanotube fiber fabrication**

CNTFs were produced from these thin films using the wet-pulling technique, which involves the dry transfer of CNT thin films to a substrate, their wetting with a solvent which aids in densification and subsequent mechanical pulling which converts the films into fibers as they wrap around themselves during the pulling procedure. The fabrication procedure has been detailed in previous works [7,85,88]. To summarize the method, the process may be broken down into 3 main steps, and has been schematically represented in Figure 4. In step (1), CNT thin films are transferred from the cellulose filter onto a glass slide by dry transfer technique. Step (2) includes wetting this thin film with a few drops of

solvent. In step (3), the film is held with tweezers and then pulled in one direction causing the film to fold and wrap into a CNTF. The described method of CNTF fabrication is based on the effect of solvent evaporation and CNT film folding due to surface tension. In this work, ethanol was used as the wetting and densification solvent. Once the fibers were produced, they were placed on glass substrates, with their ends fixed to the substrate using conductive silver glue. Their dimensions were measured using an optical microscope and their electrical resistance values noted using a Keithley multimeter. Their conductivity was calculated using the standard formula for the resistivity of solids, which was inversed to obtain the conductivity value [88].

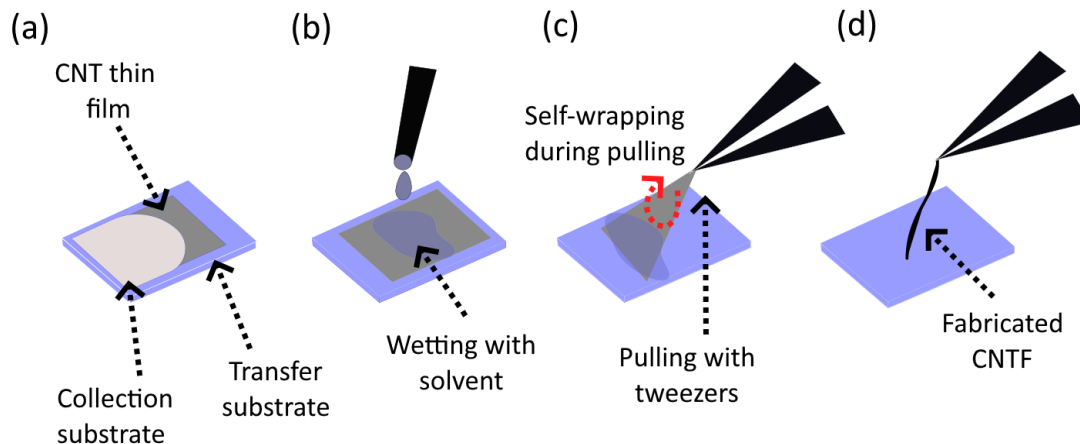


**Figure 4: Representation of the wet-pulling technique; steps (a-c) show the 3 steps and (d) shows the fabricated CNTF.**

### 3.4 Carbon nanotube nanocomposite manufacturing

The thermoset nanocomposites were produced using a standardized manufacturing route, outlined in Figure 5, using a combination of ultrasonication and high-speed shear mixing. In the first stage, the correct amount of masterbatch was weighed according to the

intended final weight percentage of the nanocomposite. For example, for a 100g nanocomposite batch of 0.25% wt. MWCNTs, 1g of masterbatch (25% wt. by manufacturer) was used. This amount was then soaked in 5 ml of acetone overnight to ensure that the dense masterbatch could disperse during the following processing stages. The soaked masterbatch was then subjected to ultrasonication in an ultrasonic bath for 30 minutes to help soften the masterbatches and create a pre-dispersion. Once this was completed, a weighed amount of thermoset resin, without the associated hardener, was added and the mixture was then shear mixed using an IKA T-25 Ultra Turrax homogenizer. The mixture was first homogenized at the lowest RPM of 3200 for 3 minutes, followed by mixing at 7500 RPM for 45 minutes and finally at 10,000 RPM for 15 minutes. Once the homogenizing step was completed, the mixture was then ultrasonicated for a second time for 1 hour to help improve dispersion while degassing the mixture. Following this, the mixture was placed in a vacuum chamber and degassed for 30 minutes before the weighed amount of hardener was added. The mixture was then slowly hand mixed for 10 minutes, followed by a second degassing step of 10 minutes. Finally, the nanocomposite mixture was then taken and hand poured into silicon molds corresponding to ISO 527. Samples were cured at room temperature for 24 hours before being post-cured at 60 degrees for 12 hours in a laboratory oven. Sample dimensions were as follows: an overall length of 170 mm, a gauge length of 75 mm and a thickness of 3.6-4.1 mm. These samples were created in groups, herewith referred to as batches. Equipment limitations allowed a maximum amount of material worth 5 samples to be processed using this route. Hence, each group or batch or material was used for one type of electrode system. Different electrode systems

were made from different batches which may lead to a batch to batch nanocomposite property variance.

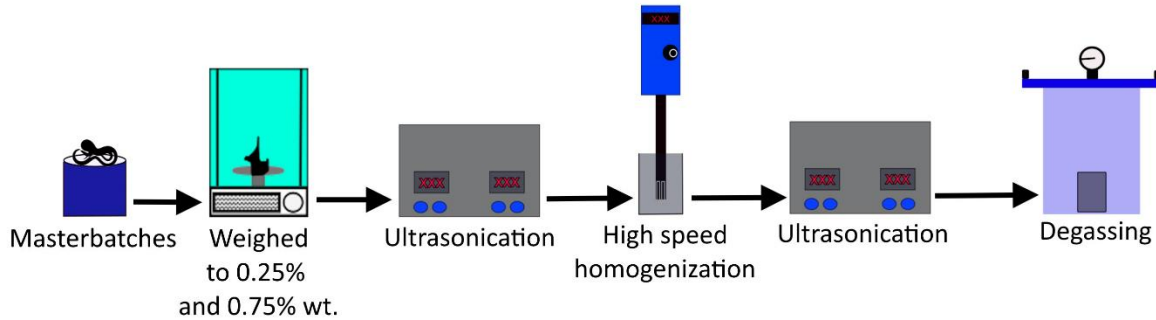


**Figure 5: The various steps of nanocomposite processing**

### **3.5 Material selection and optimization**

As part of this thesis, it was important during initial material selection to choose CNTF and CNT forms which would best represent materials in literature as well elucidate on the mechanisms of their interaction when combined together. Hence, techniques were explored to determine if CNT and CNTF optimization could be conducted before nanocomposite production and CNTF integration. For CNT optimization for nanocomposite production, CNT powders were subjected to compression and expansion to produce powders with different bulk densities. These were then used to produce CNT nanocomposites, as described further, and their properties compared to nanocomposites produced with masterbatches. This phase of the investigation provided information regarding what bulk CNT form to use for further experiments, what the electrical conductivity trends of the CNT nanocomposites are and if any differences in functional properties was present.

For CNTF optimization, mechanical densification applied after initial fabrication was applied to increase CNTF density, electrical conductivity and reduce surface and volume porosity. This process led to an electrical performance increase and reduction in defects and the mechanism of this improvement was identified.

### ***3.5.1 Carbon nanotube fiber density alteration***

CNTFs were subjected to physical twisting for additional densification and the procedure begins by placing the two ends of the free-standing fibers in a custom-made twisting machine. Control of the twisting degree was performed by counting the twist number where one twist is equal to one full 360-degree rotation. An ethanol reservoir was placed directly beneath the middle section of the fiber. Twisting was conducted in steps of 25 twists (*i.e.*, 25, 50, 75, *etc.*) until the density, calculated through the fiber diameter and verified by optical microscopy, was as near to the theoretical maximum limit as possible (120). It was noticed that after 120 twists, CNTFs with a length of ~2 cm break immediately and further processing was infeasible. Schematic illustration of the process has been shown in Figure 6. SEM was used to visualize surface and volume microstructural changes. This particular technique was chosen instead of alternative options because it has previously been reported by the laboratory where this work was conducted [7,85], provided a facile route for initial investigations and did not chemically alter the CNTF as with chemical based techniques [87].

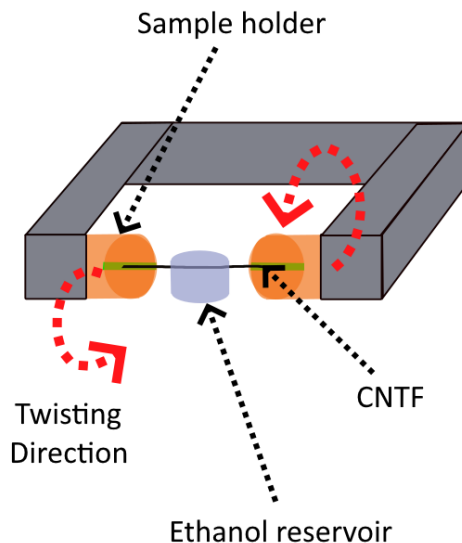


**Figure 6: Schematic diagram for the twisting procedure**

During the twisting procedure the CNTF edges spin at the point of being held, causing the rest of the CNTF to twist, overlap and wrap around itself. The process causes a transmittance of compressional force onto the length of the CNTF, which eventually causes a decrease in fiber diameter. This decrease in diameter caused by compression in turn causes the voids and defects of the CNTF to be removed by essentially pressing the fiber material together. The technique has been detailed in previous works by this laboratory [85] as well as others for CNTF production and densification [100].

### **3.5.2 Bulk density alteration of CNTs**

Four types of SWCNT forms were used to determine the effect that different bulk densification states may have on nanocomposite properties. The details of the additives have been compiled in Table 2 and illustratively shown in Figure 7. A bulk density range of more than two orders of magnitude is studied and weight percentages investigated included 0.005, 0.01, 0.05, 0.1, 0.25, 0.5, 1.0 and 2.0 wt.%.

**Table 2 Designations and parameters of the SWCNT additives. The same designations are assigned to the nanocomposites produced from the respective additives.**

Designation	Powder type	Bulk density (g/l)	Specific surface area (m <sup>2</sup> /g)	I <sub>G</sub> /I <sub>D</sub> **	Manufacturing
Briquettes	Consolidated	450	570	70 ± 40	Commercial powder subjected to compression.
MB	Masterbatches	~ 97*	-	-	Commercial masterbatch, produced through three-roll milling.
Pristine	Unaltered	18	580	80 ± 20	Commercial powder, no pre-dispersion.
RESS	RESS-expanded	1.6	560	70 ± 10	Commercial powder subjected to RESS.

\* bulk density of SWCNTs within the masterbatch is estimated considering the density of the material (0.97 g/cm<sup>3</sup>) and weight concentration of SWCNTs (10 wt.%).

\*\*I<sub>G</sub>/I<sub>D</sub> refers the reciprocal defect concentration within SWCNT

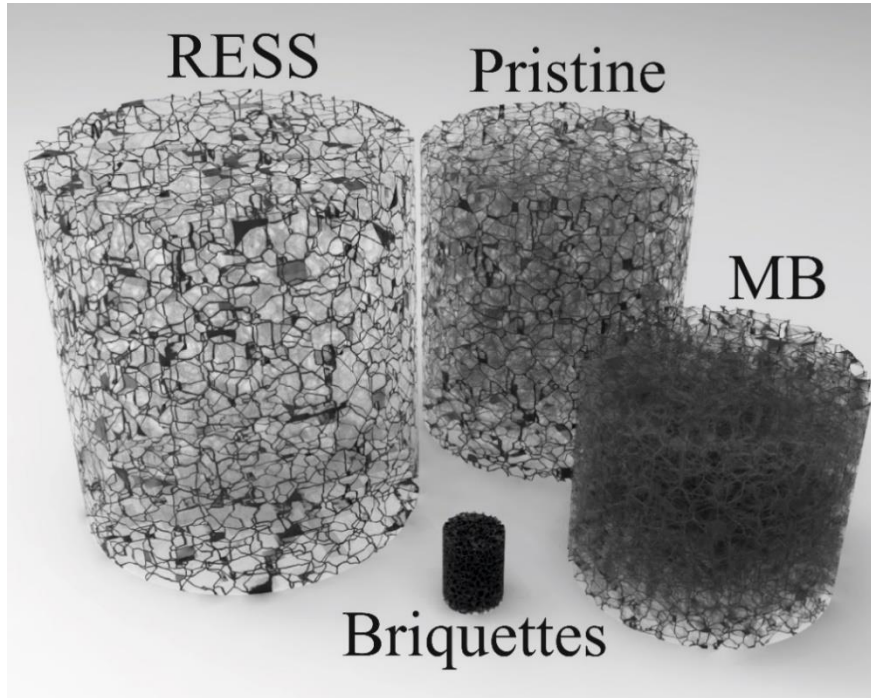


**Figure 7: Illustrative representation of the bulk density difference between the SWCNTs used showing the cylinders of the same mass.**

The masterbatch, described previously, was used as the reference to determine whether it would be suitable for further study. The RESS and briquette type powders were manufactured from pristine SWCNT powder from the same manufacturer (OCSiAl, Russia). The manufacturer data sheets of the SWCNT powder showed the diameter to be  $1.6 \pm 0.4$  nm with a mean length of  $> 5$   $\mu\text{m}$ . The estimated aspect ratio of the SWCNTs is about 3000 [101].

Briquette type powders were manufactured through the pneumatic compression (Allied High Tech Products, USA) of pristine powders at 6 atm without any heating. Powders were held at this pressure for a 5-minute period before being removed in the briquette form. RESS powder was manufactured according to a previously described method [99, 100]. Briefly, SWCNT powder was placed in a high-pressure vessel (volume is 25 ml) and then exposed to supercritical fluid (nitrogen, 150 atm, 40 °C) for 30 min. Next, this supercritical suspension was injected into a larger vessel (500 ml) kept at ambient conditions. Due to the high difference in pressures, rapid expansion of the suspension took place, leading to an intensive decrease in bulk density of the SWCNTs (11 times) along with de-bundling [102].

Scanning electron microscopy (SEM) and transmission electron microscopy (TEM) was conducted to determine whether the SWCNTs showed any differences in microstructural evolution during powder and nanocomposite manufacturing for the alternative SWCNT types. The findings were correlated to electrical performance and the nanocomposites were manufactured with the thermoset matrix using the processing route previously described. To properly visualize the internal volume and to avoid excessive

plastic deformation and associated CNT pullout for the nanocomposites, samples were frozen in liquid nitrogen for 15 min before being broken to obtain a fracture surface which was used for observations.

### **3.6 Nanocomposite fabrication with embedded electrodes**

For manufacturing samples with embedded and surface applied electrodes, the metallic and CNTF-based electrodes were carefully placed in the gauge length of the sample molds prior to nanocomposite molding, at a distance of 5 mm from each other. 2 and 4 electrodes were embedded within the samples to allow a comparison between measurements from the two techniques. Copper wiring, with a diameter of 100 – 150  $\mu\text{m}$ , was used to make the metallic embedded electrodes since wiring of a smaller caliber was difficult to manipulate and broke during the demolding process and additional wiring attachment. Such wiring is common for multifunctional nanocomposites [103] and was chosen based on two principles. The first being that such wiring is already used in the case of multifunctional composites, either as part of a sensing system, as the contacts for sensing themselves or as part of a system to impart multifunctional properties. Secondly, the dimensions of the electrodes were chosen to be similar to the diameters shown by the CNTFs, to remove ambiguity regarding the effect on mechanical properties. Samples with externally applied silver glue-based electrodes, as is common in literature with multifunctional nanocomposites [104–106], followed the same design principle with lines of the silver glue being made on the sample surfaces in the same region all along the sample periphery. Schematic representations of the sample types have been shown in Figure 8.

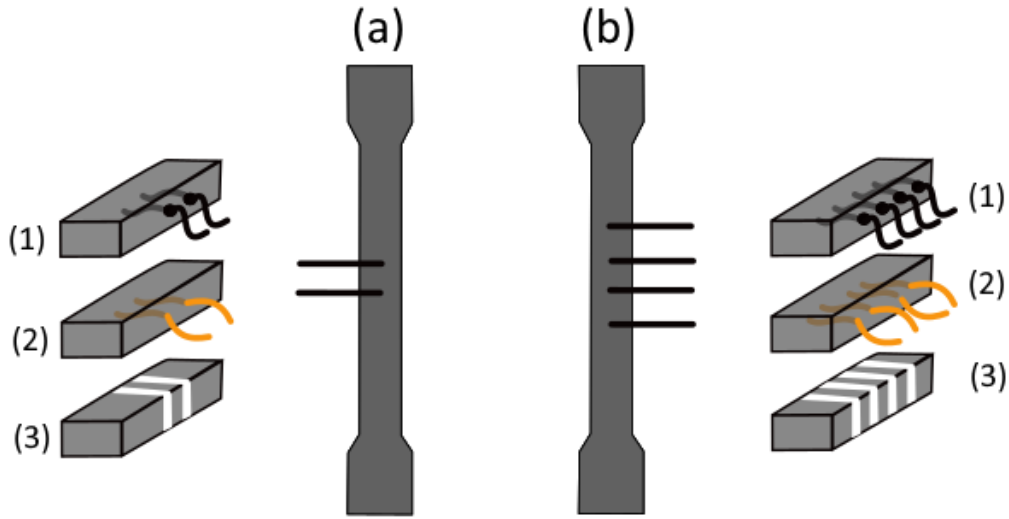


**Figure 8: (a) 2- and (b) 4-point sample schematics. (1,2,3) show the embedded CNTF, metallic and surface silver electrodes side view, respectively.**

After sample fabrication, samples were first tested for their electrical resistivity using the embedded and surface applied electrodes. Nanocomposite electrical resistivity was calculated using the same method used for CNTF electrical conductivity. The piezoresistive response of the samples was measured under two conditions, the first being uniaxial tensile loading and the second being uniaxial cyclic loading. For piezoresistive measurements, the resistance of the samples and its change was measured during mechanical loading by attaching the embedded electrodes to a Keithley multimeter. The gauge factor (GF) of the samples was calculated using the following equation, where  $R$  is the resistance value measured,  $R_0$  is the initial resistance of the sample and  $\epsilon$  is the strain:

$$GF = \frac{\frac{R-R_0}{R_0}}{\epsilon} \quad (1)$$

Tensile loading was carried out with a traverse head speed of 1mm/min on an Instron 5969 universal testing machine. Strain measurements were made using a digital

image correlation system (DIC), LIMESS (Correlated Solutions, USA). 5-megapixel cameras were used for image capturing and VIC-3D software was used for calculating strain. DIC was employed since it did not interfere with electrode placement in the gauge length of the samples and helped avoid anomalous material behavior [3]. The mechanical properties of interest that were measured were the ultimate tensile strength (UTS), Young's modulus and Poisson ratio. The UTS represents the maximum stress sustained by the material before failure, the Young's modulus is a measure of material stiffness and the Poisson ratio is the ratio of transverse to axial deformation during tensile loading. The UTS was calculated using the Bluehill software which is native to the Instron 5969. The Young's modulus was calculated using the stress to strain ratio in the elastic deformation range of the samples. The Poisson ratio was calculated using the VIC-3D software using two digital extensometers (one vertical and one horizontal) placed in the captured images during processing.

The cyclic loading was carried out using a modified version of ISO 13003, a modified ISO 527 tensile testing method, which is an approach commonly employed for measuring cyclic uniaxial loading [107]. This was done on an Instron Electropulse 3000 at 10 Hz at 60% of the UTS measured during the tensile testing. This value was chosen as (1) it is considered high for the cyclic testing of polymers and (2) the higher the stress load, the greater the chance of sample breakage at sites of inclusions and defects, allowing a comparison of whether the embedded electrodes negatively affected the mechanical properties of the multifunctional nanocomposite. After mechanical testing, samples were visually inspected at sites of breakage, followed by SEM visualization using a Helios G4

PFIB. All experiments and characterizations were conducted at ambient room conditions (temperature between 22-25 °C and humidity between 30-50%).

## **Chapter 4. Nanocomposites with embedded electrodes**

### **4.1 Material selection and optimization**

As previously stated, initial experimentation varied CNT and CNTF bulk density to determine which material states may be best for the investigation of their interaction. The wet pulling technique is a manual procedure for CNTF fabrication and factors such as pulling speed, angle and adhesion to the transfer substrate all impact the film folding and densification process during solvent evaporation. This, in turn affects the morphology and, as a result, the electrical performance of the produced fibers. Hence, mechanical densification through a twisting procedure was investigated to determine if it may produce CNTFs conducive to the thesis objectives.

CNTFs which underwent twisting in a wet state do not possess visible surface defects and the required degree of porosity, neither when visualized from the side view or at the cross-section, proving that such defects as well as macro voids and holes are almost eliminated by the twisting procedure. These fibers also showed the smallest diameter variability, indicating that the process indeed led to greater densification and tighter fiber packing. Visual comparisons of these fibers made with SEM are shown in Figure 9.

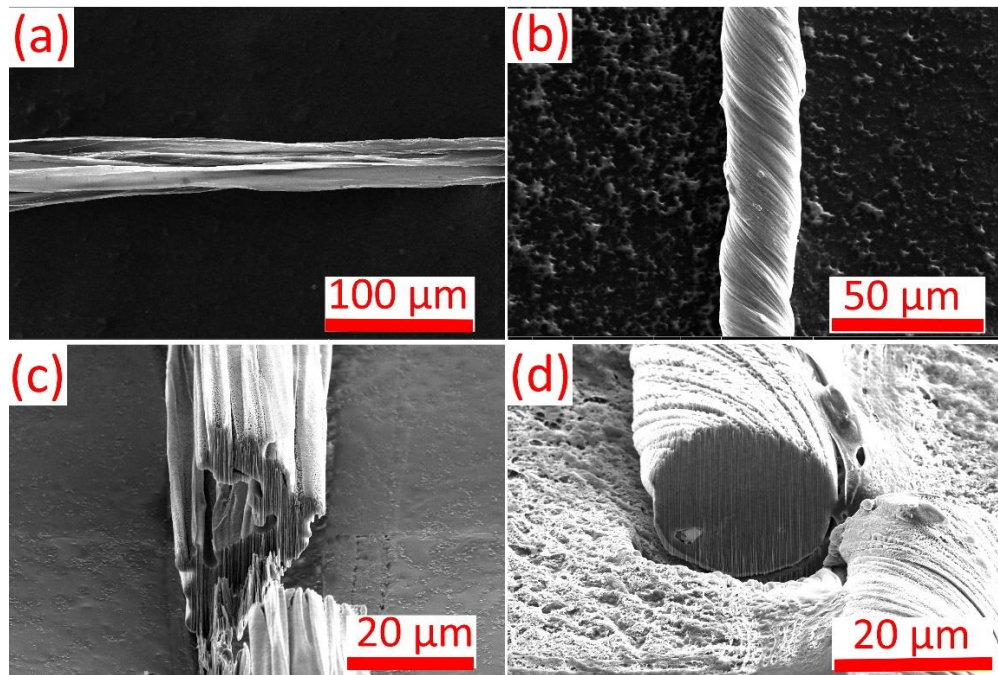


**Figure 9: SEM comparison of (a,c) as-produced CTNFs and (b,d) twisted CNTFs. Note the reduction in surface defects and surface and volume porosity.**

Although morphological improvements were noted, the directly measured electrical resistance of these twisted fibers tended to increase as the twisting number increased, while the amount of defects and porosity decreased. The densification procedure was seen to produce almost ideal, circular cross-section shaped fibers with smaller diameters. Counterintuitively, this was due to the cross-sectional area which resulted in a lower calculated resistivity.

When considering the changes brought about using this technique, and the fact that defects decreased while measured resistance values increased, the changes and their effects on electrical performance were not straightforward. Combined with the fact that the technological process involved was intensive and not scalable, the process and changes were deemed unfavorable. Further, when the microstructure is analyzed, it can be seen that

the surface porosity of the fibers and the canyon like areas decreases, which would result in a theoretically lower surface area for contact with the carbon nanotubes within the nano-reinforced matrix system. These factors led to the twisting of fibers not being investigated further for nano-reinforced matrix system embedding.

CNT bulk density alteration was also investigated for the same purpose. Surprisingly, the microstructure of SWNCTs of different bulk density powders in SEM and TEM images do not indicate considerable changes, as seen in Figure 10 and 11. Slight differences can be noticed at the lowest magnification where agglomerates of several hundred microns are present in pristine and high density SWCNTs while RESS SWCNTs possess a rather fibrous structure. Nonetheless, at higher magnifications where SWCNT bundles are already distinguishable, no significant changes in morphology after both the RESS and compression pre-processing procedures were noted. In each case, SWCNT bundles form an entangled network with apparently equal density. TEM images, usually used for bundling degree estimation [108], do not demonstrate noticeable differences between nanotubes of different types as well. Thick bundles of 10–20 nm (corresponding to 5–15 nanotubes per bundle) are characteristic to each SWCNT types. Thus, electron microscopy of the powders did not indicate crucial differences in the SWCNTs of different bulk densities. This allowed understanding that the masterbatches used for nanocomposite fabrication would perform the same as other CNT types, allowing the results of the microstructural and electrical investigation to be universally applicable.

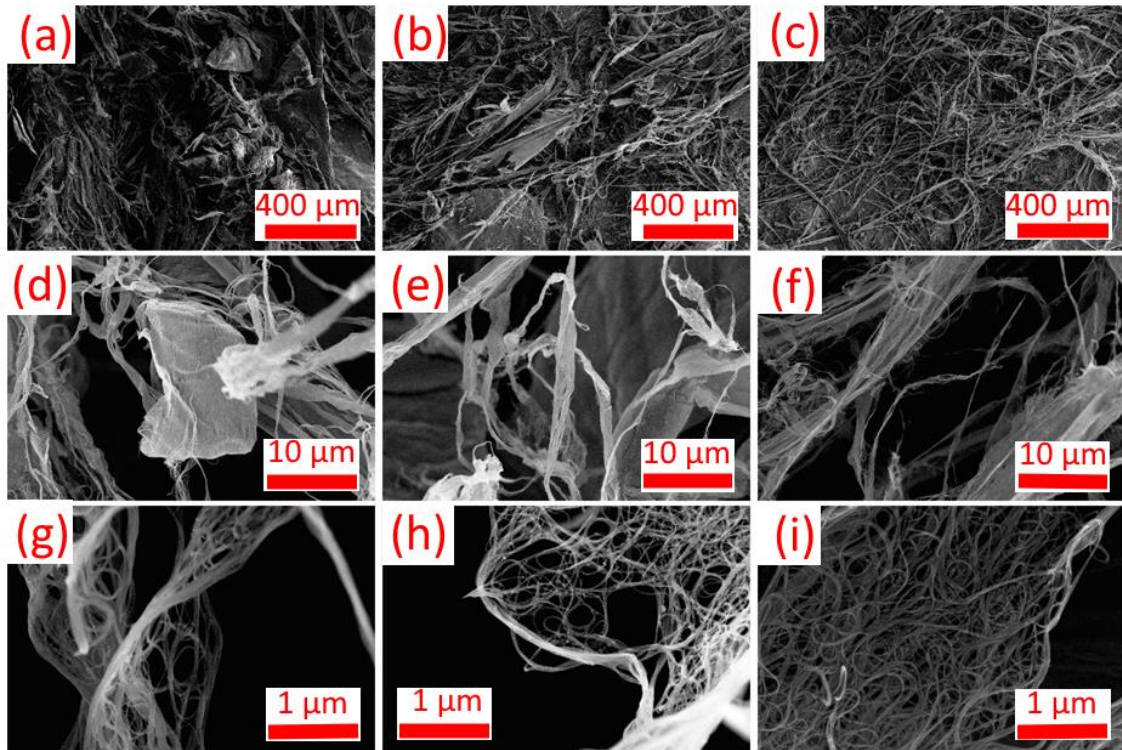


**Figure 10: SEM images of the SWCNT powders of different types: (a) briquette, (b) pristine, (c) RESS at 250x. The sample samples are examined at (d-f) 10,000x and (g-i) 100,000x, respectively.**

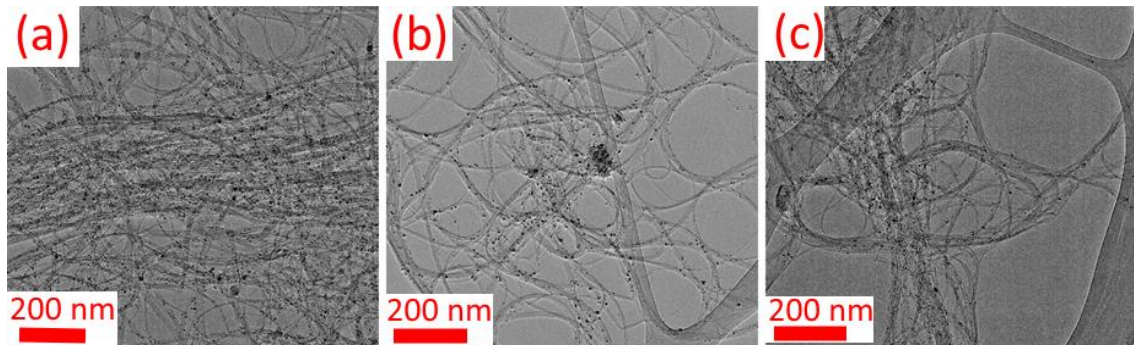


**Figure 11: TEM images of the SWCNTs of different types: (a) briquette, (b) pristine, (c) RESS.**

SEM analysis was conducted on the fracture surfaces of the nanocomposites at weight concentrations of 0.005, 0.05, 0.25 and 1.0 wt. % to ascertain differences in dispersion degree and microstructure caused by differences in densities, which could lead to a difference in electrical and piezoresistive properties. These percentages were chosen to allow for visible differences in microstructural development. At the lowest concentration

of 0.005 wt. %, the microstructure of the masterbatch-based nanocomposites is indistinguishable from the other three types. Agglomerates for all types resembled bundles or groups of bundles of SWCNTs, widely spaced between large swathes of plain epoxy. At a higher magnification, masterbatch based samples showed a microstructure with groups of bundles interconnected in regions of high CNT concentration and is known to be caused by regions of high viscosity during the fabrication process and may be the result of variances during the manufacturing procedure [44,109,110]. With higher SWCNT loadings, the composites show the formation of an interconnected nanotube system with only minor discrepancies in morphology between consolidation degrees. SEM images showing these findings have been compiled in Figures 12-15.

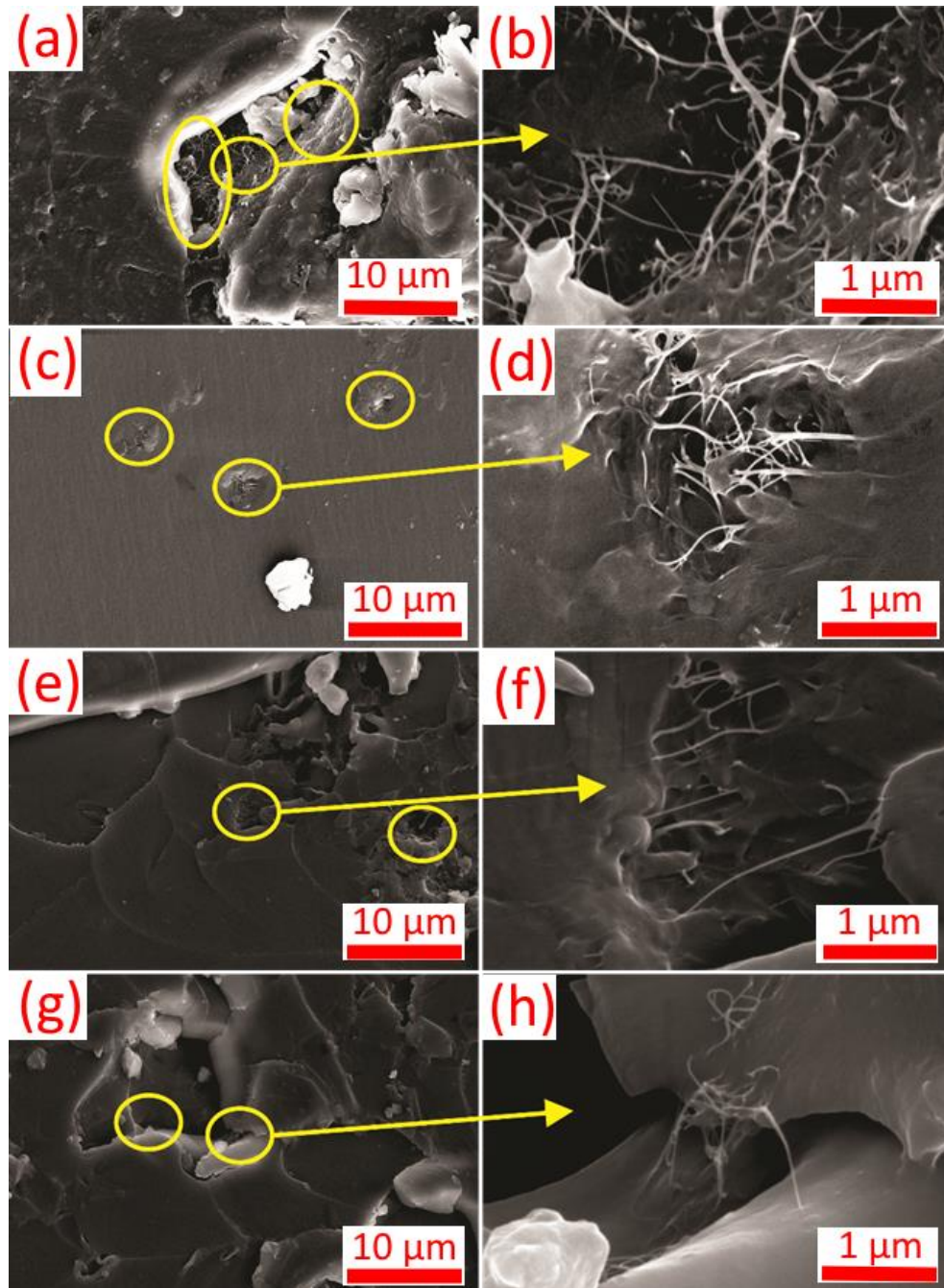


**Figure 12: SEM images for 0.005 wt. % (10,000x) for (a) briquette, (b) masterbatch, (c) pristine and (d) RESS SWCNT nanocomposites; (b,d,f,h) SEM images of the same nanocomposites taken at higher magnification, respectively (100,000x)**

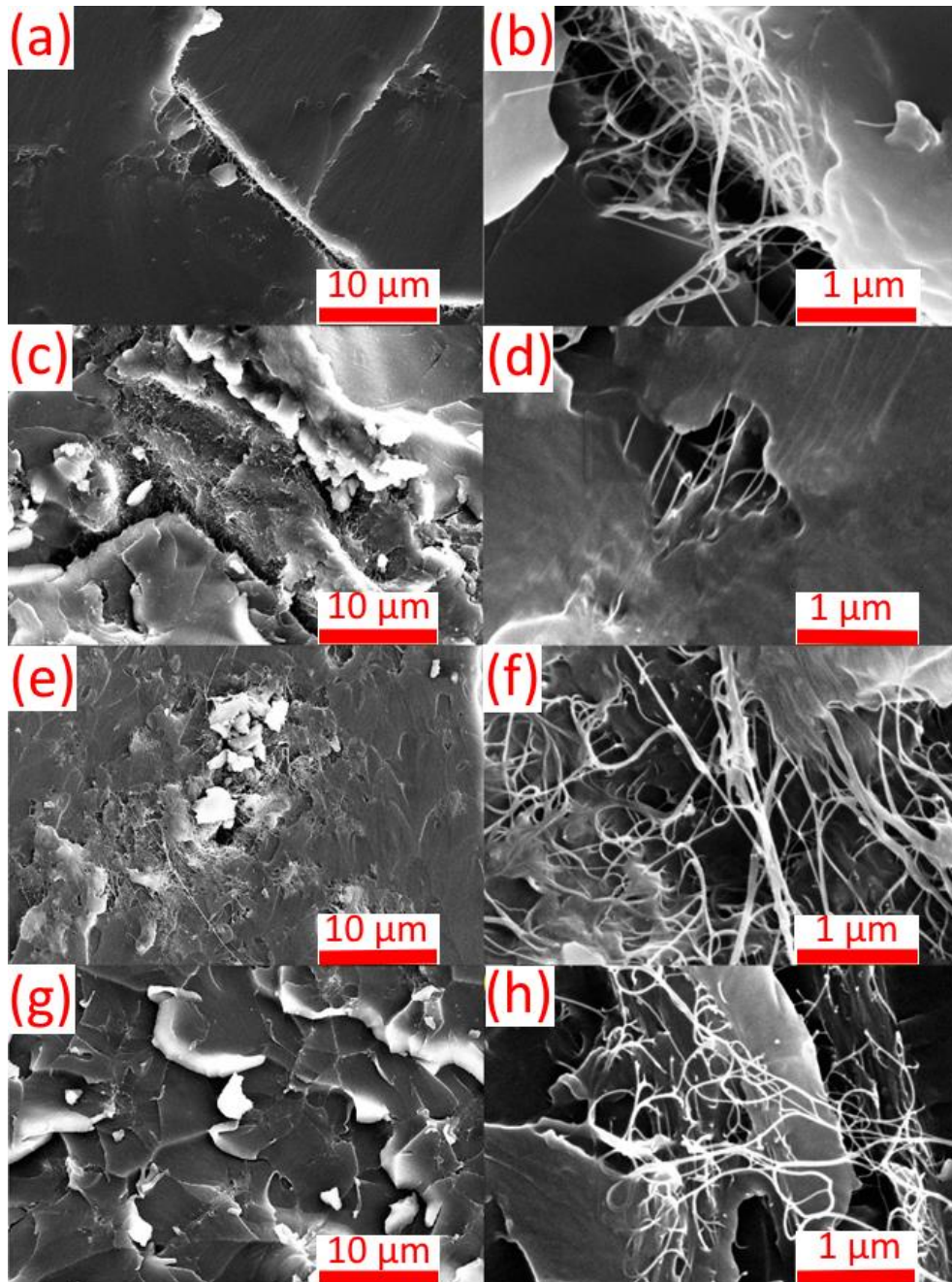


**Figure 13: SEM images of Briquettes (A,B), Masterbatch (C,D), Pristine (E,F) and RESS (G,H) nanocomposites at 0.05% wt. Images A,C,E and G are taken at 10,000x while images B,D,F and H are taken at 100,000x**

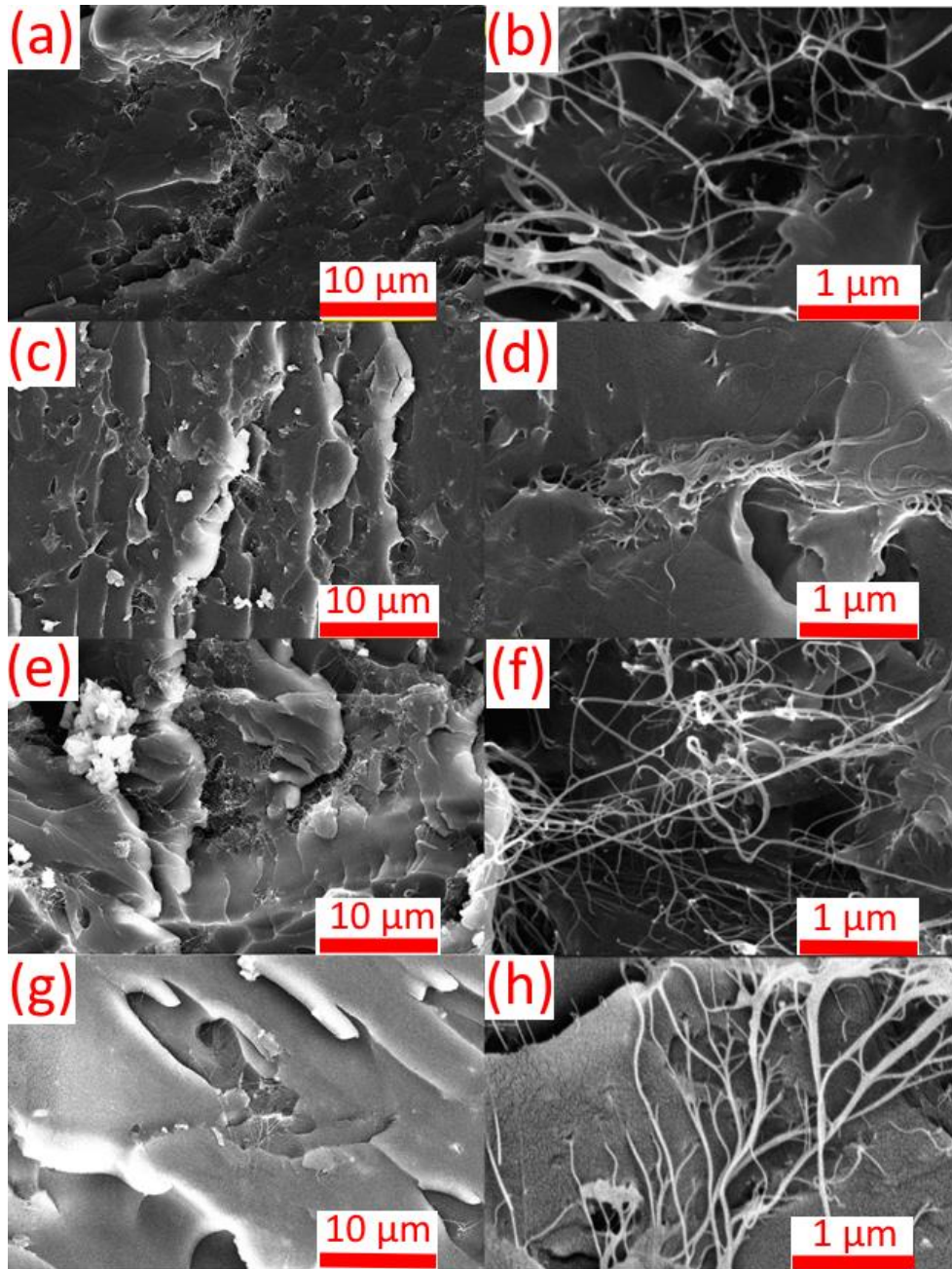


**Figure 14: SEM images of Briquettes (A,B), Masterbatch (C,D), Pristine (E,F) and RESS (G,H) nanocomposites at 0.25% wt. Images A,C,E and G are taken at 10,000x while images B,D,F and H are taken at 100,000x**

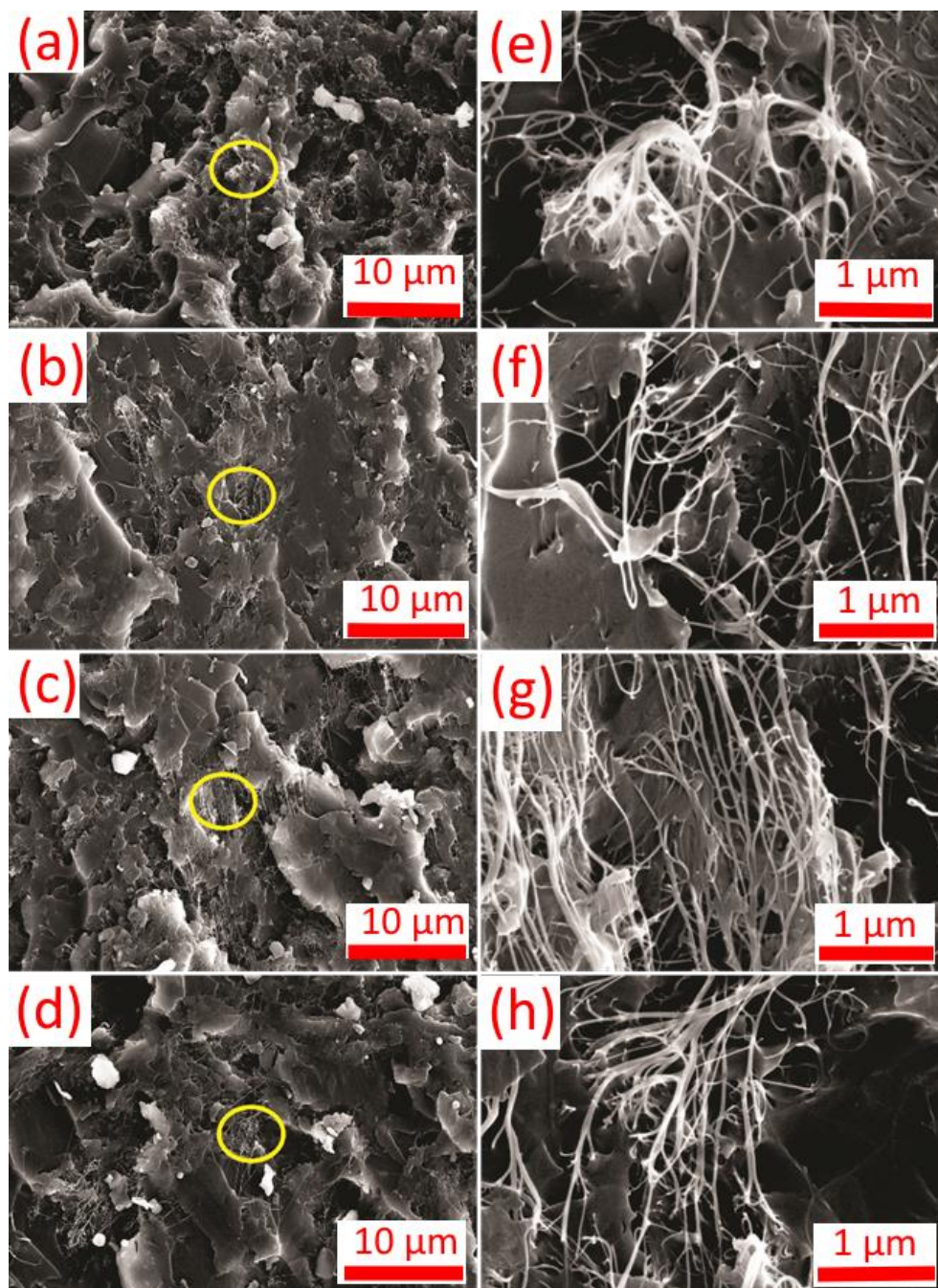


**Figure 15: SEM images for 1.0 wt. % (10,000x) for (a) briquette, (b) masterbatch, (c) pristine and (d) RESs SWCNT nanocomposites; (e-h) SEM images of the same nanocomposites taken at higher magnification (100,000x)**

At 0.05 wt.%, the nanocomposites again show very similar microstructures. All nanocomposites show the presence of CNTs in specific areas in the form of large agglomerates or matted bundled structures, typical for CNT based nanocomposites and attributed to a high concentration of CNTs within the matrix in specific regions. At 0.25 wt.%, the differences between microstructures are again practically indistinguishable. The higher weight percentage has led to a more dense, interconnected microstructure in comparison to the lower weight percentages for all nanocomposite types. At the highest weight percentage of 1.0 wt. %, the microstructure is again seen to be indistinguishable between nanocomposite types and almost no pristine epoxy matrix is seen whatsoever in any of the samples. For all the samples, agglomerates have taken the form of dense bundles with a matted structure within the epoxy.

Summarizing, we may conclude that the masterbatch-based samples show the typical morphological behavior of SWCNT/epoxy nanocomposites, with weaker percolation networks being seen at lower weight percentages. As the concentration of SWCNTs within the matrix increases, the percolation network moves towards a higher degree of interconnectivity and percolation. The samples showed a bundle-based microstructure and any large agglomerates were seen to be groups of CNT bundles. This is quite different from a typical observation for nanocomposites with multi-walled CNTs, where agglomerates are extremely densely packed, spherical or ellipsoidal in shape with little or no bundles or branching [3,111]. Hence, it was proven that further experimentation relying on masterbatch-based nanocomposites would represent a spectrum of CNT

nanocomposites, and that microstructurally, the results would be applicable across the board.

The electrical conductivity of the nanocomposites produced from different density states of CNT powder was also examined to see if the lack of microstructural differences translated into the same trend for multifunctional properties. This allowed certification of usage of masterbatches for nanocomposite production from a multifunctional property monitoring standpoint.

Analysis of the DC electrical behavior of the nanocomposites revealed no significant deviations in conductivity with SWCNT concentration, regardless of the consolidation degree of starting SWCNTs, as can be seen from Figure 16. The only visible difference in the electrical conductivity values are expectedly found for the lowest weight concentration of 0.005 wt.%, where briquette-based samples perform slightly lower than comparative types (within one order of magnitude of  $\sim 10^{-6}$  S/cm, nonetheless). Nanocomposites manufactured with low amounts of additives are known to produce properties with relatively high variations [112,113] owing to statistical deviations or minor differences caused by processing variables.

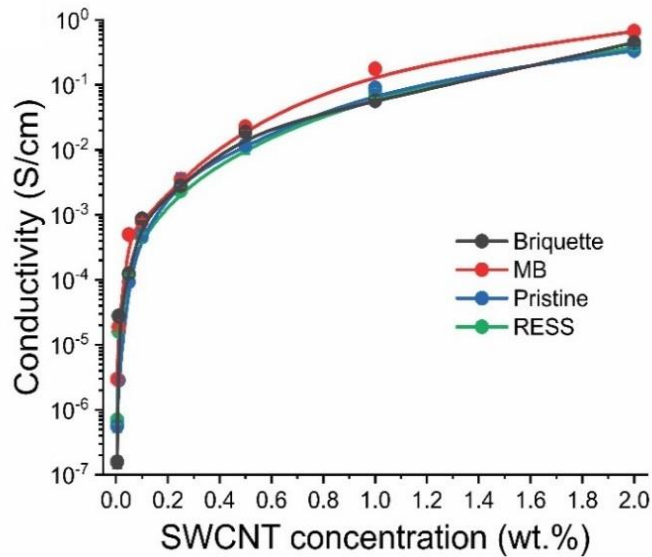


**Figure 16: Electrical conductivity of the nanocomposites made from different bulk density CNTs. The masterbatch nanocomposites perform with no significant difference**

At the higher weight percentages studied (0.25 – 2.0 wt.%), all nanocomposites show electrical performance in the same magnitude range as comparative alternatives. This is also in agreement with the SEM previously stated. The general high conductivity of the nanocomposites from all the series is also worth noting since SWCNT/epoxy nanocomposites fabricated by the presented route possess electrical conductivities of 0.3 – 0.67 S/cm at 2.0 wt.%, which is comparable to the values provided by large manufacturers of nanocomposite masterbatches [101,114].

Thus, from a detailed microstructural and electrical analysis of the performance of various densities of CNTs, it was noted that the masterbatches perform on par with all alternatives. This confirmed that further experimentation for monitoring the multifunctional nanocomposites could be made using nanocomposites produced from masterbatches. Although this experimentation resulted in a CNT bulk form which had its

own advantages for nanocomposite manufacturing, the multifunctional performance was essentially the same as masterbatch-based nanocomposites.

#### **4.2 Embedded electrodes and multifunctional property monitoring**

As the CNTFs used in this study were being tested for their feasibility as embedded electrodes for the monitoring of multifunctional properties both during manufacturing and post-manufacturing, a single step inclusion approach was used. CNTFs were placed in the gauge length of the nanocomposite samples with an equidistant spacing to allow for 2- or 4-point electrical measurements during the manufacturing stage. Continuous electrical measurement of the samples was conducted during the nanocomposite molding process, with measurements being started a few minutes before the matrix transfer and running for 24 hours until the polymer mixture was cured at room temperature. The CNTFs were not removed from the samples once curing had completed and were used as electrical connections for multifunctional property measurements during the post-manufacturing stage. Two types of nanocomposites were manufactured where the CNTFs were embedded, one based on SWCNTs and the second on MWCNTs. For both, two concentrations of CNTs were used (0.25% and 0.75% mass fraction) to determine the sensitivity of the CNTFs to the multifunctional properties and CNT concentration.

Selection of the weight percentages for study were based on several factors. Previous investigations conducted showed that weight percentages for MWCNT nanocomposites resulted in extremely low values of electrical conductivity below 0.5% by weight [115,116] . This provided the opportunity for investigating CNTF sensitivity to nanocomposites with low electrical conductivity, percolation networks consisting of

MWCNTs and their properties, and the nanocomposite viscosity values within processing limits of the techniques employed in this work. For SWCNTs, the same weight percentage values were chosen to provide a direct comparison, determine sensitivity of the CNTFs to stronger percolation networks with a higher degree of functional properties and also because the viscosity of the nanocomposite mixtures at this weight percentage were within the operating limits of the equipment employed. Values close to percolation were not chosen for study since the interaction of the materials was unknown and the detection sensitivity of the CNTFs could not be accurately predicted or compared. Figure 17 shows the scheme of the experimental scheme.

Hence, this section deals with the various steps of the core work of the thesis. The work was broken into segments which dealt with (1) the manufacturing of CNTFs, (2) embedded the CNTFs into the nanocomposites and monitoring the manufacturing process and (3) monitoring the manufactured nanocomposites with embedded electrodes and determining the property detection performance while understanding the effects the electrodes played mechanically.

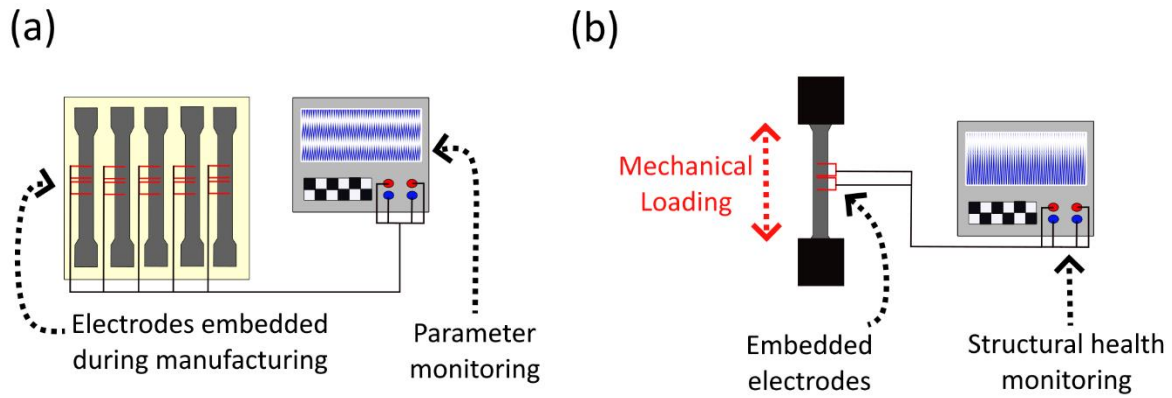


**Figure 17: The combined (a) manufacturing and (b) post manufacturing property monitoring of the nanocomposites using embedded and surface electrodes.**

### 4.3 Carbon nanotube fibers

The CNTFs produced for this thesis were wet-pulled from two initial thin film dimensions to ascertain the changes in structure and properties that may be brought about and utilized for the detection of the multifunctional properties of the CNT nanocomposites. Before being used as embedded electrodes, it was imperative that a feasible initial starting width of the film be chosen. The first thin film set was made with the dimensions of 3 cm length and 0.5 cm width while the second dimensions set was 3 cm in length and 1.0 cm in width. Once wet pulling was conducted and fibers were produced, they were placed on a glass slide so that their dimensions could be ascertained from optical microscopy. In order to measure the CNTF diameter, an optical microscope (DM4500, Leica GmbH, Germany) was employed. For diameter measurements needed for density calculations, at least 6 measurements were made in each of the 5 segments of each fiber.

Once placed on the glass slides for characterization, a Silver paste (Ted Pella Inc., USA) was applied to provide low resistance contacts between fibers and electrodes during

resistance measurements. Electrical resistance measurements were conducted using the two-point method with a Keysight 34972A DMM (Keysight Technologies, Inc. USA). Four-point measurements were initially made and showed no significant variation when compared to the values obtained with the two-point method. Silver-based paste was applied at the contacts between the machine and CNTFs to ensure good electrical contacts during measurements. The conductivity of a fiber,  $\sigma$ , was determined by its electrical resistance,  $R$ , and its dimensions (length,  $L$ , and diameter,  $D$ ):

$$\sigma = \frac{4L}{\pi D^2 R}. \quad (2)$$

The results of the diameter relationship to electrical conductivity have been compiled in Figure 18 (a), and (b) displays a SEM visualization of a CNTF. The CNTFs were produced with films of two different widths in order to create fibers with a noticeable diameter difference to help ascertain if this parameter affected sensing performance and which diameter of CNTF to choose for further investigation. As the results show, the thinner width of film resulted in CNTFs with a smaller diameter and higher conductivity and that a substantial difference in diameter was present comparing to CNTFs created from the wider films. This is already reported on, with films of smaller widths being more efficiently converted into fibers with a higher packing density, leading to greater electrical conductivity [7,85]. The values are in good correlation ( $10^3$ - $10^4$  S/m) with previous works showing the diameter and electrical conductivity of CNTFs produced through the wet-pulling technique [7,83], and were therefore suitable for investigating as embeddable electrodes. For embedding and functional property detection of the nanocomposites, electrodes were paired depending on the diameter and conductivity shown (i.e., for 4-point

measurements, 4 similar electrodes were chosen per sample and for 2-point measurements, 2 similar electrodes were chosen). Both diameter sets were investigated to determine manufacturing parameter monitoring performance.

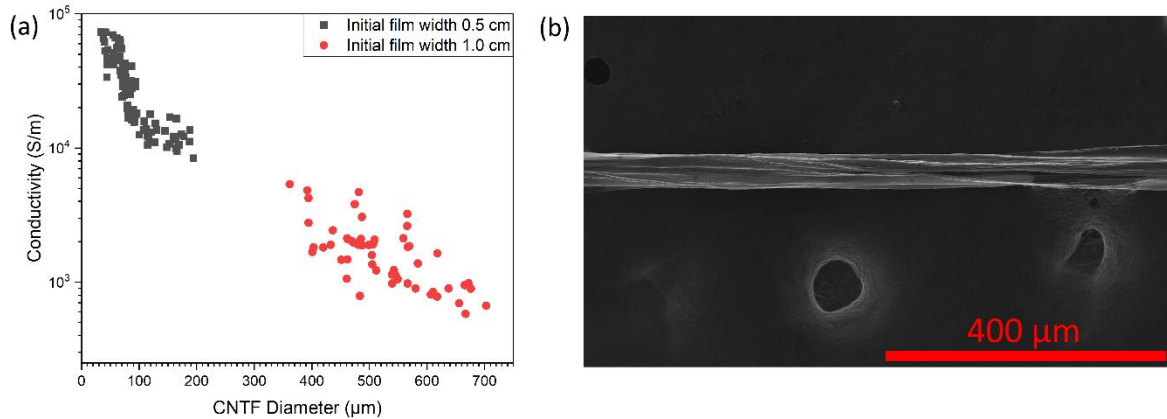


**Figure 18: (a) The distribution of diameter and electrical conductivity of the CNTFs and (b) a SEM image of a CNTF.**

SEM imagery conducted during this phase of the thesis, and previously confirm that the wet-pulled fibers have a porous structure, which is conducive to the intended application of embedded electrodes. The porous structure is more conducive to allowing CNT reinforced polymer to seep into the fiber via infiltration [95,96], allowing a strong wetting degree and connection with the carbon nanotubes in the matrix which form the percolation network. In comparison to metallic electrodes which have a smooth surface and surface oxide layer, this type of electrode is better suited for low contact resistance readings which allows the actual electrical conductivity and piezoresistive response of the materials they are embedded in to be measured.

#### **4.4 Manufacturing parameter monitoring**

To determine whether the CNTFs were feasible for monitoring the multifunctional properties of the CNT thermoset nanocomposites during the manufacturing stage, both 2- and 4-point electrical measurements were made during the manufacturing process. First, 2-point measurements were conducted with fibers produced from both widths of thin films (0.5 and 1 cm). This allowed the determination of whether the diameter of the fibers resulted in any differences in measurements and whether the CNTFs were sensitive to SWCNTs and MWCNTs in different concentrations. The two types of fillers were used at two weight percentages of 0.25 and 0.75% wt. The electrical monitoring results were then compared to 4-point measurements to determine if contact resistance was present and how it manifests in electrical readings. The measurements made using CNTFs were compared to metallic embedded electrodes to compare performance, silver glue was not used during the manufacturing stage measurements due to the fact that the base of the glue is a polymer and may result in material-based deviation in electrical measurements. In addition, the usage of silver glue as embedded electrodes would not be feasible on an industrial scale and would be impractical for a one-step embedding process since the contacts would be inaccessible after matrix coverage. Figures 19 and 20 compile the manufacturing stage resistance curves obtained from 2-point measurements made with different diameter CNTFs for the nanocomposite matrices.

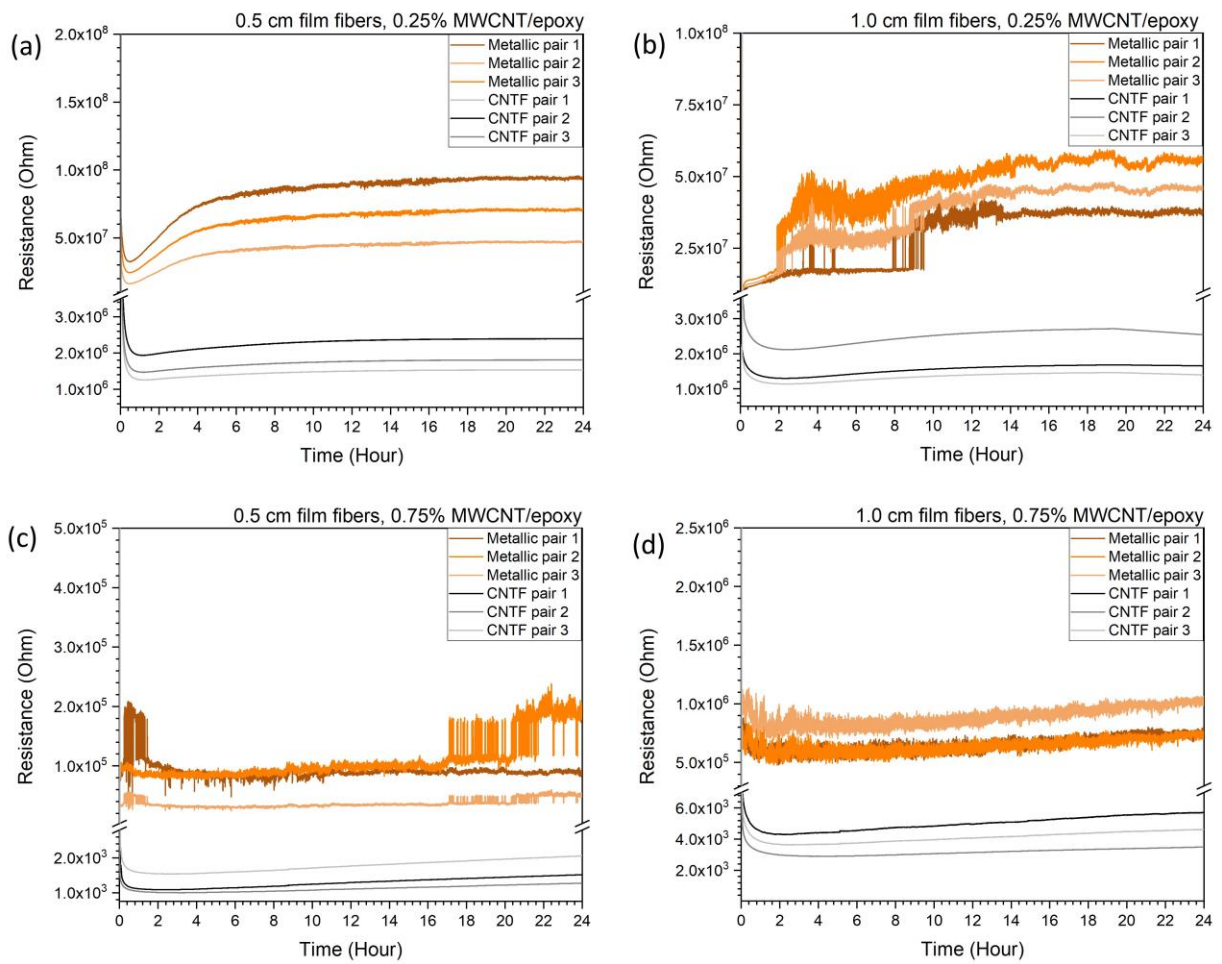


**Figure 19: 2-point electrical measurements for the MWCNT nanocomposite matrices with (a, c) 0.5 cm and (b, d) 1.0 cm film fibers**

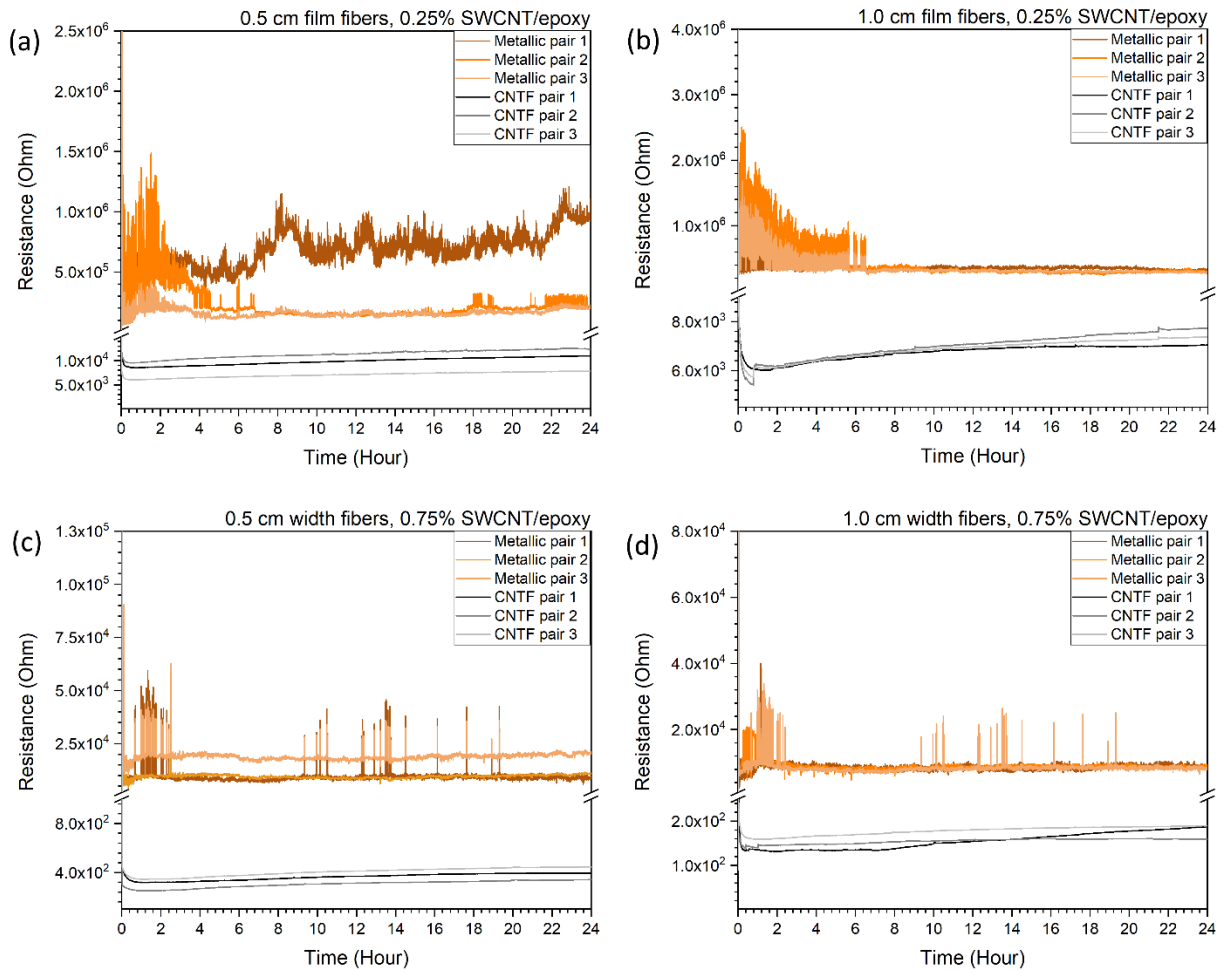


**Figure 20: 2-point electrical measurements for the SWCNT nanocomposite matrices with (a, c) 0.5 cm and (b, d) 1.0 cm film fibers**

The manufacturing stage monitoring of the nanocomposite matrices with the 2-point technique has shown quite remarkable features. First to note is that regardless of the diameter of the CNTFs used for monitoring (difference in diameter is related to the width of the film used for manufacturing, as shown in Figure 18), the measured electrical resistance values are almost identical for the same type of nanocomposite mixture as can be seen in Figures 19 and 20. This is shown to be true when measuring both SWCNT and MWCNT nanocomposite mixtures at both weight percentages. Minor differences in the measured values are related to the fact that each experiment required a separate batch of

nanocomposite mixture to be produced, resulting in variations in their inherent electrical properties. These minor differences in batch production have already been shown to present with the materials under study [3,28]. By comparing the performance of measuring electrical resistance throughout the curing process, it can be seen that the CNTF diameters provide what can be considered to be negligible difference for both SWCNT and MWCNT mixtures, regardless of the concentration. The reason behind this property is further explored in the microstructure and mechanism section.

When comparing to the embedded metallic electrodes, the lack of contact resistance, displayed in the form of electrical noise, is also apparent for all nanocomposite mixtures and fiber types. For the metallic electrodes, readings experience noise up to 0.5 magnitude of the resistance values measured, while the measurements made using CNTF electrodes do not show such behavior. During the curing process, the electrical resistance shows a slight tendency to increase with time for both the metallic and CNTF electrodes and this behavior is attributed to the increase in resistance experienced by CNT-thermoset nanocomposite systems during the process of curing [68,115]. In short, in the 2-point measurement scheme, the CNTF embedded electrodes provide a more stable, reliable and noise-free electrical measurement of the nanocomposite mixtures, regardless of the diameter, concentration of CNTs in the nanocomposite as well as type of CNT additive used.

Here, it is also noted that in all cases with the 2-point scheme, the resistance value measured during manufacturing monitoring is 1-2 orders of magnitude smaller than the values obtained by using embedded metallic electrodes. The CNTFs are seen to be less

susceptible to contact resistance when measuring electrical properties attributed to the percolation network of the nanocomposite matrix, regardless of whether SWCNT or MWCNTs have been used. Also, the electrical measurements and lower noise not seen to be affected by the concentration of CNTs, making the fibers an ideal low-noise candidate for measuring the filtration effect that may take place when nanocomposite matrices are used to create fiber reinforced nanocomposites, as stated previously.

To investigate whether 4-point measurements differed from the 2-point, the same experimentation was repeated with the 4-point technique. Since the initial experimentation showed that the diameter of the embedded CNTFs did not affect functional property measurement, only fibers produced from thin films with a width of 0.5 cm were investigated. The measurements have been compiled in Figure 21.

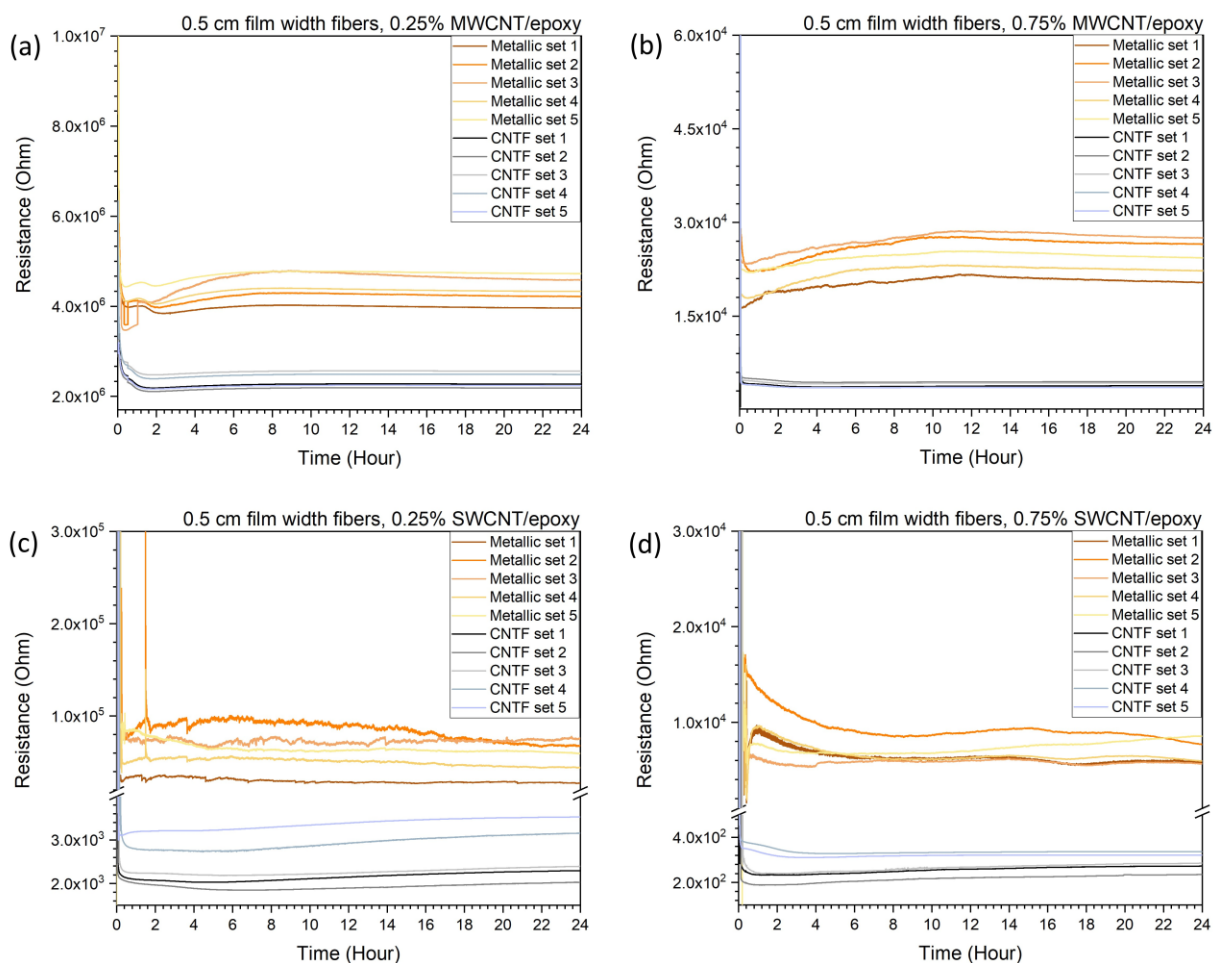


**Figure 21: 4-point electrical measurements for the nanocomposite matrices with (a, c) MWCNTs and (b, d) SWCNTs**

Comparing with the 2-point measurements made earlier, the difference in results is apparent. The noise displayed during the 2-point measurements has been almost completely eliminated for the metallic embedded electrodes for all nanocomposite batches, while no change in behavior or noise level is detected for the CNTF embedded electrodes. This further confirms that the CNTF-based electrodes provide a better electrical connection to the multifunctional nanocomposite matrices for measuring electrical properties. The metallic electrodes consistently show a value which is 1 order of magnitude smaller than the values for 2-point measurements, indicating that this technique has managed to

eliminate electrical noise as well as magnitudinal contact resistance. The CNTF embedded electrodes however, show a strong match to the magnitude values previously seen, indicating that no contact resistance, either in the form of noise or the form of higher resistance values, is present for these electrodes. Variance in detected values can be seen, but it is relatively insignificant and is attributed to batch to batch processing variance.

Hence, the electrical testing and manufacturing monitoring proved that CNTF-based electrodes are less susceptible to contact resistance as compared to metallic electrodes regardless of measurement technique. Since contact resistance is shown to be negligible, the CNTFs seem to display a better interaction with the conductive nanoparticles in the nanocomposite matrices. The CNTFs have also shown themselves to be able to detect electrical properties developed in the nanocomposites due to the CNTs. They provide different electrical measurements to different concentrations of the CNTs, showing that they have the potential to be used for CNT filtration detection in nanocomposite materials. The measurements they provide are comparatively more reliable and stable. The reason behind these enhanced properties is further explained in the microstructural section. Besides confirming the advantages listed above, the results have shown that the CNTFs are more versatile than embedded metallic electrodes. The CNTF-based electrodes show a consistent reading of electrical values whether the 2 or 4-point measurement scheme is utilized. This is extremely important as it reduces the amount of electrical connections and electrodes needed to monitor a material by exactly half, giving the benefits of ease of installation, reliability and reduced areas of inhomogeneity where embedded electrodes may cause mechanical property loss. The consistency of electrical readings allows the

CNTF-based electrodes to be used in either 2-point or 4-point measurement schemes without the loss of sensitivity or performance.

#### **4.5 Post-manufacturing parameter monitoring**

As the aim of this work was to determine whether CNTFs are a suitable future alternative for the one-step inclusion and monitoring of functional properties of CNT nanocomposites, the post-manufacturing monitoring consisted of measuring the electrical resistivity and piezoresistive response through the embedded CNTFs. The electrical and piezoresistive measurements were compared to those obtained by metallic embedded electrodes as well as the standard method of creating electrical contacts through applied silver-based glue. Piezoresistive measurements were made both during uniaxial tensile strain as well as uniaxial cyclic testing for measuring the reliability of performance.

##### ***4.5.1 Electrical resistivity measurements***

As electrical resistivity or conductivity is one of the main areas where CNT multifunctional nanocomposites are at the forefront and attract a large amount of industrial and research attention [58,59], this was the first property tested in the post-manufacturing stage with CNTFs. Electrical characterization of the nanocomposites was carried using the DC based technique and is shown in Figure 22. DC resistance measurements were conducted using a Keysight 34410A digital multimeter. Resistance measurements were used to calculate the conductivity of the samples using the following equation, where  $R$  is the resistance of the sample,  $\sigma$  is the calculated conductivity,  $L$  is the length between electrodes and  $A$  is the cross-sectional area (equal to the product of the sample thickness and width,  $H \cdot W$ , respectively):

$$\sigma = \frac{L}{R \cdot A} = \frac{L}{R \cdot W \cdot H} \quad (3)$$

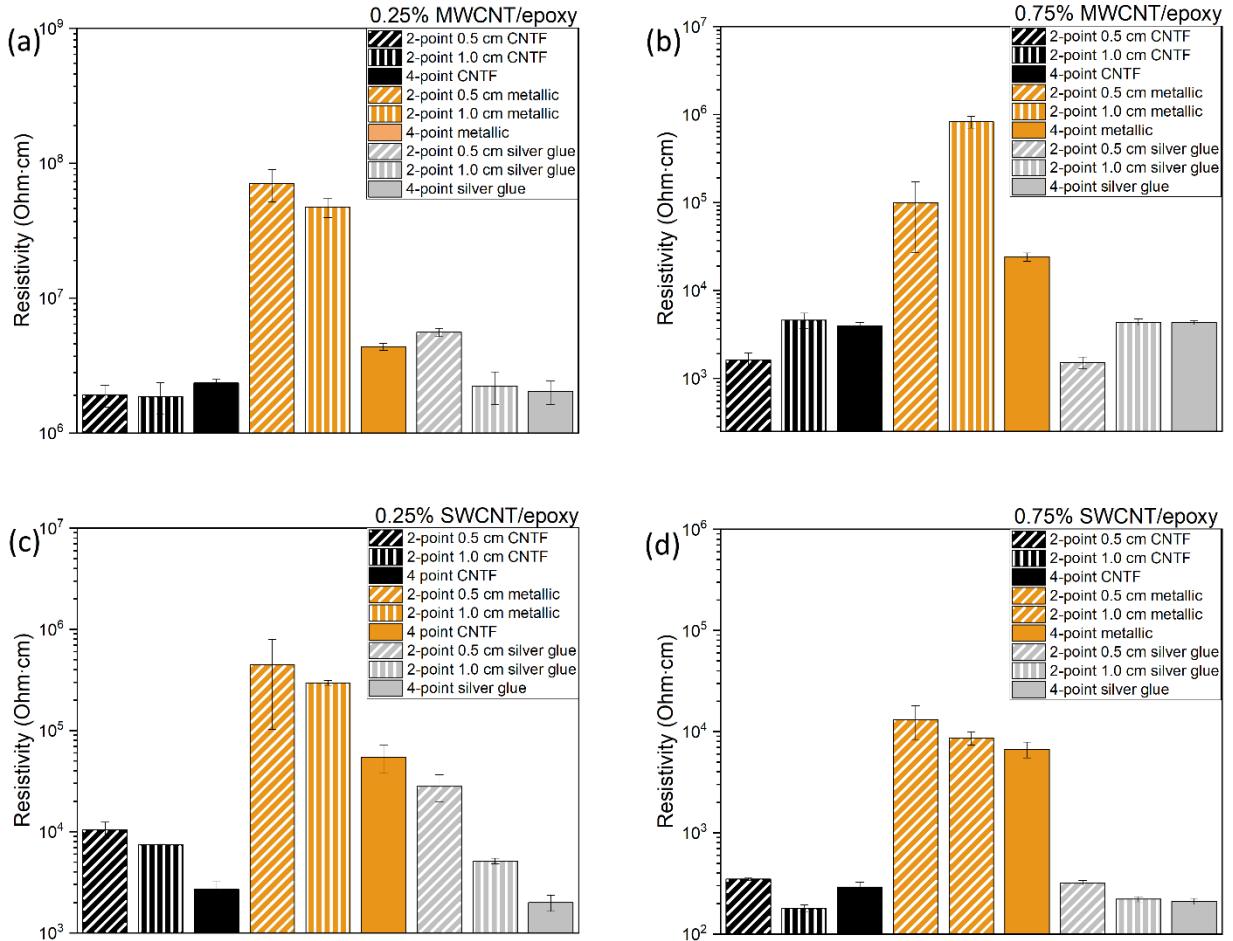


**Figure 22: Electrical resistivity measured using the different electrodes and schemes for (a, b) MWCNT and (c, d) SWCNT nanocomposites.**

As can be seen from the figure, it is worth noting that the nanocomposites produced and tested with the silver-based glue, which acted as the benchmark and standard test method for electrode performance as it has been used in various publications [29,48,54,116], show electrical resistivity values aligned with those seen in literature. The values obtained from these electrodes also show a batch to batch variance, which was also noted and explained in the manufacturing monitoring section. For the SWCNT

nanocomposites measured using silver standard electrodes, the resistivity values for 0.25 % and 0.75 % by weight are in the range of  $\sim 10^3$  and  $\sim 10^2$  Ohm·cm respectively, which matches literature values for the stated processing route [6]. For the same weight percentages, the MWCNT nanocomposites show electrical resistivities of  $\sim 10^6$  and  $\sim 10^3$  Ohm·cm respectively, which also coincide or are better than what is seen in literature [3,60]. This shows that the nanocomposites being tested with the novel CNTF electrodes represent samples whose performance is known and comparable, and are thus suitable for examining the detection capability of the CNTF electrodes.

The trend of showing lower resistance and thus lower resistivity values for both SWCNT and MWCNT nanocomposites by the CNTF electrodes has continued even after sample production, regardless of the use of 2- or 4-point measurement schemes. Compared to the metallic electrodes used, the CNTFs show a 1-2 orders of magnitude value smaller for all nanocomposite weight percentages tested for both schemes. This is also seen to be the case when larger diameter CNTFs are used, further cementing earlier conclusions that the CNTFs display negligible contact resistance when used to measure the multifunctional nanocomposite matrices. When compared with the silver standard electrodes, the resistivity values detected by the CNTF electrodes show no significant difference for any of the batches. This shows that the CNTFs are making a stronger electrical contact with the percolation network of the nanocomposites as compared to embedded metallic electrodes, whereas their performance matches that of a standard electrode material. Here, the CNTFs show that not only do they have the advantage of being able to be embedded in the nanocomposites during production and then used for lifecycle measurements, but also

provide the added benefits of reduced cost, detection performance matching that of a commonly used standard material as well as a simpler application route.

#### ***4.5.2 Tensile piezoresistive response and properties***

One of the main multifunctional properties exhibited by CNT-thermoset nanocomposites is that of piezoresistive response, which has made the material a prime candidate for smart materials and structural health monitoring. Since the CNTFs in this study are being evaluated for usage as embedded electrodes, it was necessary to determine whether they caused any mechanical property loss when combined with the nanocomposites for monitoring. Tensile testing was conducted using the parameters previously described, and simultaneous electrical measurements were taken to establish any difference in piezoresistive response which may have been caused by electrode types as well as determining the feasibility of the CNTFs to detect functional property changes. Figure 23 displays the piezoresistive response of the nanocomposites with different electrodes. The tensile testing curves have been compiled in Figure 24. Table 3 compiles the information obtained from the tensile mechanical tests.

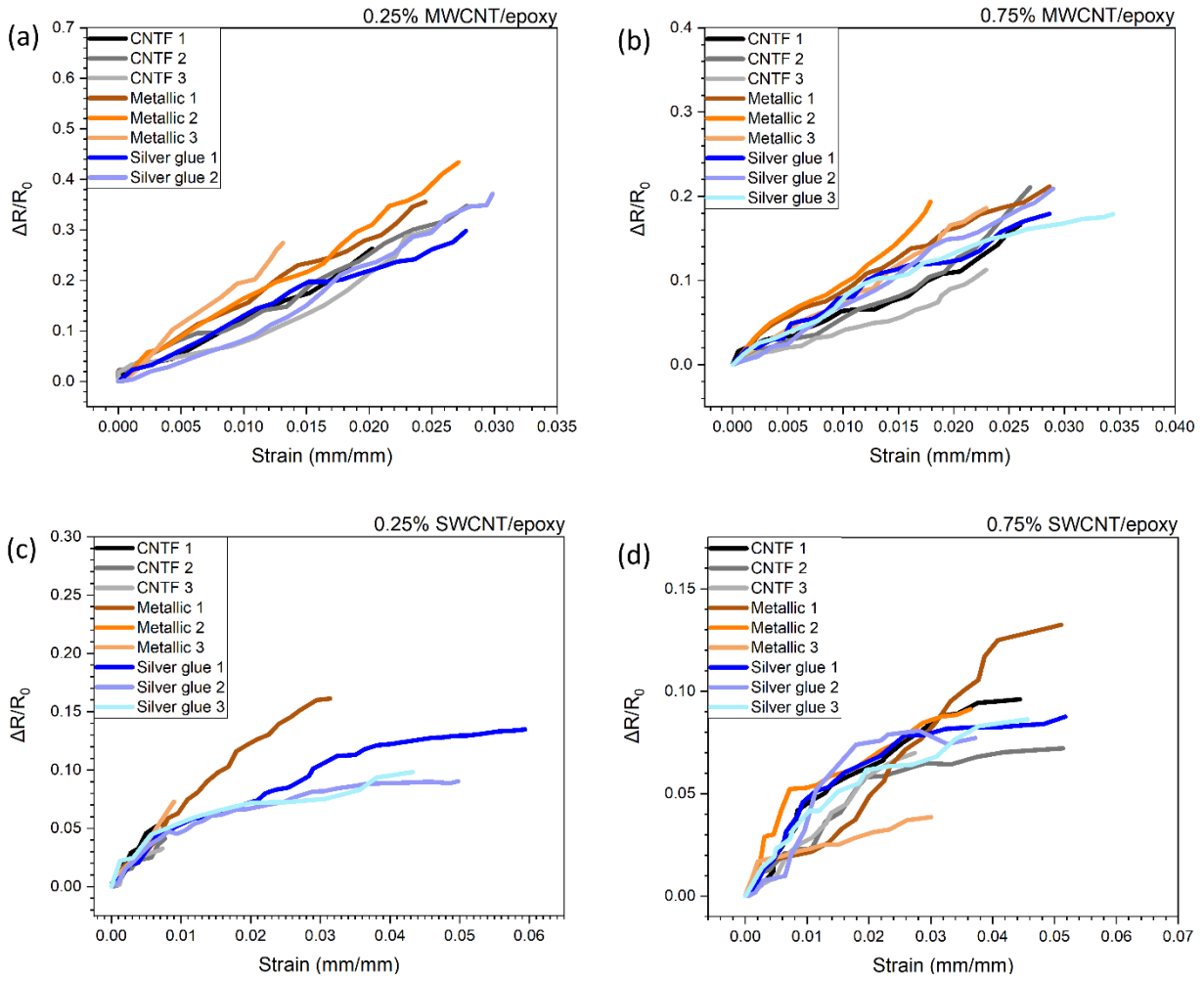


**Figure 23: Piezoresistive curves for the nanocomposites measured using different electrode systems. (a) and (b) show MWCNT, while (c) and (d) show SWCNT nanocomposites at 0.25% and 0.75% wt., respectively**

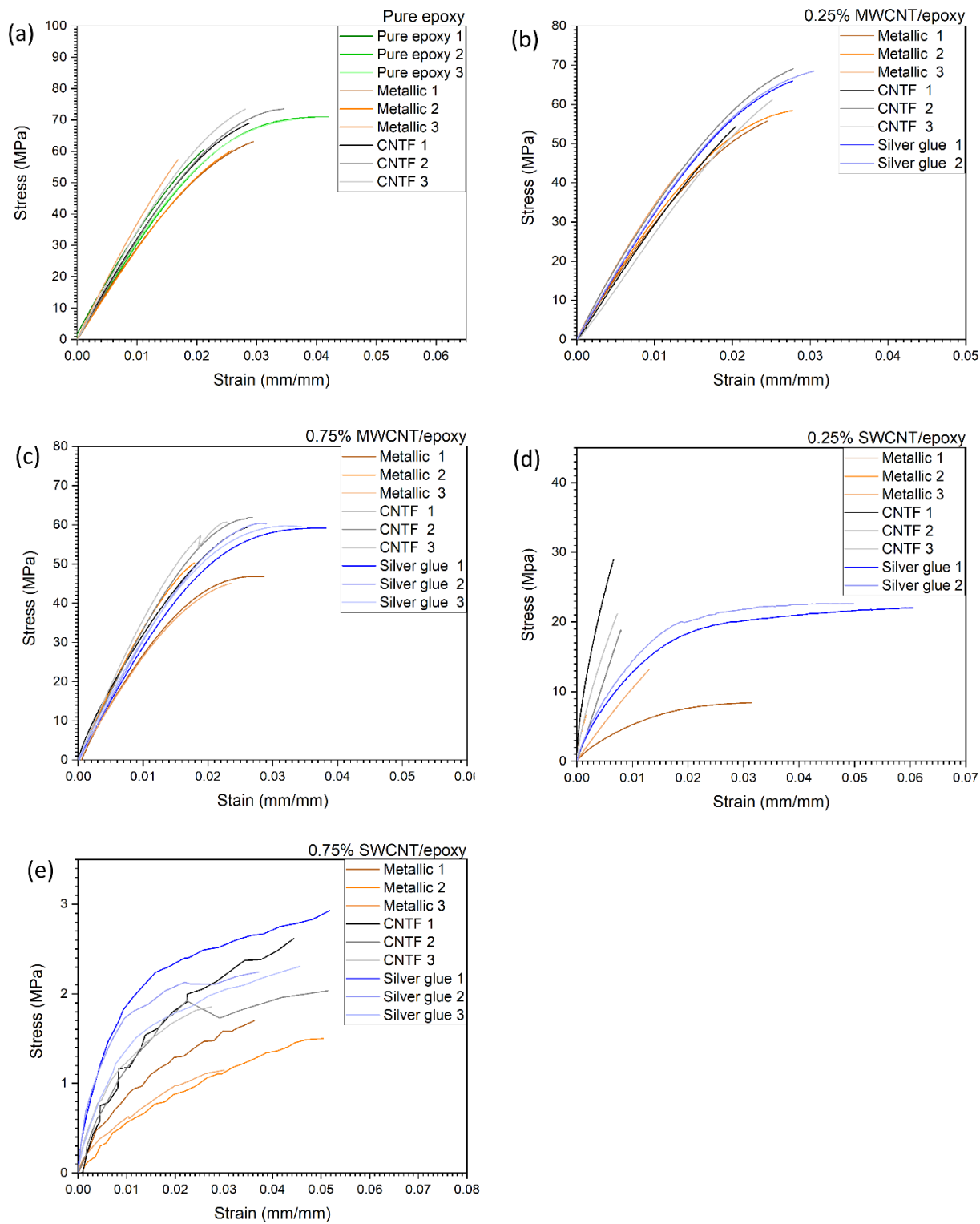


**Figure 24: Tensile testing curves for the various electrode systems for (a) pure epoxy and embedded electrodes, (b, c) MWCNT and (d, e) SWCNT nanocomposites.**

**Table 3: Material and electrode type piezoresistive performance and mechanical properties**

<b>Materials and electrode types</b>	<b>Ultimate tensile strength (MPa)</b>	<b>Average Gauge factor</b>	<b>Young's modulus (GPa)</b>	<b>Poisson Ration</b>
<b>Epoxy</b>	$71.8 \pm 1.3$	-	$3.15 \pm 0.97$	$0.33 \pm 0.02$
<b>Epoxy + CNTF</b>	$72.3 \pm 2.1$	-	$3.37 \pm 0.15$	$0.36 \pm 0.01$
<b>Epoxy + metallic</b>	$59.6 \pm 3.2$	-	$3.59 \pm 0.19$	$0.34 \pm 0.02$
<b>0.25% MWCNT + silver glue</b>	$68.2 \pm 0.5$	$11.6 \pm 0.8$	$3.18 \pm 0.03$	$0.39 \pm 0.01$
<b>0.25% MWCNT + CNTF</b>	$61.5 \pm 6.2$	$12.5 \pm 0.4$	$2.93 \pm 0.28$	$0.40 \pm 0.01$
<b>0.25% MWCNT + metallic</b>	$52.3 \pm 6.8$	$17.1 \pm 2.7$	$3.07 \pm 0.26$	$0.40 \pm 0.02$
<b>0.75% MWCNT + silver glue</b>	$59.8 \pm 0.5$	$6.6 \pm 0.5$	$2.89 \pm 0.15$	$0.39 \pm 0.01$
<b>0.75% MWCNT + CNTF</b>	$60.7 \pm 1.1$	$6.4 \pm 1.2$	$3.13 \pm 0.35$	$0.41 \pm 0.03$
<b>0.75% MWCNT + metallic</b>	$47.4 \pm 2.2$	$8.8 \pm 1.5$	$2.60 \pm 0.43$	$0.41 \pm 0.01$

<b>0.25% SWCNT + silver glue</b>	$22.3 \pm 0.3$	$4.3 \pm 0.7$	$0.44 \pm 0.04$	$0.43 \pm 0.05$
<b>0.25% SWCNT + CNTF</b>	$22.6 \pm 3.8$	$5.8 \pm 1.3$	$0.36 \pm 0.05$	$0.41 \pm 0.02$
<b>0.25% SWCNT + metallic</b>	$9.6 \pm 2.7$	$6.9 \pm 0.7$	$0.46 \pm 0.09$	$0.42 \pm 0.01$
<b>0.75% SWCNT + silver glue</b>	$2.5 \pm 0.3$	$3.1 \pm 0.3$	$0.03 \pm 0.01$	$0.44 \pm 0.04$
<b>0.75% SWCNT + CNTF</b>	$2.2 \pm 0.3$	$2.9 \pm 1.7$	$0.03 \pm 0.01$	$0.44 \pm 0.02$
<b>0.75% SWCNT + metallic</b>	$1.6 \pm 0.4$	$3.7 \pm 0.6$	$0.03 \pm 0.01$	$0.45 \pm 0.01$

To understand the performance of the electrode systems in terms of piezoresistive monitoring performance, one must take a look at the base material mechanical characteristics. For all nanocomposite samples, it was seen that the addition of CNTs results in a change in mechanical properties mechanical properties. The SWCNTs were seen to deteriorate mechanical properties severely, in both the elastic and plastic range, while the MWCNTs were only seen to lower plastic range performance in terms of UTS. This is portrayed by the decrease in UTS, Young's modulus and the increase in the Poisson

ratio, leading to the conclusion that the nanocomposites tend towards a plastic or viscoelastic response as the addition of CNTs in the polymer increases. This has been well reported, with the mechanism of property loss being based on the interference of CNTs in the polymerization reaction and eventual decrease in overall curing degree [68,115,117]. What is important to note here is that each batch of material and electrodes has shown similar Young's modulus and Poisson ratio, meaning that the base material behavior is essentially the same and a significant difference in UTS may be attributed to the inclusion of electrodes.

The initial difference in UTS is evident from testing with plain epoxy, with the metallic embedded electrodes showing a ~17% loss. The CNTF embedded electrodes however, showed no significant difference in UTS values. For the nanocomposite with 0.25% wt. MWCNT addition, the metallic embedded electrodes showed a UTS value which was ~24% lower than that of the samples with surface applied electrodes and a piezoresistive gauge factor of 17, which was ~55% higher than its counterparts. The higher gauge factor is not surprising, since during the electrical testing it was shown that the metallic embedded electrodes show a consistently higher resistivity value due to the presence of contact resistance. In comparison, the samples containing CNTF electrodes show a UTS and gauge factor which is almost the same as the samples which contain no embedded electrode system, making their performance almost identical to that of a commonly used standard material. For nanocomposites with 0.75% wt. MWCNTs, the CNTF electrode containing samples show no significant changes to UTS or gauge factor, whereas the metallic electrodes maintain a slightly overestimated gauge factor and a ~21%

loss in UTS. For the MWCNT nanocomposites, at both weight percentages, the CNTF electrode system showed a performance almost identical to that of the surface applied silver standard electrodes, but surprisingly showed no loss in tensile mechanical properties.

Nanocomposites manufactured with SWCNTs on the other hand, showed severe mechanical property degradation, even at the smaller wt.% in this study. The property loss is again attributed to changes in polymerization, as cited previously. However, this provided the opportunity to study the CNTF electrodes with a material which is relatively highly conductive as well as shows highly plastic or viscoelastic behavior. Nanocomposites batches manufactured with 0.25% SWCNTs showed the same trend as seen with MWCNTs, where the CNTF electrodes caused no significant changes in piezoresistive strain detection or UTS. The samples incorporating embedded metallic electrodes however, showed slightly higher gauge factors combined with a ~60% loss in UTS performance. The nanocomposites created with 0.75% wt. SWCNT loading narrowed the piezoresistive detection difference, with the metallic electrodes performing no different than the CNTF and silver glue-based samples when variance is taken into account. However, they did show a 37% decrease in UTS. For nanocomposites with SWCNTs, the electrical resistivity values are extremely low, and when considering the order of magnitude of difference seen, may be the reason why a large difference in gauge factors is not present as compared to nanocomposites containing MWCNTs.

During this stage of testing, the feasibility of CNTFs as embedded electrodes for sensing of multifunctional nanocomposite properties during strain was verified. The CNTFs caused no discernable property loss, performed on par with standard electrode

materials and provided no overestimated piezoresistive response. Although metallic embedded electrodes seem to be suitable for piezoresistive monitoring of relatively conductive nanocomposites, their negative influence on mechanical properties cannot be overlooked. It is fundamental to note that during this testing, all samples containing metallic embedded electrodes failed at the location of the embedded electrodes, often following the electrode path. This was not the case for embedded CNTFs or surface applied electrodes. This is further discussed in the microstructural and mechanism section and the example images of these failures are provided in Figure 25.

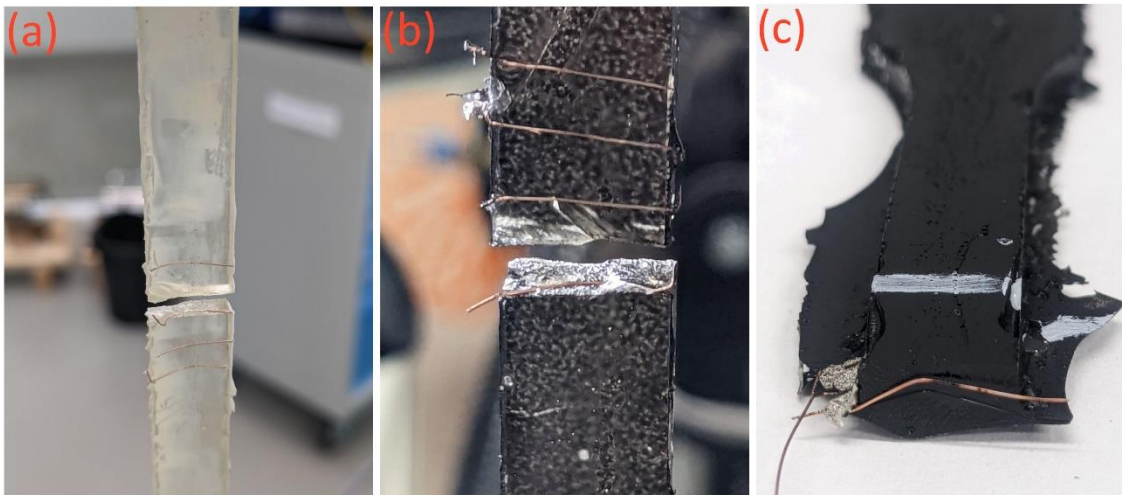


**Figure 25: Samples showing fracture path along metallic embedded electrodes for (a) pure thermoset polymer, (b) MWCNT and (c) SWCNT samples.**

An additional interesting find was that during testing, although samples with metallic embedded electrodes provided regions of inhomogeneity which were conducive to sample fracture and failure, the surface applied silver electrodes would detach upon the extreme shock force experienced by the materials during breakage. Single frames from DIC are shown Figure 26 showing this taking place. Although the surface applied silver-glue is suitable for static material measurement, this work shows that they may not be

suitable for applications where the force experienced by the nanocomposite matrices is greater than the bonding strength of certain adhesives, limiting their usage in large-scale real-world scenarios, unlike the CNTF-based electrodes.

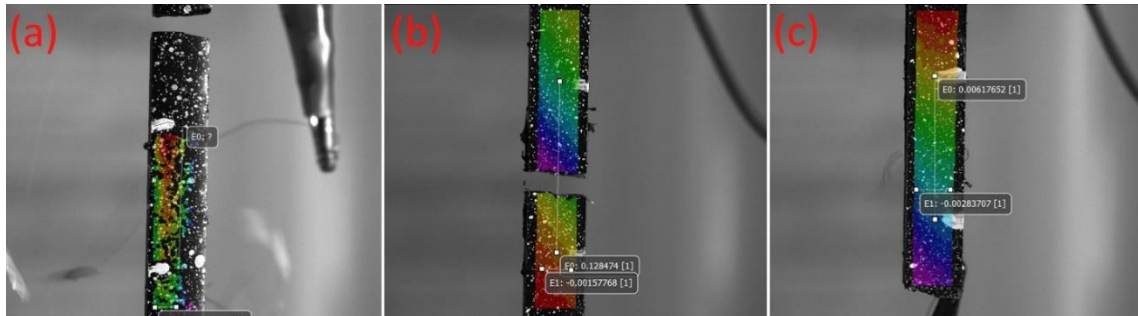


**Figure 26: DIC frames showing (a) detaching of silver-glue electrodes during fracture, (b) fracture taking place along metallic embedded electrode and (c) CNTF electrodes outside fracture region. Digital extensometers may be ignored.**

#### ***4.5.3 Cyclic piezoresistive response and properties***

Cyclic testing of the nanocomposites was conducted to determine whether any electrode-based drift was present in the sensing of piezoresistive response. Cyclic testing also allowed the determination of whether any of the electrode types may cause failure of the samples under alternating loads, representing real world usage of the materials and how embedded electrodes may affect sensing performance. Sample cyclic responses have been shown in Figure 27 and 28.

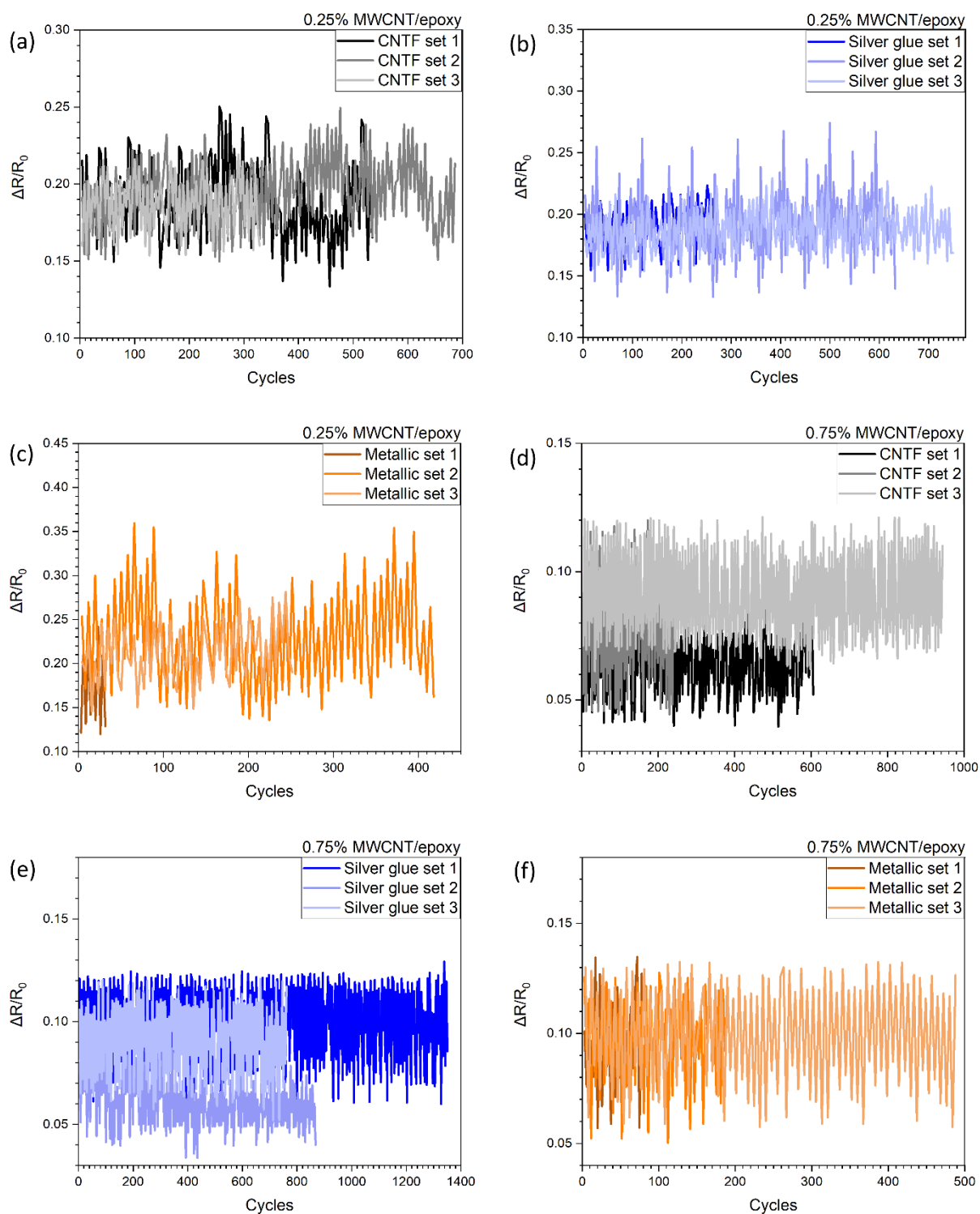


**Figure 27: Cyclic response curves for the various electrodes for MWCNT nanocomposites**

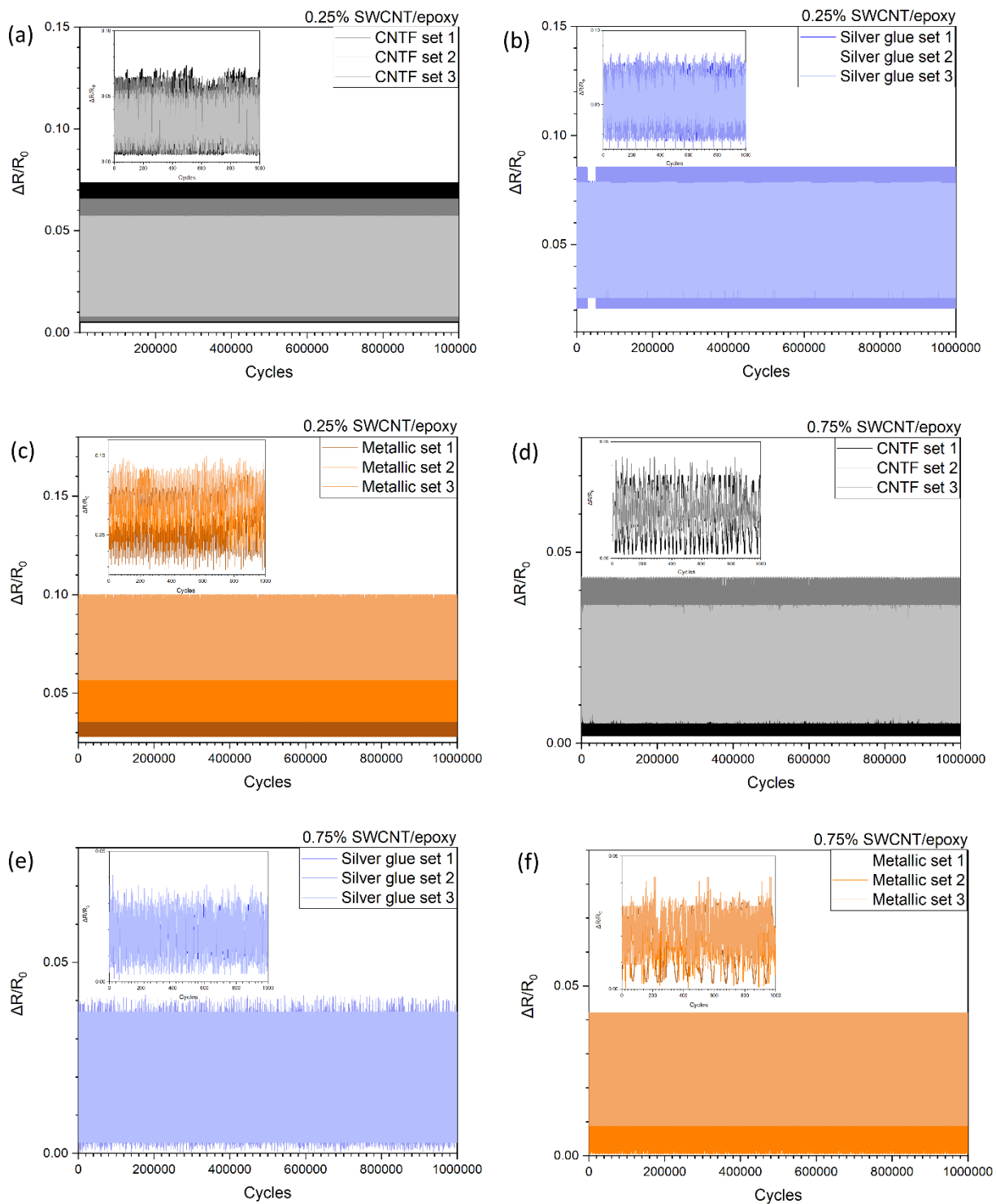


**Figure 28: Cyclic response curves for the various electrodes for MWCNT nanocomposites**

The cyclic response of the nanocomposites showed results which corresponded to the trends seen during tensile testing. For nanocomposites made with 0.25% wt. MWCNTs, the CNTF electrodes show a similar response to that of the standard silver electrodes whereas the metallic embedded electrodes show a heightened response at a slightly lower applied force. The same is noted for the nanocomposites with 0.75% wt. MWCNTs, where on average, the response of the embedded metallic electrodes was higher in comparison to the samples with CNTFs and silver standard electrodes. The higher response of the metallic electrodes ties in with the microstructural analysis, showing that the poor interface between the nanocomposite matrix and electrodes causes a higher response due to contact and tunneling resistance. It should be noted that for both these weight percentages, the nanocomposites showed no major drift, highlighting that the base nanocomposite may be a reliable material for structural health monitoring. An additional finding of interest was that the samples which contained embedded metallic electrodes would fail at the site of the electrode placement. The same failure behavior was not seen for samples containing CNTFs or samples with standard silver contacts. Although the samples that contained embedded metallic electrodes failed at a lower number of cycles as compared to their counterparts, the number of cycles was not very significantly lower. Although the metallic electrodes may provide a heightened response and sensitivity, they provide a region for stress concentration and are conducive to failure, which is not the case with the embedded CNTFs. In addition, it is noted that the metallic electrodes provide a slightly slower cyclic response. This is most probably due to the development of plastic deformation in the form of microcracks which eliminate weak connection points, leaving stronger connections

which are less susceptible to deformation. The delayed response may also be due to the multimeter taking additional time to adjust and provide a stable current for 4-point measurements when these deformations occur.

The SWCNT nanocomposites, showing electrical resistivity values which differ by only 1 order of magnitude between their weight percentages, showed similar and subdued responses. Given the low testing force based on the UTS displayed and the shift to more viscoelastic properties of the matrix, all samples for both weight percentages completed 1 million cycles without failure. To allow for visualization, a segment of their responses have been shown in Figure 27. For the samples created with 0.25% SWCNTs, the responses of the different electrode systems become similar, with the embedded metallic electrodes showing a slightly higher response. This is not unexpected as the higher the conductivity achieved in nanocomposites, the lower the overall piezoresistive response becomes [116,118]. As the weight percentage of SWCNTs is increased to 0.75%, a very slow cyclic response is noted from all materials, with the degree of sensitivity almost the same. Considering the microstructure seen in the SEM analysis, the response from these nanocomposites is not surprising, given that the percolation network formed in the nanocomposites is extremely dense, with a large number of interconnections between the SWCNTs due to the high aspect ratio, a high dispersion degree and relatively large weight percentage. Again, no major drift was seen in any of the samples from the different electrode types, showing that the base material was being measured in a similar way by all electrodes.

The cyclic testing allowed some important conclusions to be made regarding the usage of the CNTF electrodes. First, it showed that for nanocomposites made with either MWCNTs or SWCNTs, the CNTF are able to pick up cyclic electrical changes similar to silver standard electrodes, meaning that the measurements made are reliable and comparable to utilized standard techniques. Secondly, the same trend of similarity is shown by the CNTFs at both high and low forces of testing, for both relatively stiff nanocomposites as well as for viscoelastic nanocomposites. This makes the CNTFs as versatile as existing embedded and surface applied electrode systems, without the drawback of mechanical property loss. Thirdly, the CNTFs have been shown to register electrical changes in nanocomposites which are relatively highly conductive or are on the border of what is considered to be electrically insulative, making them extremely versatile and tailorable for a number of nanocomposites and applications. Last but not least, these findings combined with the fact that they can be embedded during the manufacturing process and can provide information regarding the uniaxial tensile mechanical loading which does not affect the nanocomposite matrix in any measurable way give the CNTF embedded electrodes an advantage over contemporary measurement systems.

#### ***4.5.4 Microstructural analysis and mechanism of working***

As seen from the manufacturing and post-manufacturing monitoring results, the CNTF electrodes display properties similar to that of standard surface applied electrode systems without the drawbacks of conventional embedded metallic electrodes. To understand if the performance is rooted in the microstructure and interaction of the different

materials in the hierarchical nanocomposite, optical imagery and SEM analysis was conducted.

Initial optical imagery showed that the CNTFs displayed an internal infiltration of the nanocomposite matrices into the fiber. Figure 29 shows how when a droplet of nanocomposite matrix is placed on a CNTF, the matrix infiltrates the fiber through its surface porosity and dented irregular surface paths at places. The irregular surface provides paths within the diameter of the fiber for the flow of the nanocomposite matrix, allowing an enhanced interaction between the CNTs of both materials. It was noted during initial testing that the fibers were completely wetted by the matrix (both SWCNT and MWCNT) in areas where the nanocomposite matrix was placed and also that in regions along where the infiltration of the droplet was present, the fibers obtained a stiffness without any matrix present on the surface. In comparison, the metallic embedded electrodes did not show a similar affinity when examined with optical microscopy, but rather displayed regions of inhomogeneous connection with the matrices as well as regions of separation of matrix constituents. It is postulated that the porous nature of the CNTFs allows not only for enhanced interaction with the nanocomposite matrices, but through the infiltration effect, maintains a volume of CNTs at the interface through CNT (from the matrix) to CNT (in the fibers) affinity. This mechanism is what is most likely responsible for the lack of contact resistance seen during electrical testing, whereas the inhomogeneous connection of the metallic embedded electrode with the matrix contributes and is responsible for the measurable contact resistance.

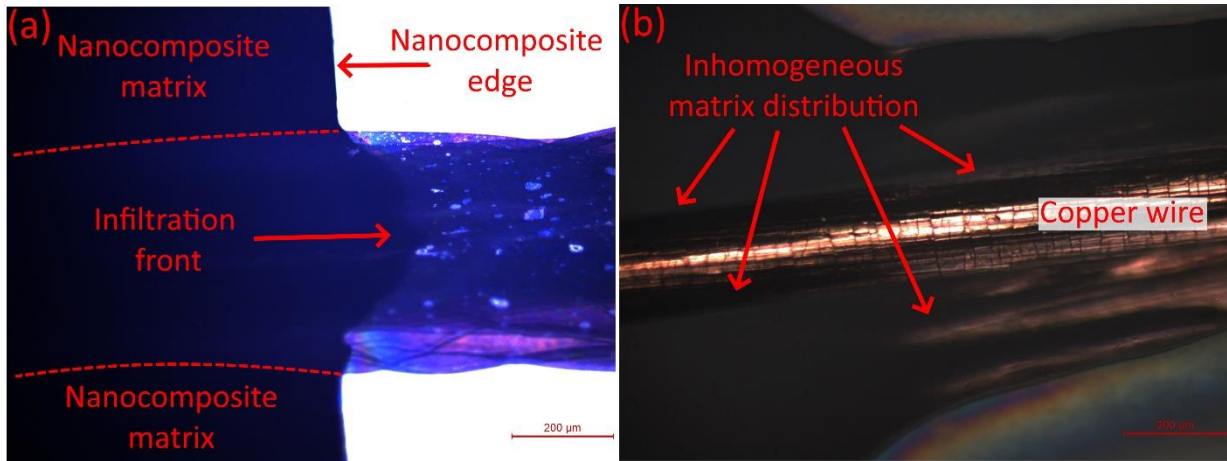


**Figure 29: Optical images showing (a) the infiltration of the matrix along the irregular region of the fiber and (b) inhomogeneous regions of connection between the metallic embedded electrode and matrix.**

To examine these characteristics further, SEM was conducted on the fracture surfaces of the metallic embedded samples which were used in piezoresistive testing. Since samples with the embedded CNTF electrodes did not break at the point of insertion or length of the electrodes, samples were carefully cut using a handheld Dremel saw at the point of insertion. Samples prepared from surface applied silver electrodes were used as the baseline for microstructural comparison and images are provided Figure 30, while images of samples with embedded electrodes are provided in Figure 31 and 32.

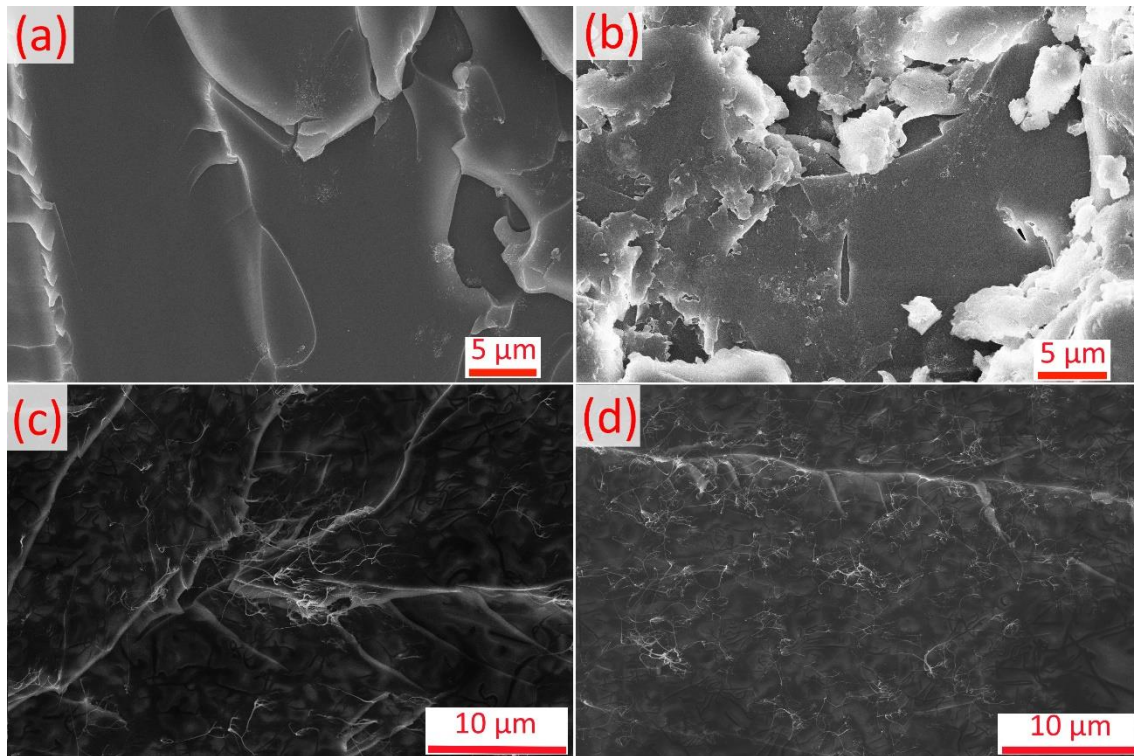


**Figure 30: SEM images of matrices with (a) 0.25% MWCNTs, (b) 0.75% MWCNTs, (c) 0.25% SWCNTs and (d) 0.75% SWCNTs.**

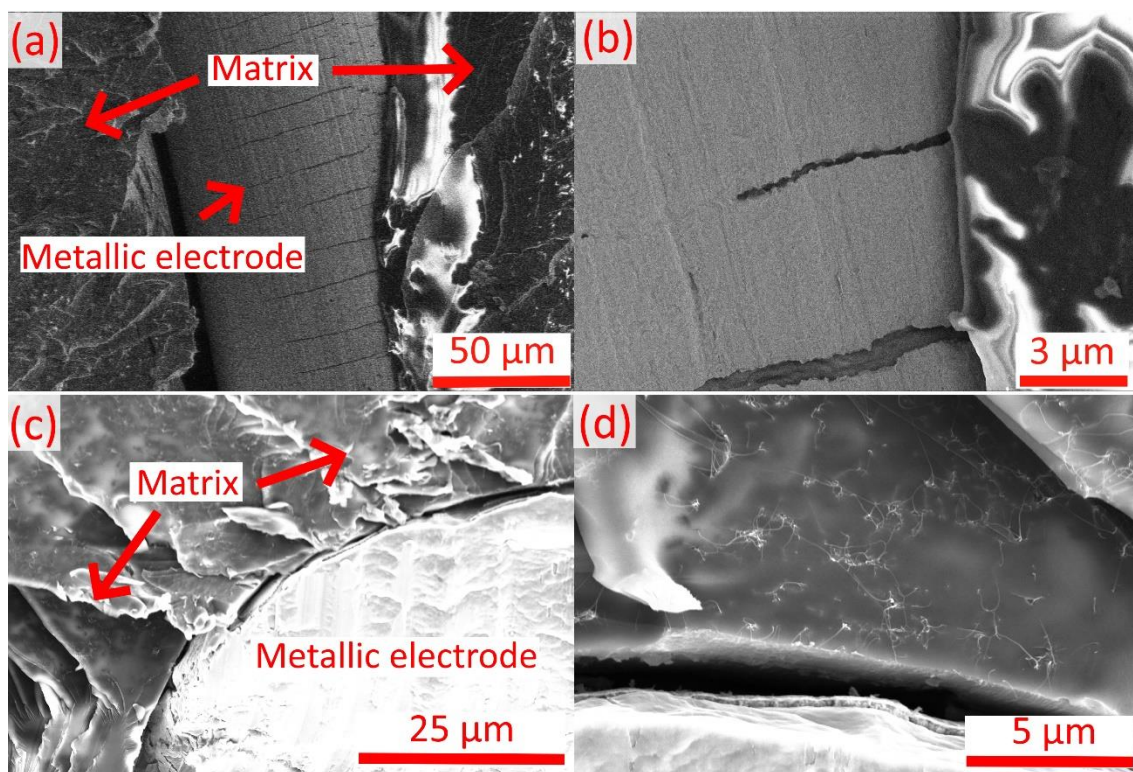
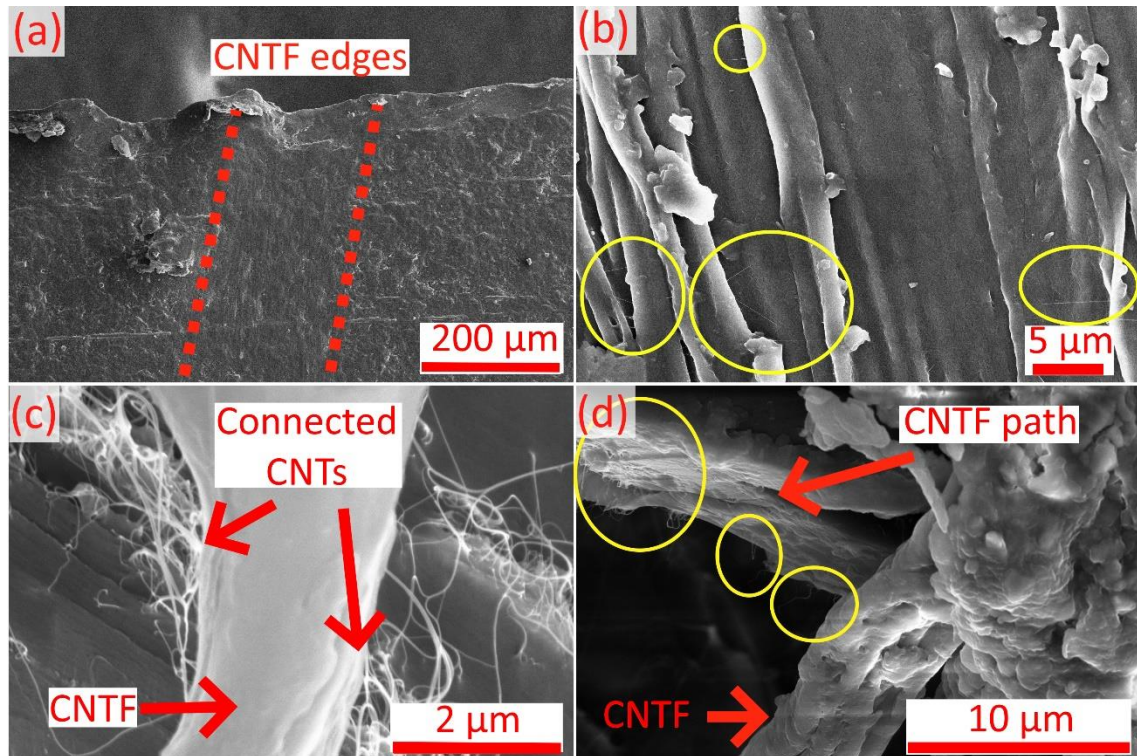


Figure 31: SEM images of embedded metallic electrodes within nanocomposites with MWCNTs at (a) 2000X, (b) 20,000X and SWCNTs at (c)3000X and (d) 18000X.



**Figure 32: SEM images of CNTFs embedded within nanocomposites with MWCNTs at (a) 500X, (b) 10000X and SWCNTs at (c) 60000X and (d) 16000X. Yellow circles indicate CNT bridging from CNTs in the matrix.**

The SEM results elucidated on the interaction of the nanocomposite matrices with the embedded electrodes and confirmed that both the functional property measurements and measured piezoresistive response were highly influenced by the interfaces of the materials in the hierarchical nanocomposite. As seen in Figure 31, the embedded metallic electrodes display poor adhesion to both the MWCNT and SWCNT nanocomposite matrices, which contributed to them acting as mechanical failure promoting structures. The surfaces of the electrodes in the samples examined seem pristine, again indicating that regardless of the microcracks present in the electrodes, the adhesion between the materials was indeed poor, and thus fracture paths and delamination existed along the length of the electrodes. A careful inspection of the interface area shows the presence of CNTs at the

interface between the electrodes and matrices, but that no CNT bridging is taking place between the two, also indicating a lack of strong contact between the CNTs in the nanocomposites and the electrodes. This is most likely the cause of the existence of the contact resistance and higher electrical values seen during the earlier phases of the study. In homogeneously dispersed nanocomposites where the CNTs form a highly electrically conductive percolation network surrounded by a strong dielectric material, as is the case in this study, the CNTs are considered to be solely responsible for the any electrical conductivity through ohmic contacts and the tunneling mechanism [40]. A lack of connection with this percolation network, especially when CNTs are often covered by the polymer making an insulating layer, results in an overestimation of both the electrical resistivity and piezoresistive response.

The samples with CNTF embedded electrodes provided the most interesting microstructural properties, explaining why they caused no loss in mechanical properties and a multifunctional property measurement closer to what is seen for standard surface applied electrodes. As shown in Figure 32, the CNTFs are completely wetted by the nanocomposite matrices, with no clear boundary visible between the two materials, except the directional density of CNTs forming the CNTF. This indicated that not only is the infiltration mechanism seen in the optical microscopy correct and present, but that the surface of the CNTFs present a stronger adhesion to the nanocomposite matrices in comparison with metallic embedded electrodes due to their porous surface (additional images of surface porosity are provided in Figure 33). Furthermore, in both MWCNT and SWCNT samples, CNT concentration near the interface of the electrodes and matrices was

present and visible, with CNT bridging taking place between the CNTs of the matrices and the CNTF surface (highlighted with yellow circles). In Figure 32 (c), complete large bundles can be seen adhering to the CNTF at the interface. This points to the fact that the not only does the strong interfacial connection between the electrodes and CNTs in the matrices allow for no significant loss in mechanical properties, but that the percolation network of the nanocomposite matrices and the CNTFs interact. This interaction of the two is what allows the elimination of contact resistance seen during multifunctional property measurement and enables more accurate and precise measurement since they are able to reduce the tunneling distance caused by the thermoset polymer matrix and promote ohmic contacts.

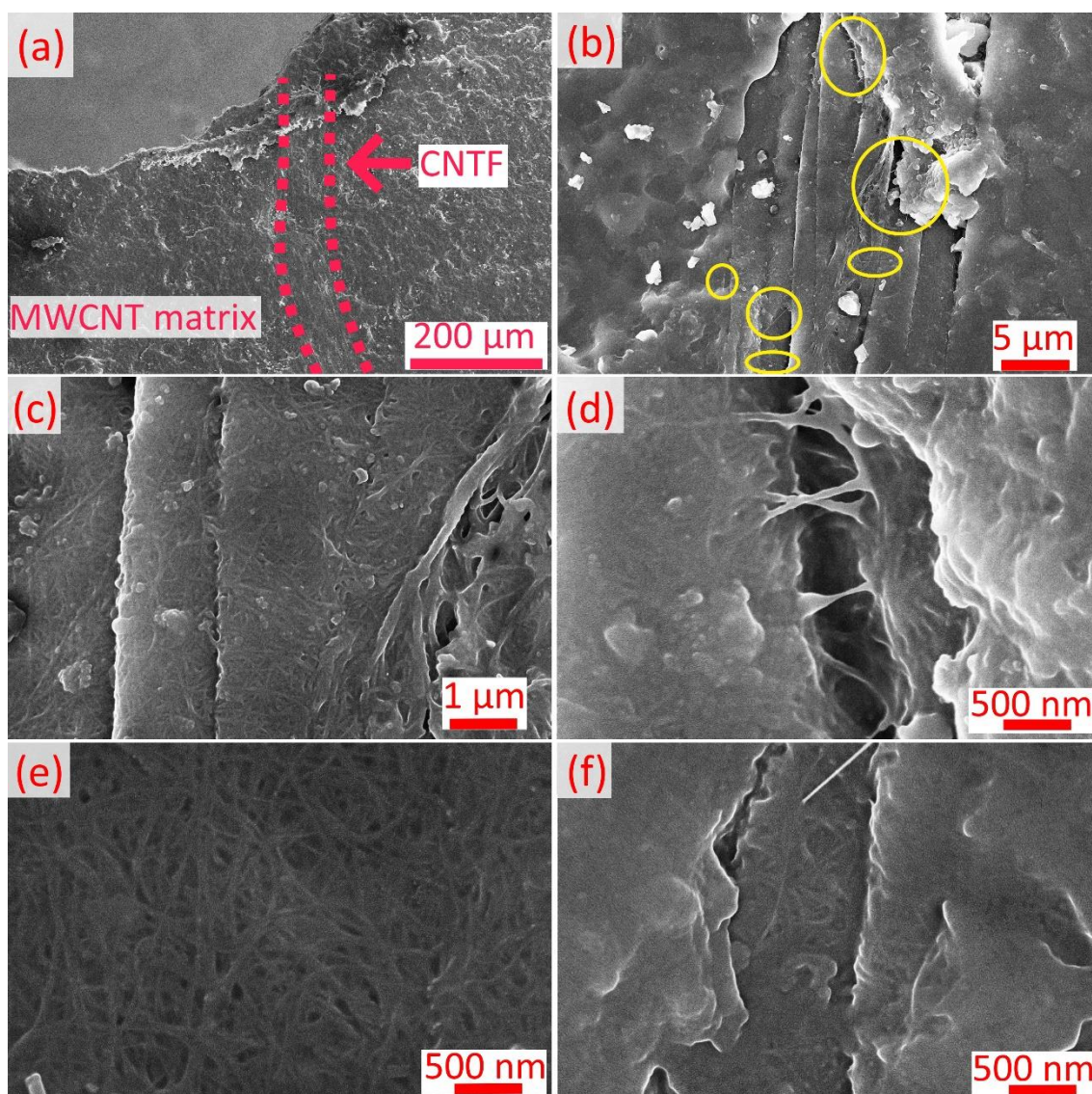


**Figure 33: SEM images showing (a) complete impregnation of CNTF with nanocomposite matrix, (b) CNT bridging between matrix and fiber, (c) impregnated surface of CNTF with matrix, (d) CNT bridging, (e) surface porosity of CNTF and (f) impregnated surface porosity with CNT bridging.**

Hence, the working mechanism and performance of the CNTF embedded electrodes can be explained by the enhanced microstructural interaction with the nanocomposite matrices. The infiltration of the nanomodified matrices into the internal diameter of the fibers through surface defects (as seen in Figures 32 and 33) along with surface infiltration through porosity allows for strong interfacial bonding and reduces areas

of inhomogeneity, causing no significant difference in nanocomposite mechanical performance. At the same time, this enhanced interaction allows a higher contact area and CNT bridging between the CNTs of the electrodes and the nanocomposites, which in turn causes the contact resistance between the materials to be insignificant, resulting in more accurate and precise measurements of multifunctional properties.

## Chapter 5. Conclusions and Future Outlook

This thesis examines the novel application of CNTFs made through the wet pulling technique. It reports on the first reported combination of CNTFs with CNT matrices, both SWCNTs and MWCNTs, for the purpose of multifunctional property measurement both during and after nanocomposite manufacturing with one-step integration. For this work, two multifunctional nanocomposite matrix types were created at two weight percentages (0.25% and 0.75%) and both were tested for their properties using (1) silver-based glue electrodes as the standard, (2) embedded metallic electrodes and (3) embedded CNTF electrodes.

During the manufacturing stage, the CNTF electrodes showed sensitivity to the concentration of both types of CNTs, proving that they have the potential to be utilized for the detection of filtration effects and different concentrations of different CNTs within a nanocomposite matrix. The electrodes showed almost identical resistance readings with negligible variance regardless of whether 2- or 4-point measurements were made, providing the advantages of reducing the number of electrodes needed for monitoring, reducing chances for regions of inhomogeneity which may cause later mechanical failure and allowing an inexpensive material-based manufacturing monitoring solution. Electrical measurements for the nanocomposites were between  $10^2$ - $10^3$  Ohm and  $10^3$ - $10^6$  for SWCNTs and MWCNTs at 0.25% and 0.75%, respectively. Comparatively, metallic embedded electrodes have the disadvantage of high noise, presence of contact resistance and inconsistency between batches, with measured values 1-2 orders of magnitude higher. The contact resistance noticed during both 2- and 4- point measurements for the embedded

metallic electrodes is due to poor interfacial connections formed with the CNTs in the nanocomposite matrices. During the manufacturing stage, the inconsistencies in readings between batches seen for the metallic electrodes are associated with the same phenomenon, where the CNTs form different levels of connection with the electrodes. These connections cause the development of contact resistance during manufacturing while the polymer is undergoing curing and becoming more electrically insulative. As the polymer cures, tunneling distances are affected during the solidification of the polymer, and ohmic contacts are negatively affected as polymer chains density increases around the CNTs.

The lifecycle monitoring also showed the CNTFs to be superior than alternatives. They showed electrical resistivity values with no significant difference (within sample to sample and batch to batch variance) when compared with the standard silver electrodes. Measured resistivity for the nanocomposites were between  $10^2$ - $10^3$  Ohm·cm and  $10^3$ - $10^6$  for SWCNTs and MWCNTs at 0.25% and 0.75%, respectively. Metallic electrodes again showed a 1-2 orders of magnitude larger measurement, with a generally higher variance. Tensile testing showed that samples incorporating CNTFs show a piezoresistive responses similar to the samples measured with standard silver electrodes (gauge factor between ~2-12), whereas the samples with metallic electrodes showed higher responses at lower force values. Metallic electrode integration was conducive to tensile mechanical property loss, with samples failing at points of insertion as they acted as regions of stress concentration and inhomogeneity. The cyclic testing corresponded to the tensile results, with CNTF incorporating samples providing cyclic responses similar to the standard samples. CNTF samples sustained more cycles at higher forces than the samples with metallic embedded

electrodes, but the difference was not significantly larger. Microstructural analysis proved that the performance of the CNTFs was due to matrix infiltration, both through the porous surface and into the volume of the fiber through surface artefacts, which allowed for an enhanced connection between the CNTs of the nanocomposites and the CNTFs. This was also the reason for the lack of contact resistance seen during multifunctional property measurement.

Here the superiority of a CNTF-based one-step monitoring solution for multifunctional nanocomposites utilizing CNTs as the additive has been shown. This thesis provides the scientific groundwork for further investigations into these advanced hierarchical nanocomposites and factors such as CNTF production technique, precursor quality, density, porosity, thickness and well as CNT type, functionalization and dispersion degree are now opened for further in-depth investigations. The thesis is the first to document this unique material interaction and properties and allow further scientific work to be conducted in this direction. In particular, in-depth studies which focus on primary variables such as CNTF densification and packing degree, morphology and interaction with various polymers should be addressed. Such studies will lay further groundwork as to what exact properties of CNTFs are required to sense which particular properties of CNT/nanocomposites. Further along the road, functionalization would be of particular interest since the variety of chemical groups which can be attached to CNTFs may make them very sensitive to chemical changes, such as those during polymer curing.

Practically, the thesis has proved the concept for a material-based dual-stage monitoring solution for multifunctional, smart and self-diagnostic nanocomposites.

Although the thesis shows that the CNTFs are sensitive to CNTs, the behavior should be consistent for all electrically conductive nanoparticles such as graphene and its derivatives, nanometals and nanorods. Defect management and structural health monitoring of next generation composites and nanocomposites, electromagnetic absorbers and reflectors, smart materials and sensors are highly possible based off of this work. When compared with equipment intensive techniques currently employed by the industry for composite monitoring and which lie in the price range of 1500- 15,000 USD (excluding overheads), the outlined technique offers a promising alternative which currently costs between 50-800 USD for 1 meter of monitored material (including overheads).

Further practical applications of the method outlined in the dissertation will be most attractive where hierarchical fiber reinforced nanocomposites incorporating CNTs will be used. As the CNTFs showed that they provide electrical responses which may help determine the concentration of CNTs in composites, this field would be the first place where they may be applied. Fiber reinforced composites are often subject to the filtration effect during manufacturing, and having a one-step solution for dual stage monitoring will be both feasible and attractive. With the proper protocol of embedding, which would ideally be a grid like format which is premade on the fiber reinforcement, holes, notches, macrocracks and microdamage (if the grid size is small enough) should be theoretically detectable. Particular forms of damage may be detectable due to the unique range of change of resistance, but more accurate and precise equipment will be required.

In the case of other forms of mechanical loading, the piezoresistive response of the base nanocomposite will dictate the response detected by the CNTFs. Generally, for

complex mechanical deformation, the piezoresistive response is the same over a monitored area, where the resistance increases with deformation. Compression is one of the only examples where piezoresistive response for such nanocomposites is negative, i.e. the conductivity is seen to increase with compression since the percolation network is forced together. The CNTFs should, by all results seen in this dissertation, be able to pick up such responses. This has been added into the dissertation.

An interesting aspect for investigation might include the area of AC conductivity measurement. AC measurements should not affect the performance of the CNTFs, as they themselves have a high conductivity and will show as typical resistors. The base nanocomposite properties will determine changes in behavior and it would be of interest to see how the CNTFs may respond to frequency dependent conductivity.

## Bibliography

- [1] I.V. Novikov, D.V. Krasnikov, A.M. Vorobei, Y.I. Zuev, H.A. Butt, F.S. Fedorov, S.A. Gusev, A.A. Safonov, E.V. Shulga, S.D. Konev, I.V. Sergeichev, S.S. Zhukov, T. Kallio, B.P. Gorshunov, O.O. Parenago, A.G. Nasibulin, Multifunctional Elastic Nanocomposites with Extremely Low Concentrations of Single-Walled Carbon Nanotubes, *ACS Appl. Mater. Interfaces*. 14 (2022) 18866–18876. <https://doi.org/10.1021/acsami.2c01086>.
- [2] H. A. Butt, G. V. Rogozhkin, A. Starkov, D. V. Krasnikov, A. G. Nasibulin, Multifunctional Carbon Nanotube Reinforced Polymer/Fiber Composites: Fiber-Based Integration and Properties, in: Longbiao Li, António B. Pereira, A. L. Pereira (Eds.), *Next Generation Fiber-Reinforced Composites - New Insights*, IntechOpen, 2023. <https://doi.org/10.5772/intechopen.108810>.
- [3] H.A. Butt, S.V. Lomov, I.S. Akhatov, S.G. Abaimov, Self-diagnostic carbon nanocomposites manufactured from industrial epoxy masterbatches, *Composite Structures*. 259 (2021) 113244. <https://doi.org/10.1016/j.compstruct.2020.113244>.
- [4] M. Choudhary, A. Sharma, S. Aravind Raj, M.T.H. Sultan, D. Hui, A.U.M. Shah, Contemporary review on carbon nanotube (CNT) composites and their impact on multifarious applications, *Nanotechnology Reviews*. 11 (2022) 2632–2660. <https://doi.org/10.1515/ntrev-2022-0146>.
- [5] M.H. Islam, S. Afroj, M.A. Uddin, D.V. Andreeva, K.S. Novoselov, N. Karim, Graphene and CNT-Based Smart Fiber-Reinforced Composites: A Review, *Adv Funct Materials*. 32 (2022) 2205723. <https://doi.org/10.1002/adfm.202205723>.
- [6] H.A. Butt, M. Owais, A. Sulimov, D. Ostrizhiniy, S.V. Lomov, I.S. Akhatov, S.G. Abaimov, Y.A. Popov, CNT/Epoxy-Masterbatch Based Nanocomposites: Thermal and Electrical Properties, in: *2021 IEEE 21st International Conference on Nanotechnology (NANO)*, IEEE, Montreal, QC, Canada, 2021: pp. 417–420. <https://doi.org/10.1109/NANO51122.2021.9514322>.
- [7] M.A. Zhilyaeva, E.V. Shulga, S.D. Shandakov, I.V. Sergeichev, E.P. Gilshteyn, A.S. Anisimov, A.G. Nasibulin, A novel straightforward wet pulling technique to fabricate carbon nanotube fibers, *Carbon*. 150 (2019) 69–75. <https://doi.org/10.1016/j.carbon.2019.04.111>.
- [8] M. Monthieux, V.L. Kuznetsov, Who should be given the credit for the discovery of carbon nanotubes?, *Carbon*. 44 (2006) 1621–1623. <https://doi.org/10.1016/j.carbon.2006.03.019>.
- [9] L. Radushkevich, V.á. Lukyanovich, The Structure of Carbon Forming in Thermal Decomposition of Carbon Monoxide on an Iron Catalyst, *Russian Journal of Physical Chemistry*. 26 (1952) 88–95.
- [10] T.W. Hughes, C.R. Chambers, *Manufacture of Carbon Filaments*, 1889.
- [11] C Pélabon, H Pélabon, Sur une variété de carbone filamenteux, *C R Acad Sci Paris*. 137 (1903) 706–708.
- [12] S. Iijima, T. Ichihashi, Single-shell carbon nanotubes of 1-nm diameter, *Nature*. 363 (1993) 603–605. <https://doi.org/10.1038/363603a0>.

- [13] P.R. Bandaru, Electrical Properties and Applications of Carbon Nanotube Structures, *J Nanosci Nanotechnol.* 7 (2007) 1239–1267. <https://doi.org/10.1166/jnn.2007.307>.
- [14] John S. Bulmer, Adarsh Kaniyoor, James A. Elliott, A Meta-Analysis of Conductive and Strong Carbon Nanotube Materials, *Advanced Materials.* 33 (2021). <https://doi.org/10.1002/adma.202008432>.
- [15] Z. Zhao, K. Teng, N. Li, X. Li, Z. Xu, L. Chen, J. Niu, H. Fu, L. Zhao, Y. Liu, Mechanical, thermal and interfacial performances of carbon fiber reinforced composites flavored by carbon nanotube in matrix/interface, *Composite Structures.* 159 (2017) 761–772. <https://doi.org/10.1016/j.compstruct.2016.10.022>.
- [16] J. Cai, S. Chawla, M. Naraghi, Piezoresistive effect of individual electrospun carbon nanofibers for strain sensing, *Carbon.* 77 (2014) 738–746. <https://doi.org/10.1016/j.carbon.2014.05.078>.
- [17] D. Sengupta, S.-H. Chen, A. Michael, C.Y. Kwok, S. Lim, Y. Pei, A.G.P. Kottapalli, Single and bundled carbon nanofibers as ultralightweight and flexible piezoresistive sensors, *Npj Flex Electron.* 4 (2020) 9. <https://doi.org/10.1038/s41528-020-0072-2>.
- [18] L. Kou, T. Huang, B. Zheng, Y. Han, X. Zhao, K. Gopalsamy, H. Sun, C. Gao, Coaxial wet-spun yarn supercapacitors for high-energy density and safe wearable electronics, *Nat Commun.* 5 (2014) 3754. <https://doi.org/10.1038/ncomms4754>.
- [19] Z. Eivazi Zadeh, A. Solouk, M. Shafieian, M. Haghbin Nazarpak, Electrospun polyurethane/carbon nanotube composites with different amounts of carbon nanotubes and almost the same fiber diameter for biomedical applications, *Materials Science and Engineering: C.* 118 (2021) 111403. <https://doi.org/10.1016/j.msec.2020.111403>.
- [20] F. Daneshvar, H. Chen, K. Noh, H.-J. Sue, Critical challenges and advances in the carbon nanotube–metal interface for next-generation electronics, *Nanoscale Adv.* 3 (2021) 942–962. <https://doi.org/10.1039/D0NA00822B>.
- [21] Y. Zhao, A. Kim, G. Wan, B.C.K. Tee, Design and applications of stretchable and self-healable conductors for soft electronics, *Nano Convergence.* 6 (2019) 25. <https://doi.org/10.1186/s40580-019-0195-0>.
- [22] A. Naeemi, J.D. Meindl, Carbon Nanotube Interconnects, (n.d.).
- [23] P. Lambin, Electronic structure of carbon nanotubes, *Comptes Rendus Physique.* 4 (2003) 1009–1019. [https://doi.org/10.1016/S1631-0705\(03\)00101-4](https://doi.org/10.1016/S1631-0705(03)00101-4).
- [24] R.H. Baughman, A.A. Zakhidov, W.A. De Heer, Carbon Nanotubes--the Route Toward Applications, *Science.* 297 (2002) 787–792. <https://doi.org/10.1126/science.1060928>.
- [25] G. Rahman, Z. Najaf, A. Mehmood, S. Bilal, A. Shah, S. Mian, G. Ali, An Overview of the Recent Progress in the Synthesis and Applications of Carbon Nanotubes, *C.* 5 (2019) 3. <https://doi.org/10.3390/c5010003>.
- [26] F. Yang, M. Wang, D. Zhang, J. Yang, M. Zheng, Y. Li, Chirality Pure Carbon Nanotubes: Growth, Sorting, and Characterization, *Chem. Rev.* 120 (2020) 2693–2758.
- [27] E.L. Ivchenko, B. Spivak, Chirality effects in carbon nanotubes, *Phys. Rev. B.* 66 (2002) 155404. <https://doi.org/10.1103/PhysRevB.66.155404>.

- [28] H.A. Butt, I.V. Novikov, D.V. Krasnikov, A.V. Sulimov, A.K. Pal, S.A. Evlashin, A.M. Vorobei, Y.I. Zuev, D. Ostrizhiniy, D. Dzhurinskiy, Y.A. Popov, O.O. Parenago, A.G. Nasibulin, Binder-free, pre-consolidated single-walled carbon nanotubes for manufacturing thermoset nanocomposites, *Carbon*. 202 (2023) 450–463. <https://doi.org/10.1016/j.carbon.2022.10.088>.
- [29] Alamusi, N. Hu, H. Fukunaga, S. Atobe, Y. Liu, J. Li, Piezoresistive Strain Sensors Made from Carbon Nanotubes Based Polymer Nanocomposites, *Sensors*. 11 (2011) 10691–10723. <https://doi.org/10.3390/s111110691>.
- [30] K. Aly, A. Li, P.D. Bradford, Compressive piezoresistive behavior of carbon nanotube sheets embedded in woven glass fiber reinforced composites, *Composites Part B: Engineering*. 116 (2017) 459–470. <https://doi.org/10.1016/j.compositesb.2016.11.002>.
- [31] Ayesha Kausar, Corrosion prevention prospects of polymeric nanocomposites: A review, *Journal of Plastic Film & Sheeting*. 0 (2018) 1–22. <https://doi.org/10.1177/875608791880602>.
- [32] S. Araby, B. Philips, Q. Meng, J. Ma, T. Laoui, C.H. Wang, Recent advances in carbon-based nanomaterials for flame retardant polymers and composites, *Composites Part B: Engineering*. 212 (2021) 108675. <https://doi.org/10.1016/j.compositesb.2021.108675>.
- [33] T.R. Pozegic, J.V. Anguita, I. Hamerton, K.D.G.I. Jayawardena, J.-S. Chen, V. Stolojan, P. Balocchi, R. Walsh, S.R.P. Silva, Multi-Functional Carbon Fibre Composites using Carbon Nanotubes as an Alternative to Polymer Sizing, *Sci Rep*. 6 (2016) 37334. <https://doi.org/10.1038/srep37334>.
- [34] M.S. Islam, Y. Deng, L. Tong, S.N. Faisal, A.K. Roy, A.I. Minett, V.G. Gomes, Grafting carbon nanotubes directly onto carbon fibers for superior mechanical stability: Towards next generation aerospace composites and energy storage applications, *Carbon*. 96 (2016) 701–710. <https://doi.org/10.1016/j.carbon.2015.10.002>.
- [35] O. Gohardani, M.C. Elola, C. Elizetxea, Potential and prospective implementation of carbon nanotubes on next generation aircraft and space vehicles: A review of current and expected applications in aerospace sciences, *Progress in Aerospace Sciences*. 70 (2014) 42–68. <https://doi.org/10.1016/j.paerosci.2014.05.002>.
- [36] M.B. Bryning, M.F. Islam, J.M. Kikkawa, A.G. Yodh, Very Low Conductivity Threshold in Bulk Isotropic Single-Walled Carbon Nanotube-Epoxy Composites, *Adv. Mater*. 17 (2005) 1186–1191. <https://doi.org/10.1002/adma.200401649>.
- [37] M.B. Bryning, D.E. Milkie, M.F. Islam, J.M. Kikkawa, A.G. Yodh, Thermal conductivity and interfacial resistance in single-wall carbon nanotube epoxy composites, *Applied Physics Letters*. 87 (2005) 161909. <https://doi.org/10.1063/1.2103398>.
- [38] F.H. Gojny, M.H.G. Wichmann, B. Fiedler, I.A. Kinloch, W. Bauhofer, A.H. Windle, K. Schulte, Evaluation and identification of electrical and thermal conduction mechanisms in carbon nanotube/epoxy composites, *Polymer*. 47 (2006) 2036–2045. <https://doi.org/10.1016/j.polymer.2006.01.029>.
- [39] Y. Zare, K.Y. Rhee, Simulation of Percolation Threshold, Tunneling Distance, and Conductivity for Carbon Nanotube (CNT)-Reinforced Nanocomposites Assuming Effective CNT Concentration, *Polymers*. 12 (2020) 114. <https://doi.org/10.3390/polym12010114>.

- [40] N.A. Gudkov, S.V. Lomov, I.S. Akhatov, S.G. Abaimov, Conductive CNT-polymer nanocomposites digital twins for self-diagnostic structures: Sensitivity to CNT parameters, *Composite Structures*. 291 (2022).
- [41] W. Bauhofer, J.Z. Kovacs, A review and analysis of electrical percolation in carbon nanotube polymer composites, *Composites Science and Technology*. 69 (2009) 1486–1498. <https://doi.org/10.1016/j.compscitech.2008.06.018>.
- [42] C. Pramanik, J.R. Gissinger, S. Kumar, H. Heinz, Carbon Nanotube Dispersion in Solvents and Polymer Solutions: Mechanisms, Assembly, and Preferences, *ACS Nano*. 11 (2017) 12805–12816. <https://doi.org/10.1021/acsnano.7b07684>.
- [43] S.M. Fatemi, M. Foroutan, Recent developments concerning the dispersion of carbon nanotubes in surfactant/polymer systems by MD simulation, *J Nanostruct Chem*. 6 (2016) 29–40. <https://doi.org/10.1007/s40097-015-0175-9>.
- [44] J.-H. Du, J. Bai, H.-M. Cheng, The present status and key problems of carbon nanotube based polymer composites, *Express Polym. Lett*. 1 (2007) 253–273. <https://doi.org/10.3144/expresspolymlett.2007.39>.
- [45] L.J. Lanticse, Y. Tanabe, K. Matsui, Y. Kaburagi, K. Suda, M. Hoteida, M. Endo, E. Yasuda, Shear-induced preferential alignment of carbon nanotubes resulted in anisotropic electrical conductivity of polymer composites, *Carbon*. 44 (2006) 3078–3086. <https://doi.org/10.1016/j.carbon.2006.05.008>.
- [46] J.O. Aguilar, J.R. Bautista-Quijano, F. Aviles, Influence of carbon nanotube clustering on the electrical conductivity of polymer composite films, *Express Polym. Lett*. 4 (2010) 292–299. <https://doi.org/10.3144/expresspolymlett.2010.37>.
- [47] M. Aravand, S.V. Lomov, I. Verpoest, L. Gorbatikh, Evolution of carbon nanotube dispersion in preparation of epoxy-based composites: From a masterbatch to a nanocomposite, *Express Polym. Lett*. 8 (2014) 596–608. <https://doi.org/10.3144/expresspolymlett.2014.63>.
- [48] T. Tarlton, E. Sullivan, J. Brown, P.A. Derosa, The role of agglomeration in the conductivity of carbon nanotube composites near percolation, *Journal of Applied Physics*. 121 (2017) 085103. <https://doi.org/10.1063/1.4977100>.
- [49] D. Martin, R.F. Minchin, M. Belkina, A. Milev, G.S. Kamali Kannangara, Toxicity and regulatory perspectives of carbon nanotubes, in: *Polymer–Carbon Nanotube Composites*, Elsevier, 2011: pp. 621–653. <https://doi.org/10.1533/9780857091390.2.621>.
- [50] C.S. Davis, J.W. Woodcock, J.W. Gilman, Preparation of Nanoscale Mutli-walled Carbon Nanotube Dispersions in a Polyetheramine Epoxy for Eco-Toxicological Assessment, National Institute of Standards and Technology, 2015. <https://doi.org/10.6028/NIST.SP.1200-9>.
- [51] K.B. Knudsen, T. Berthing, P. Jackson, S.S. Poulsen, A. Mortensen, N.R. Jacobsen, V. Skaug, J. Szarek, K.S. Hougaard, H. Wolff, H. Wallin, U. Vogel, Physicochemical predictors of Multi-Walled Carbon Nanotube–induced pulmonary histopathology and toxicity one year after pulmonary deposition of 11 different Multi-Walled Carbon Nanotubes in mice, *Basic & Clinical Pharmacology & Toxicology*. 124 (2019) 211–227. <https://doi.org/10.1111/bcpt.13119>.
- [52] A.H. Korayem, M.R. Barati, G.P. Simon, X.L. Zhao, W.H. Duan, Reinforcing brittle and ductile epoxy matrices using carbon nanotubes masterbatch, *Composites Part*

- A: Applied Science and Manufacturing. 61 (2014) 126–133. <https://doi.org/10.1016/j.compositesa.2014.02.016>.
- [53] Alexander Korzhenko, Mickael Havel, Catherine Bluteau, Masterbatch for manufacturing a drilling fluid, US 2012/0277125 A1, 2012.
- [54] A. Chafidz, M.A. Ali, R. Elleithy, Morphological, thermal, rheological, and mechanical properties of polypropylene-nanoclay composites prepared from masterbatch in a twin screw extruder, *J Mater Sci.* 46 (2011) 6075–6086. <https://doi.org/10.1007/s10853-011-5570-0>.
- [55] F. Wang, S. Liu, L. Shu, X.-M. Tao, Low-dimensional carbon based sensors and sensing network for wearable health and environmental monitoring, *Carbon.* 121 (2017) 353–367. <https://doi.org/10.1016/j.carbon.2017.06.006>.
- [56] B. Earp, J. Simpson, J. Phillips, D. Grbovic, S. Vidmar, J. McCarthy, C. Luhrs, Electrically Conductive CNT Composites at Loadings below Theoretical Percolation Values, *Nanomaterials.* 9 (2019) 491. <https://doi.org/10.3390/nano9040491>.
- [57] P. Sheng, E.K. Sichel, J.I. Gittleman, Fluctuation-Induced Tunneling Conduction in Carbon-Polyvinylchloride Composites, *PHYSICAL REVIEW LETTERS.* 40 (1978).
- [58] N. Hu, Y. Karube, C. Yan, Z. Masuda, H. Fukunaga, Tunneling effect in a polymer/carbon nanotube nanocomposite strain sensor, *Acta Materialia.* 56 (2008) 2929–2936. <https://doi.org/10.1016/j.actamat.2008.02.030>.
- [59] A. Terenzi, M. Natali, R. Petrucci, M. Rallini, L. Peponi, M. Beaumont, A. Eletsii, A. Knizhnik, B. Potapkin, J.M. Kenny, Analysis and simulation of the electrical properties of CNTs/epoxy nanocomposites for high performance composite matrices, *Polymer Composites.* 38 (2017) 105–115. <https://doi.org/10.1002/pc.23565>.
- [60] Y. Shimamura, T. Yasuoka, A. Todoroki, STRAIN SENSING BY USING PIEZORESISTIVITY OF CARBON-NANOTUBE/FLEXIBLE-EPOXY COMPOSITE, (n.d.).
- [61] S. Gong, Z.H. Zhu, S.A. Meguid, Carbon nanotube agglomeration effect on piezoresistivity of polymer nanocomposites, *Polymer.* 55 (2014) 5488–5499. <https://doi.org/10.1016/j.polymer.2014.08.054>.
- [62] R. Talreja, Manufacturing defects in composites and their effects on performance, in: *Polymer Composites in the Aerospace Industry*, Elsevier, 2020: pp. 83–97. <https://doi.org/10.1016/B978-0-08-102679-3.00004-6>.
- [63] Y.K. Hamidi, M.C. Altan, Process Induced Defects in Liquid Molding Processes of Composites, *International Polymer Processing.* 32 (2017) 527–544. <https://doi.org/10.3139/217.3444>.
- [64] S.Z.H. Shah, S. Karuppanan, P.S.M. Megat-Yusoff, Z. Sajid, Impact resistance and damage tolerance of fiber reinforced composites: A review, *Composite Structures.* 217 (2019) 100–121. <https://doi.org/10.1016/j.compstruct.2019.03.021>.
- [65] H. Altenbach, A. Ganczarski, eds., *Advanced Theories for Deformation, Damage and Failure in Materials*, Springer International Publishing, Cham, 2023. <https://doi.org/10.1007/978-3-031-04354-3>.
- [66] Y. Fu, X. Yao, A review on manufacturing defects and their detection of fiber reinforced resin matrix composites, *Composites Part C: Open Access.* 8 (2022) 100276. <https://doi.org/10.1016/j.jcomc.2022.100276>.

- [67] B. Wang, S. Zhong, T.-L. Lee, K.S. Fancey, J. Mi, Non-destructive testing and evaluation of composite materials/structures: A state-of-the-art review, *Advances in Mechanical Engineering*. 12 (2020) 168781402091376. <https://doi.org/10.1177/1687814020913761>.
- [68] L.S. Cividanés, E.A.N. Simonetti, M.B. Moraes, F.W. Fernandes, G.P. Thim, Influence of carbon nanotubes on epoxy resin cure reaction using different techniques: A comprehensive review, *Polym Eng Sci*. 54 (2014) 2461–2469. <https://doi.org/10.1002/pen.23775>.
- [69] B. Yenilmez, E. Murat Sozer, A grid of dielectric sensors to monitor mold filling and resin cure in resin transfer molding, *Composites Part A: Applied Science and Manufacturing*. 40 (2009) 476–489. <https://doi.org/10.1016/j.compositesa.2009.01.014>.
- [70] J.S. Chilles, A.F. Koutsomitopoulou, A.J. Croxford, I.P. Bond, Monitoring cure and detecting damage in composites with inductively coupled embedded sensors, *Composites Science and Technology*. 134 (2016) 81–88. <https://doi.org/10.1016/j.compscitech.2016.07.028>.
- [71] I.-B. Kwon, K.-S. Choi, Fiber optic sensors and their applications on structural health monitoring in South Korea, in: Y. Liao, W. Jin, D.D. Sampson, R. Yamauchi, Y. Chung, K. Nakamura, Y. Rao (Eds.), Beijing, , China, 2012: pp. 84210I-84210I–8. <https://doi.org/10.1117/12.979784>.
- [72] W. Hufenbach, F. Adam, W.-J. Fischer, A. Kunadt, D. Weck, Effect of Integrated Sensor Networks on the Mechanical Behaviour of Textile-Reinforced Thermoplastics, *Procedia Materials Science*. 2 (2013) 153–159. <https://doi.org/10.1016/j.mspro.2013.02.018>.
- [73] K. Shivakumar, L. Emmanwori, Mechanics of Failure of Composite Laminates with an Embedded Fiber Optic Sensor, *Journal of Composite Materials*. 38 (2004) 669–680. <https://doi.org/10.1177/0021998304042393>.
- [74] A. Huijjer, C. Kassapoglou, L. Pahlavan, Acoustic Emission Monitoring of Carbon Fibre Reinforced Composites with Embedded Sensors for In-Situ Damage Identification, *Sensors*. 21 (2021) 6926. <https://doi.org/10.3390/s21206926>.
- [75] M. Yourdkhani, W. Liu, S. Baril-Gosselin, F. Robitaille, P. Hubert, Carbon nanotube-reinforced carbon fibre-epoxy composites manufactured by resin film infusion, *Composites Science and Technology*. 166 (2018) 169–175. <https://doi.org/10.1016/j.compscitech.2018.01.006>.
- [76] G. Szebényi, Y. Blößl, G. Hegedüs, T. Tábi, T. Czigany, R. Schledjewski, Fatigue monitoring of flax fibre reinforced epoxy composites using integrated fibre-optical FBG sensors, *Composites Science and Technology*. 199 (2020) 108317. <https://doi.org/10.1016/j.compscitech.2020.108317>.
- [77] P. Hofmann, A. Walch, A. Dinkelman, S.K. Selvarayan, G.T. Gresser, Woven piezoelectric sensors as part of the textile reinforcement of fiber reinforced plastics, *Composites Part A: Applied Science and Manufacturing*. 116 (2019) 79–86. <https://doi.org/10.1016/j.compositesa.2018.10.019>.
- [78] K.I. Tifkitsis, A.A. Skordos, A novel dielectric sensor for process monitoring of carbon fibre composites manufacture, *Composites Part A: Applied Science and Manufacturing*. 123 (2019) 180–189. <https://doi.org/10.1016/j.compositesa.2019.05.014>.

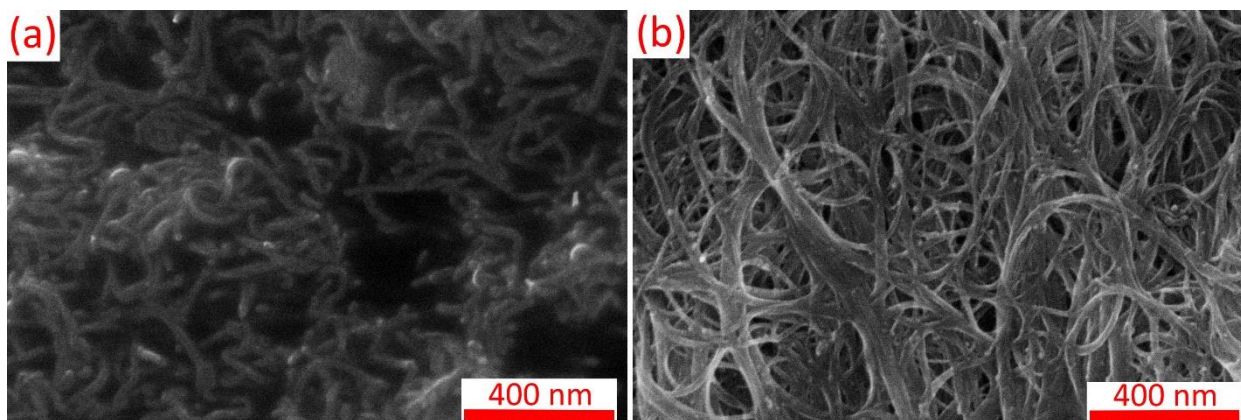
- [79] T. Feng, Y. Wang, J. Yang, Y. Li, P. Xu, H. Wang, H.-X. Peng, F. Qin, Real-time self-monitoring and smart bend recognizing of fiber-reinforced polymer composites enabled by embedded magnetic fibers, *Composites Science and Technology*. 232 (2023) 109869. <https://doi.org/10.1016/j.compscitech.2022.109869>.
- [80] S. Khadka, J. Hoffman, M. Kumosa, FBG monitoring of curing in single fiber polymer composites, *Composites Science and Technology*. 198 (2020) 108308. <https://doi.org/10.1016/j.compscitech.2020.108308>.
- [81] C.-S. Shin, L.-W. Chen, Damage Monitoring of Composite Adhesive Joint Integrity Using Conductivity and Fiber Bragg Grating, *Polymers*. 15 (2023) 1575. <https://doi.org/10.3390/polym15061575>.
- [82] A. Dimopoulos, S.J. Buggy, A.A. Skordos, S.W. James, R.P. Tatam, I.K. Partridge, Monitoring cure in epoxies containing carbon nanotubes with an optical-fiber Fresnel refractometer, *J of Applied Polymer Sci*. 113 (2009) 730–735. <https://doi.org/10.1002/app.30115>.
- [83] Y. Meyer, R. Lachat, G. Akhras, A review of manufacturing techniques of smart composite structures with embedded bulk piezoelectric transducers, *Smart Mater. Struct*. 28 (2019) 053001. <https://doi.org/10.1088/1361-665X/ab0fab>.
- [84] A. Allue, P. Corte-León, K. Gondra, V. Zhukova, M. Ipatov, J.M. Blanco, J. Gonzalez, M. Churyukanova, S. Taskaev, A. Zhukov, Smart composites with embedded magnetic microwire inclusions allowing non-contact stresses and temperature monitoring, *Composites Part A: Applied Science and Manufacturing*. 120 (2019) 12–20. <https://doi.org/10.1016/j.compositesa.2019.02.014>.
- [85] S.D. Shandakov, A.V. Kosobutsky, A.I. Verzhinina, O.G. Sevostyanov, I.M. Chirkova, D.M. Russakov, M.V. Lomakin, M.S. Rybakov, T.V. Glushkova, E.A. Ovcharenko, M.A. Zhilyaeva, A.G. Nasibulin, Electromechanical properties of fibers produced from randomly oriented SWCNT films by wet pulling technique, *Materials Science and Engineering: B*. 269 (2021) 115178. <https://doi.org/10.1016/j.mseb.2021.115178>.
- [86] J. Lee, D.-M. Lee, Y. Jung, J. Park, H.S. Lee, Y.-K. Kim, C.R. Park, H.S. Jeong, S.M. Kim, Direct spinning and densification method for high-performance carbon nanotube fibers, *Nat Commun*. 10 (2019) 2962. <https://doi.org/10.1038/s41467-019-10998-0>.
- [87] L.W. Taylor, O.S. Dewey, R.J. Headrick, N. Komatsu, N.M. Peraca, G. Wehmeyer, J. Kono, M. Pasquali, Improved properties, increased production, and the path to broad adoption of carbon nanotube fibers, *Carbon*. 171 (2021) 689–694. <https://doi.org/10.1016/j.carbon.2020.07.058>.
- [88] M.A. Zhilyaeva, O.A. Asiyanbola, M.V. Lomakin, D.M. Mironov, B.S. Voloskov, B. Mikladal, D.O. Tsetserukou, F.S. Fedorov, A.I. Verzhinina, S.D. Shandakov, A.G. Nasibulin, Tunable force sensor based on carbon nanotube fiber for fine mechanical and acoustic technologies, *Nanotechnology*. 33 (2022) 485501. <https://doi.org/10.1088/1361-6528/ac8b18>.
- [89] H.W. Zhu, C.L. Xu, D.H. Wu, B.Q. Wei, R. Vajtai, P.M. Ajayan, Direct Synthesis of Long Single-Walled Carbon Nanotube Strands, *Science*. 296 (2002) 884–886. <https://doi.org/10.1126/science.1066996>.

- [90] W. Zhou, J. Vavro, C. Guthy, K.I. Winey, J.E. Fischer, L.M. Ericson, S. Ramesh, R. Saini, V.A. Davis, C. Kittrell, M. Pasquali, R.H. Hauge, R.E. Smalley, Single wall carbon nanotube fibers extruded from super-acid suspensions: Preferred orientation, electrical, and thermal transport, *Journal of Applied Physics*. 95 (2004) 649–655. <https://doi.org/10.1063/1.1627457>.
- [91] X. Zhong, Y. Li, Y. Liu, X. Qiao, Y. Feng, J. Liang, J. Jin, L. Zhu, F. Hou, J. Li, Continuous Multilayered Carbon Nanotube Yarns, *Advanced Materials*. 22 (2010) 692–696. <https://doi.org/10.1002/adma.200902943>.
- [92] V.A. Davis, A.N.G. Parra-Vasquez, M.J. Green, P.K. Rai, N. Behabtu, V. Prieto, R.D. Booker, J. Schmidt, E. Kesselman, W. Zhou, H. Fan, W.W. Adams, R.H. Hauge, J.E. Fischer, Y. Cohen, Y. Talmon, R.E. Smalley, M. Pasquali, True solutions of single-walled carbon nanotubes for assembly into macroscopic materials, *Nature Nanotech*. 4 (2009) 830–834. <https://doi.org/10.1038/nnano.2009.302>.
- [93] M. Miao, Electrical conductivity of pure carbon nanotube yarns, *Carbon*. 49 (2011) 3755–3761. <https://doi.org/10.1016/j.carbon.2011.05.008>.
- [94] L.M. Ericson, H. Fan, H. Peng, V.A. Davis, W. Zhou, J. Sulpizio, Y. Wang, R. Booker, J. Vavro, C. Guthy, A.N.G. Parra-Vasquez, M.J. Kim, S. Ramesh, R.K. Saini, C. Kittrell, G. Lavin, H. Schmidt, W.W. Adams, W.E. Billups, M. Pasquali, W.-F. Hwang, R.H. Hauge, J.E. Fischer, R.E. Smalley, Macroscopic, Neat, Single-Walled Carbon Nanotube Fibers, *Science*. 305 (2004) 1447–1450. <https://doi.org/10.1126/science.1101398>.
- [95] O. Rodríguez-Uicab, J.L. Abot, F. Avilés, Electrical Resistance Sensing of Epoxy Curing Using an Embedded Carbon Nanotube Yarn, *Sensors*. 20 (2020) 3230. <https://doi.org/10.3390/s20113230>.
- [96] J.L. Abot, J.C. Anike, Structural Health Monitoring Using Carbon Nanotube Fibers, in: *Nanotube Superfiber Materials*, Elsevier, 2019: pp. 219–238. <https://doi.org/10.1016/B978-0-12-812667-7.00010-0>.
- [97] S.A. Romanov, A.E. Aliev, B.V. Fine, A.S. Anisimov, A.G. Nasibulin, Highly efficient thermophones based on freestanding single-walled carbon nanotube films, *Nanoscale Horiz*. 4 (2019) 1158–1163. <https://doi.org/10.1039/C9NH00164F>.
- [98] A.G. Nasibulin, A. Moisala, D.P. Brown, H. Jiang, E.I. Kauppinen, A novel aerosol method for single walled carbon nanotube synthesis, *Chemical Physics Letters*. 402 (2005) 227–232. <https://doi.org/10.1016/j.cplett.2004.12.040>.
- [99] G.A. Ermolaev, A.P. Tsapenko, V.S. Volkov, A.S. Anisimov, Y.G. Gladush, A.G. Nasibulin, Express determination of thickness and dielectric function of single-walled carbon nanotube films, *Applied Physics Letters*. 116 (2020) 231103. <https://doi.org/10.1063/5.0012933>.
- [100] F. Wang, S. Zhao, Q. Jiang, R. Li, Y. Zhao, Y. Huang, X. Wu, B. Wang, R. Zhang, Advanced functional carbon nanotube fibers from preparation to application, *Cell Reports Physical Science*. 3 (2022) 100989. <https://doi.org/10.1016/j.xcrp.2022.100989>.
- [101] M.R. Predtechenskiy, A.A. Khasin, A.E. Bezrodny, O.F. Bobrenok, D.Yu. Dubov, V.E. Muradyan, V.O. Saik, S.N. Smirnov, New perspectives in SWCNT applications: Tuball SWCNTs. Part 1. Tuball by itself—All you need to know about it, *Carbon Trends*. 8 (2022) 100175. <https://doi.org/10.1016/j.cartre.2022.100175>.

- [102] P.M. Kalachikova, A.E. Goldt, E.M. Khabushev, T.V. Eremin, K.B. Ustinovich, A. Grebenko, O.O. Parenago, T.S. Zatsepin, O.I. Pokrovskiy, E.D. Obraztsova, A.G. Nasibulin, Direct injection of SWCNTs into liquid after supercritical nitrogen treatment, *Carbon*. 152 (2019) 66–69. <https://doi.org/10.1016/j.carbon.2019.06.003>.
- [103] A.V. Shiverskii, M. Owais, B. Mahato, S.G. Abaimov, Electrical Heaters for Anti/De-Icing of Polymer Structures, *Polymers*. 15 (2023) 1573. <https://doi.org/10.3390/polym15061573>.
- [104] P. Shimpi, A. Aniskevich, D. Zeleniakene, Improved method of manufacturing carbon nanotube infused multifunctional 3D woven composites, *Journal of Composite Materials*. 56 (2022) 479–489. <https://doi.org/10.1177/00219983211055823>.
- [105] A. Sanli, A. Benchirouf, C. Müller, O. Kanoun, Piezoresistive performance characterization of strain sensitive multi-walled carbon nanotube-epoxy nanocomposites, *Sensors and Actuators A: Physical*. 254 (2017) 61–68. <https://doi.org/10.1016/j.sna.2016.12.011>.
- [106] A. Bouhamed, A. Al-Hamry, C. Müller, S. Choura, O. Kanoun, Assessing the electrical behaviour of MWCNTs/epoxy nanocomposite for strain sensing, *Composites Part B: Engineering*. 128 (2017) 91–99. <https://doi.org/10.1016/j.compositesb.2017.07.005>.
- [107] T. Barriere, X. Gabrion, S. Holopainen, J. Jokinen, Testing and analysis of solid polymers under large monotonic and long-term cyclic deformation, *International Journal of Plasticity*. 135 (2020) 102781. <https://doi.org/10.1016/j.ijplas.2020.102781>.
- [108] I.V. Novikov, E.M. Khabushev, D.V. Krasnikov, A.V. Bubis, A.E. Goldt, S.D. Shandakov, A.G. Nasibulin, Residence time effect on single-walled carbon nanotube synthesis in an aerosol CVD reactor, *Chemical Engineering Journal*. 420 (2021) 129869. <https://doi.org/10.1016/j.cej.2021.129869>.
- [109] M. Zhang, J. Li, Carbon nanotube in different shapes, *Materials Today*. 12 (2009) 12–18. [https://doi.org/10.1016/S1369-7021\(09\)70176-2](https://doi.org/10.1016/S1369-7021(09)70176-2).
- [110] A. Gbaguidi, S. Namila, D. Kim, Stochastic percolation model for the effect of nanotube agglomeration on the conductivity and piezoresistivity of hybrid nanocomposites, *Computational Materials Science*. 166 (2019) 9–19. <https://doi.org/10.1016/j.commatsci.2019.04.045>.
- [111] T.R. Frømyr, F.K. Hansen, T. Olsen, The Optimum Dispersion of Carbon Nanotubes for Epoxy Nanocomposites: Evolution of the Particle Size Distribution by Ultrasonic Treatment, *Journal of Nanotechnology*. 2012 (2012) 1–14. <https://doi.org/10.1155/2012/545930>.
- [112] T.M. Al-Saadi, S.H. Aleabi, E.E. Al-Obodi, H.A.-J. Abbas, The Effect of Multi Wall Carbon Nanotubes on Some Physical Properties of Epoxy Matrix, *J. Phys.: Conf. Ser.* 1003 (2018) 012102. <https://doi.org/10.1088/1742-6596/1003/1/012102>.
- [113] S.-H. Park, J. Hwang, G.-S. Park, J.-H. Ha, M. Zhang, D. Kim, D.-J. Yun, S. Lee, S.H. Lee, Modeling the electrical resistivity of polymer composites with segregated structures, *Nat Commun*. 10 (2019) 2537. <https://doi.org/10.1038/s41467-019-10514-4>.
- [114] M.R. Predtechenskiy, A.A. Khasin, S.N. Smirnov, A.E. Bezrodny, O.F. Bobrenok, D.Yu. Dubov, A.G. Kosolapov, E.G. Lyamysheva, V.E. Muradyan, V.O. Saik, V.V. Shinkarev, D.S. Chebochakov, M.S. Galkov, R.V. Karpunin, T.D. Verkhovod, D.V.

- Yudaev, Y.S. Myasnikova, A.N. Krasulina, M.K. Lazarev, New Perspectives in SWCNT Applications: Tuball SWCNTs. Part 2. New Composite Materials through Augmentation with Tuball., Carbon Trends. 8 (2022) 100176. <https://doi.org/10.1016/j.cartre.2022.100176>.
- [115] L.S. Cividanés, W. Franceschi, F.V. Ferreira, B.R.C. Menezes, R.C.M. Sales, G.P. Thim, How Do CNT affect the branch and crosslink reactions in CNT-epoxy, Mater. Res. Express. 4 (2017) 105101. <https://doi.org/10.1088/2053-1591/aa8d31>.
- [116] H. Tanabi, Effect of CNTs dispersion on electrical, mechanical and strain sensing properties of CNT/epoxy nanocomposites, Results in Physics. (2019).
- [117] Irfan Ahmad Mir, D. Kumar, Carbon nanotube-filled conductive adhesives for electronic applications, Nanoscience Methods. 1 (2012) 183–193. <https://doi.org/10.1080/17458080.2011.602724>.
- [118] H. Meeuw, C. Viets, W.V. Liebig, K. Schulte, B. Fiedler, Morphological influence of carbon nanofillers on the piezoresistive response of carbon nanoparticle/epoxy composites under mechanical load, European Polymer Journal. 85 (2016) 198–210. <https://doi.org/10.1016/j.eurpolymj.2016.10.027>.

## Appendix



**Appendix Figure 1: SEM images of (a) MWCNT and (c) SWCNT masterbatches taken at 250,000 X.**